Ege University

IGIC
ІЗНХ

ENVIRONMENTAL PROTECTION: FROM SORBENTS TO MEMBRANES

KYIV 2016

National Academy of Science of Ukraine
V.I. Vernadskii Institute of General and Inorganic Chemistry
Ege University, Turkish Republic

ENVIRONMENTAL PROTECTION: FROM SORBENTS TO MEMBRANES

Edited by
Nalan Kabay
Yuliya Dzyazko
Müşerref Arda
Konstantin Kazdobin

Referees: Selih Ötleş, Valerii Myronchuk, Idil Ipek, Valentina Sazonova

KYIV 2016

УДК 544.018.2: 544.472.3 + 555.11+666.22

Колективна монографія «Environmental Protection: from Sorbents to Membranes» - під ред. проф. Н. Кабай, докт. хім. наук Ю. С. Дзязько, проф. М. Арда, докт. хім. наук К.О. Каздобіна - 108 с.

Колективна монографія включає статті за матеріалами українсько-турецького семінару, який було проведено 11 листопада 2016 р. на базі Інституту загальної та неорганічної хімії ім. В. І. Вернадського НАН України за участю фахівців Егейського університету (Турецька республіка) та за підтримки Відділення хімії НАН України, Відділу міжнародних зв'язків НАН України, а також Наукової та Технічної дослідної Ради Турецької республіки TÜBİTAK. У монографії наведено результати досліджень, які направлені на вилучення токсичних і цінних компонентів із розчинів техногенного та природного походження, зокрема з біологічних рідин, із застосуванням сорбційних та мембранних методів. Результати робіт можуть бути застосовані у водопідготовці, хімічній, фармацевтичній, харчовій промисловості. Особливу увагу приділено синтезу нових матеріалів для процесів розділення та впливу структури цих матеріалів на їх функціональні властивості: проникну здатність, електропровідність, каталітичну спроможність тощо.

Монографія є корисною для фахівців в області мембранних та сорбційних технологій, а також для студентів вищих навчальних закладів.

Рецензенти: Проф. Утлеш Селіх (Егейський університет, Турецька республіка), докт. техн. наук Мирончук Валерій Григорович (Національний університет харчових технологій, Україна), докт. Іпек Іділь (Егейський університет, Турецька республіка), докт. хім. наук, проф. Сазонова Валентина Федорівна (Одеський Національний університет ім. І. І. Мечникова).

Рекомендовано до друку Вченою радою ІЗНХ ім. В. І. Вернадського НАН України (протокол № 15 від 19 жовтня 2016 р.).

ISBN 978-966-97621-2-2

CONTENT

PREFACE **5**
N. Kabay, V.M. Ogenko, V.N. Belyakov

UTILIZATION OF ION EXCHANGE TOGETHER WITH MEMBRANE PROCESSES FOR WASTEWATER RECLAMATION AND REUSE **7**
N. Kabay, M. Arda, S. Bunani, E. Altiok, D. İpekçi, M. Hacıfazlıoğlu, İ. Parlar, İ. Yilmaz İpek, M. Yüksel

NOVEL EFFECTIVE ECO-FRIENDLY NANOSIZED HETEROGENEOUS CATALYST SYSTEM FOR REDUCTION OF NITROARENES WITH HYDRAZINE HYDRATE **12**
L.F. Sharanda, P.P. Onys'ko, Ya.Ya. Khomutnyk, L S. Lysyuk, V.M. Ogenko, S.V. Volkov

LITHIUM-SELECTIVE COMPOSITE MATERIALS BASED ON TiO_2 AND MnO_2 **18**
L.M. Rozhdestvenska, M.O. Chaban, V.M. Belyakov

REMOVAL OF As(V) COMPOUNDS FROM WATER USING OPMN-P NANOFILTRATION MEMBRANE **23**
L.O, Melnik

APPLICATION OF MEMBRANE FILTRATION TO WHEY PROCESSING **27**
İ. Özdemir, Y.A. Jarma, E. Altıok, N. Kabay, S. Ötleş, M. Yüksel

ION EXCHANGE MEMBRANES AND ACTIVATED CARBON **33**
Yu.M. Volfkovich, V.E. Sosenkin, Yu.S. Dzyazko

PHOSPHORUS-CONTAINING CARBONS – A NEW TYPE OF CARBONACEOUS ADSORBENTS **43**
A.M. Puziy, O.I. Poddubnaya

ADSORPTION KINETICS OF ANTHOCYANINS FROM ELDERBERRY EXTRACTS ON BENTONITE **48**
L.M. Soldatkina, V.O. Novotna

WHEY AND WHEY PROCESSING **52**
İ. Özdemir, S. Ötleş, N. Kabay, M. Yüksel

INTERACTIONS IN THE SYSTEM AIR – WATER - NATURAL ALUMINOSILICATES AND TECHNOLOGY FOR THE ACCELERATION OF SELF- REMEDIATION IN NATURAL **58**

BASINS
K. Pershina, K. Kazdobin

NANOCOMPOSITE POLYSULFONE MEMBRANES WITH IMPROVED ANTIFOULING PROPERTIES **64**
O. Dzhodzhyk, I. Kolesnyk, V. Konovalova, A. Burban

CONCENTRATE MANAGEMENT FOR NF BRİNE OF GROUND WATER BY USİNG ELECTROMEMBRANE (ED AND EDI) PROCESSES **68**
E. Altıok, S. Bunani, D. İpekçi, N. Kabay, M.Arda, M.Yüksel

SORPTION REMOVAL OF URANIUM (VI) COMPOUNDS WITH ORGANIC-INORGANIC ION-EXCHANGERS **74**
N.O. Perlova, O.V. Perlova, I.Yu. Halutska, Yu.S. Dzyazko, A.V. Palchik, V.F. Sazonova

THE NATURE OF INTERPHASE POTENTIAL UNDER FORCED MOVEMENT OF THE PROTON IN WATER/OXYGEN SYSTEM **79**
K.D. Pershina

ELECTRODEIONIZATION REMOVAL OF $HCrO_4^-$ IONS FROM DILUTED SOLUTION. EFFECT OF MEMBRANE **84**
Yu.S. Dzyazko, Ö. Arar, L.M. Rozhdestvenska, S.L. Vasilyuk

REVERSE OSMOSIS FOR CONCENTRATIION OF SUGAR BEET JUICE AFTER THE SECOND CARBONATION **90**
Yu.G. Zmievskii, V.G. Myronchuk

REMOVAL OF Pb (II) IONS FROM WATER SOLUTIONS WITH ION EXCHANGE RESINS, OXIDES AND HYBRID SORBENTS **94**
T.V. Maltseva, K. O. Kudelko, E.A. Kolomiets

ADSORPTION OF DYES, HERBICIDES AND HEAVY METALS BY COMPOSITES OF SILICA WITH AMINO- AND SULFO CONTAINING POLYSACCHARIDES **98**
T.M. Budnyak, V.A. Tertykh, M. Błachnio, A. Deryło-Marczewska, A.W. Marczewski

BORONIC-ACID FUNCTIONALIZED MAGNETITE NANOCOMPOSITES FOR FRUCTOSE SENSING **102**
Ye.V. Pylypchuk, Yu.O. Zubchuk, P.P. Gorbyk, K.O. Doroshenko, N.G. Antoniuk

PREFACE

Water is an essential resource for life and good health. The lack of water to meet daily needs is a reality today for one in three people around the World. Globally, the problem is getting worse as cities and population grow, and the needs for water increase in agriculture, industry and households. This urgeses very one to be part of efforts to conserve and protect the water sources.

The scarcity of water is accompanied by deterioration in the quality of available water due to pollution and environmental degradation. Recently, utilization of clean technologies with the target of "**zerodischarge**" has attracted the interest of policymakers, stakeholders and industrial sectors.

In this context, an international workshop on "**Environmental Protection: from Sorbents to Membranes**" was organized at V.I. Vernadskii Institute of General and Inorganic Chemistry, Ukrainian National Academy of Sciences, Kiev, Ukraine on November 11, 2016 in order to create an international platform where the most recent researches and experiences are exchanged and presented. This workshop will focus mostly on water treatment technologies such as sorption and membrane processes. During the workshop, some specific applications such as water reclamation and whey demineralization in food industry will be also discussed.

We acknowledge TÜBİTAK and National Academy of Science of Ukraine (NASU) to support us for our biletaral project and to organize this workshop for discussing the results obtained during the project period in both countries and future collaborations.

We would like to welcome you to this workshop to get an opportunity to acquire the scientific information and experiences to be presented at V.I. Vernadskii Institute of General and Inorganic Chemistry. We wish that this workshop will let us to tackle the environmental problems and get some new ideas together for future collaborations at an international level.

Prof. NalanKabay
Ege University

Membranes and membrane processes are studied more than 250 years. The term "membrane" is of Latin origin and means literally "peel", "shell", "diaphragm". The first membrane separation process has been performed in 1748, when French Abbot Jean-Antoine Nollet tried to separate water from alcohol using pig bladders. However, German physiologists, botanists and chemists were the founders of membrane science. Physiologist Adolf Eugen Fick has set phenomenological diffusion law. Botanist Wilhem Pfeffer postulated the existence of cell membranes. This suggestion was based on the similarity between the cells and osmometers with semipermeable membranes, which were produced by chemist Moritz Traube using copper ferrocyanide. Then the investigations were continued by physical chemists.

Among them, it should be noted great names of Walther Hermann Nernts (electrochemical aspects of membrane processes) and Jacobus Henricus van 't Hoff (theory of osmotic processes).

However, the rapid development of the membrane science began only in the middle of the last century, when synthetic polymers as well as inorganic sorbents had been developed and commercialized. Actually the membranes are applied to solution of a wide spectrum of practical tasks, particularly for water conditioning and wastewater treatment, in chemical, food, pharmaceutical industries, in medicine.

In fact, membrane science is often associated with such branch of physical chemistry as adsorption and ion exchange. A number of membrane types are produced from sorbents: ion exchange resins are used for manufacture of heterogeneous membranes for electrodialysis, the raw materials for preparation of inorganic membranes are hydrated oxides of multivalent metals, Ion transport trough the ion exchange membranes and resins shows similar regularities. Membrane and sorption processes can be independent elements of a single technological scheme. Alternately they can occur simultaneously in a single cell. Thus, the membrane and sorption materials and processes should be considered within the same context.

The rich world of membrane phenomena, the possibility to combine membrane separation with other processes as well as the great potential for synthesis of polymers, ceramics and composites allow us to hope that the membrane science and membrane technologies will be developed in the near future involving more and more highly qualified professionals and young scientists. It is also expected for Ukraine as the integration of our country into the world community.

We thank the team of Turkish Republic for co-operation. We express our gratitude for the Tubitak Council, the Section of Chemistry and the International Relation Department of the NAS of Ukraine for the possibility of the meeting with our colleagues. We really appreciate the contribution of the administration of our Institute to organization of this event. We will always remember the support of our scientific direction by academician of the NAS of Ukraine, prof. Sergey Volkov, who has been a director of the Institute for long time and passed away this year.

Corresponding member of the NAS of Ukraine,
Prof. Vladimir Belyakov
Corresponding member of the NAS of Ukraine,
Prof. Vladimir Ogenko
V.I. Vernadskii Institute of General and Inorganic Chemistry

UDC 66.081

UTILIZATION OF ION EXCHANGE TOGETHER WITH MEMBRANE PROCESSES FOR WASTEWATER RECLAMATION AND REUSE

N. Kabay[1*], M. Arda[2], S. Bunani[1,2,3], E. Altıok[1], D.İpekçi[1], M.Hacıfazlıoğlu[1], İ.Parlar[1], İ. Yılmaz İpek[1], M. Yüksel[1]

[1]*Ege University, Chemical Engineering Department, Faculty of Engineering, 35100 Izmir, Turkey*
e-mail: nalan.kabay@ege.edu.tr
[2]*Ege University, Chemistry Department, Faculty of Science, 35100 Izmir, Turkey*
[3]*University of Burundi, Department of Chemistry, Faculty of Science, Bujumbura, Burundi*

Abstract. *Ion exchange resins and membranes could be successfully used in integrated systems for elimination of some pollutants, recovery of valuable substances from water and for polishing RO permeate of desalination plants. Ion exchange membranes in an electrodialysis (ED) system could be employed for the post-treatment of concentrate streams of NF/RO processes and for valorization of RO desalination brines. The ED process in combination with bipolar membranes (BMED) was developed to split an aqueous saline solution into its corresponding acid and base without addition of any chemicals. Electrodeionization (EDI) system could be also another alternative method for boiler feed water production from RO permeate of raw water. This presentation will focus on elaboration of new ideas for the utilization of ion exchange in the process schemes of wastewater treatment based on membrane technologies.*

Keywords: *Ion exchange, desalination, membrane process, wastewater treatment*

Introduction. Advanced technologies in water and wastewater treatment become important due to the fact that discharge standards are decreased and there is a need for water recovery and reuse. The commercially available ion exchange resins and ion exchange membranes are mostly used today in water treatment technologies to produce water needed for different purposes and to remove/recover some trace substances from water. Integrating ion exchange process with a membrane filtration in a hybrid process is considered to result in a higher efficiency and lower cost as compared with the traditional fixed bed ion exchange system.

The growing demand for fresh water is partially satisfied by desalination plants that increasingly use membrane technologies such as reverse osmosis (RO) to produce potable water. Operating with water recoveries from 35% to 85%, RO plants generate large volumes of concentrates containing all retained compounds that are commonly discharged to water bodies. This causes a potentially serious threat to eco-systems. Therefore, there is an urgent need for environmentally friendly management options of RO brines [1-2]. Along with traditional treatments such as evaporation and crystallization, membrane technologies such as membrane distillation, forward osmosis, and electrodialysis (ED) have been emerged recently to reduce the volume of the concentrate before disposal and with the objective of achieving zero liquid discharge and recovery of valuable compounds. Recently, integrated processes coupling RO with ED to minimize the waste fractions of the brine are shown to be more effective than the traditional evaporation techniques due to lower energy consumption [3-8].

Bipolar membrane electrodialysis (BPED) method was developed to split an aqueous saline solution into its corresponding acid and base without addition of chemicals. Bipolar membranes contain an anion-exchange layer, a cation-exchange layer and a hydrophilic interface between two layers. When a direct current is applied, the water molecules migrate into the hydrophilic layer where they split into H^+ and OH^- ions. Thus, it is possible to achieve the removal and the recovery simultaneously [9-10].

In this presentation, importance of integrated ion exchange and membrane technologies for especially wastewater reclamation and reuse will be discussed. Some data obtained will be presented.

Experimental. For wastewater reclamation, some tests were performed using a pilot membrane test system installed in the wastewater treatment plant where MBR treatment system has been employed since 2008. The EDI tests were carried out using an EDI system (Electrocell) with multi cells. Figure 1 shows the flow-scheme of multi-cells EDI system. Neosepta CMX and AMX membranes were employed in the EDI stack while Purolite-CT175 and -A500 as cation and anion exchange resins, respectively. For ED tests, TS-1-10 model ED equipment was employed.

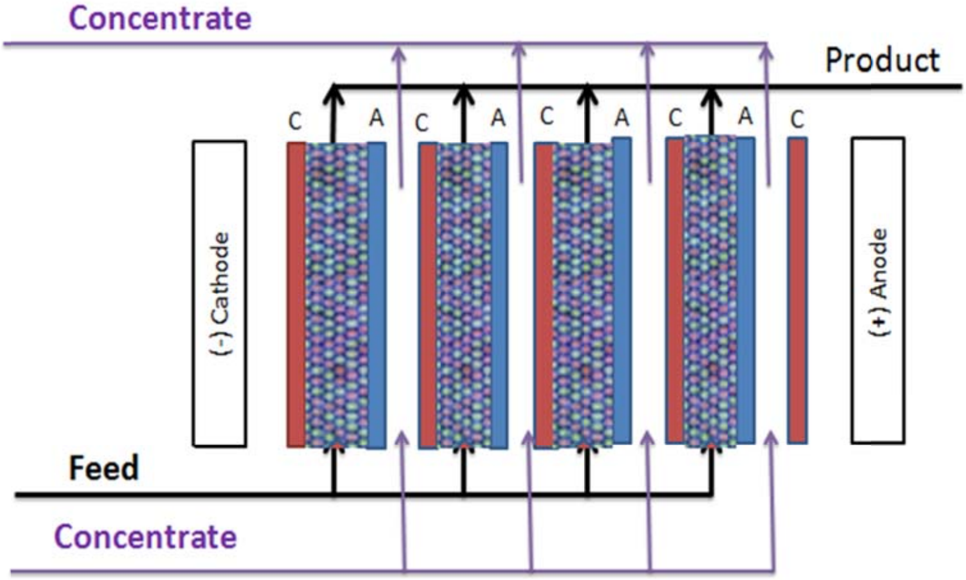

Fig. 1. *A Flow Scheme of a Multi Cell EDI System*

Results and discussion. For wastewater reclamation, RO tests were carried out at the industrial zone using a pilot RO system where MBR effluent was further treated. The collected RO permeate was fed to EDI system with a flow rate of 1 L/h. As shown in Figure 2, conductivity of diluate decreased by time as a function of applied electrical potential. It was possible to reduce conductivity of RO permeate from 40 µS/cm to 2.6 µS/cm by EDI process.

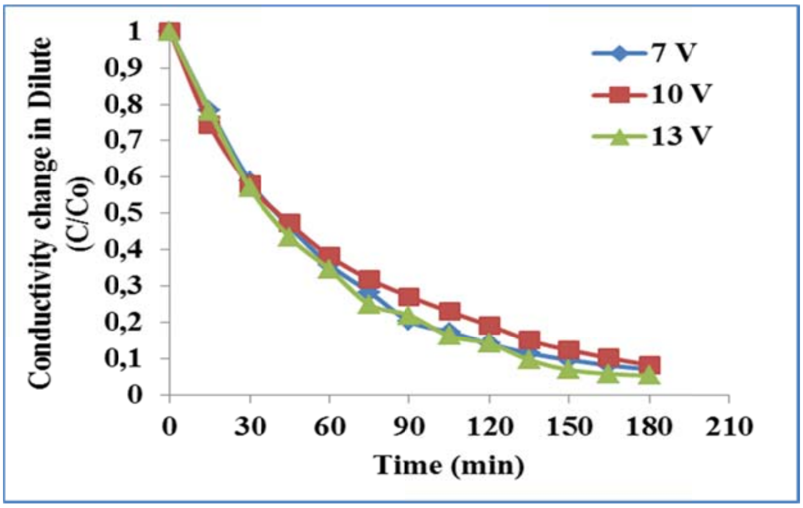

Fig. 2. *Conductivity Change vs. Time Plots for RO Permeate during EDI Operation*

In a separate test, RO brine with a conductivity of 11 mS/cm was treated with nanofiltration (NF) first for pre-treatment. By doing this, the conductivity of RO brine was reduced to 350 µS/cm. Electrodialysis was the following step to reduce this conductivity to 15 µS/cm in the diluate. Conductivity rejection from RO brine was 95% in 36 min by ED process at 10 V (Figure 3). .

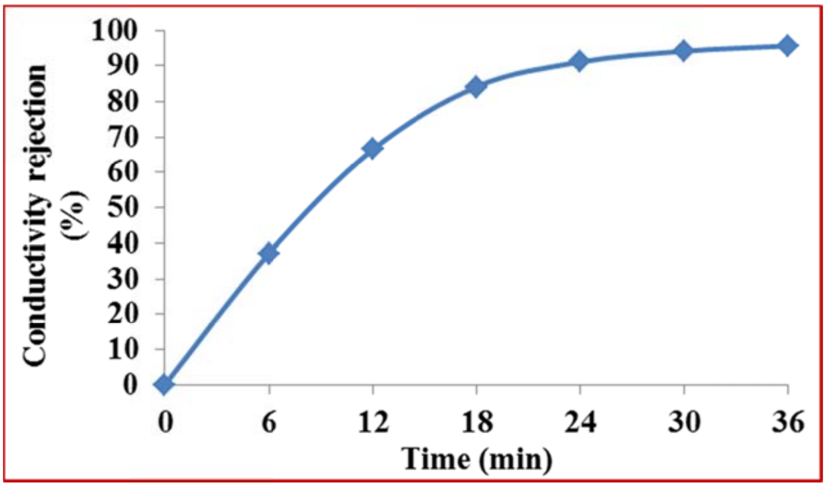

Fig. 3. *Conductivity Rejection vs. Time Plot for NF Permeate during ED Operation*

Following ED process, EDI was employed for post-treatment of ED diluate. As illustrated in Figure 4, conductivity of ED diluate was reduced to 3.0 mS/cm from 15 mS/cm with 88% of conductivity rejection at 7 V.

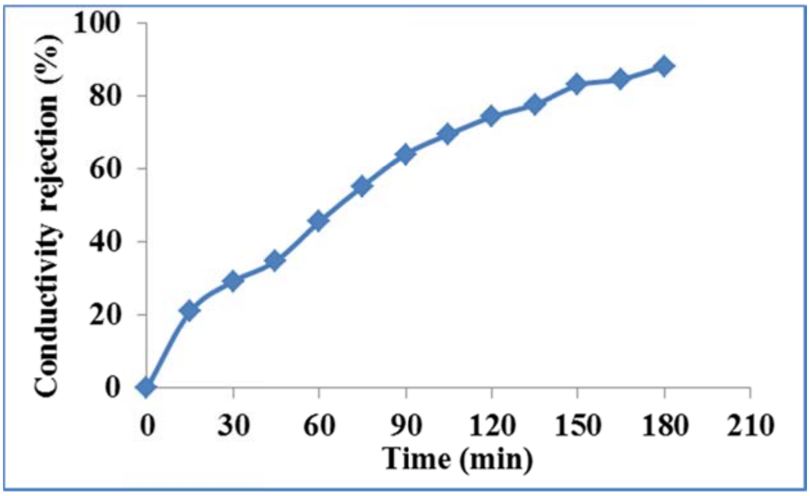

Fig. 4. *Conductivity Rejection vs. Time Plot for ED Diluate during EDI Operation*

Conclusions. Electromembrane separation can be alternative processes for water recovery from the concentrate stream of NF/RO processes employed for the treatment of MBR treated wastewater. This will contribute to wastewater reclamation and reuse, protection of available water resources and thus sustainable development.

Acknowledgements. This study has been supported by TUBITAK (Project numbers: 114M551 and 114Y500). We are grateful to ITOB Organized Industrial Zone for field tests.

References

1. *Mauguin G., Corsin P.* Concentrate and other waste disposals from SWRO plants: characterization and reduction of their environmental impact //Desalination. 2005. V. 182. P. 355-364.
2. *Roberts D.A., Johnston E.L., Knott N.A.* Impacts of desalination plant discharges on the marine environment: A critical review of published studies // Water Res. 2010. V. 44. P. 5117-5128.
3. *Reig M., Casas S., Aladjem C., Valderrama C., Gibert O., Valero F., Centeno C.M., Larrotcha E., Cortina J.L.* Concentration of NaCl from seawater reverse osmosis brines for the chlor-alkali industry by electrodialysis // Desalination. 2014. V. 342. P. 107-117.
4. *Zhang Y., Ghyselbrecht K., Vanherpe R., Meesschaert B., Pinoy L., Van der Bruggen B.* RO concentrate minimization by electrodialysis: Techno-economic analysis and environmental concerns // J. Environ. Manag. 2012. V. 107. P. 28-36.
5. *Turek M., Was J., Dydo P.* Brackish water desalination in RO-single pass EDR system. // Desal. Water Treat. 2009. V. 7. P. 263-266.
6. *Oren Y., Korngold E., Daltrophe N., Messalem R., Volkman Y., Aronov L., Weismann M., Bouriako, N., Glueckstern P., Gilron J.* Pilot studies on high recovery BWRO-EDR for near zero liquid discharge approach // Desalination. 2010. V. 261. P. 321-330.
7. *Praneeth K., Manjunath D., Suresh K. B., Tardio J., Sridhar S.* Economical treatment of reverse osmosis reject of textile industry effluent by electrodialysis–evaporation integrated process, Desalination. 2014. V. 333. P. 82-91.
8. *Jiang C., Wang Y., Zhang Z., Xu T.* Electrodialysis of concentrated brine from RO plant to produce coarse salt and freshwater // J. Membr. Sci. 2014. V. 450. P. 323-330.
9. *Bauer B., Gerner F.J., Strathmann H.* Development of Bipolar Membranes // Desalination. 1988. V. 68. P. 279-292.
10. *Wilhelm F.G.* Bipolar membrane electrodialysis, PhD Thesis, Twente University. 2001.

УДК 66.081

ЗАСТОСУВАННЯ ІОННОГО ОБМІНУ У МЕМБРАННОМУ РОЗДІЛЕННІ ДЛЯ ПЕРЕРОБКИ СТІЧНИХ ВОД З МЕТОЮ ЇХ ПОДАЛЬШОГО ВИКОРИСТАННЯ

N. Kabay[1*], M. Arda[2], S. Bunani[1,2,3], E. Altıok[1], D.İpekçi[1], M.Hacıfazlıoğlu[1], İ.Parlar[1], İ. Yılmaz İpek[1], M. Yüksel[1]

[1] Егейський університет, інженерний факультет, хіміко-технологічний факультет, 35100, Ізмір, Туреччина
*e-mail: nalan.kabay@ege.edu.tr
[2] Егейський університет, факультет природничих наук, хімічний факультет, 35100, Ізмір, Туреччина
[3]Університет Бурунді, факультет природничих наук, хімічний факультет, Бурунді

***Резюме**. Іонообмінні смоли і мембрани можуть бути успішно використані в інтегрованих системах для видалення деяких забруднюючих речовин, для вилучення з води цінних компонентів і для кондиціонування пермеату опріснювальних установок. Іонообмінні мембрани в електродіалізних системах (ЕД) можуть бути використані для подальшої обробки концентрату, який утворюється при перебігу процесів нанофільтрації/зворотного осмосу (НФ/ЗО) і нейтралізації відходів опріснювальних розсолів зворотного осмосу. Для безреагентної трансформації водного сольового розчину у відповідні кислоту та луг розроблено процес ЕД із застосуванням біполярних мембран. Для одержання води із ЗО пермеату, призначеної для живлення систем охолодження, може бути застосовано інший альтернативний метод електродеіонізації (ЕДІ). Дану презентацію сфокусовано на розробку нових ідей для використання іонного обміну в технологічних схемах очищення стічних вод із застосуванням мембранних технологій.*

***Ключові слова**: іонний обмін, опріснення води, мембранний процес, очищення стічних вод*

UDC 544.478-03;546824-31

NOVEL EFFECTIVE ECO-FRIENDLY NANOSIZED HETEROGENEOUS CATALYST SYSTEM FOR REDUCTION OF NITROARENES WITH HYDRAZINE HYDRATE

L.F. Sharanda[1], P.P. Onys'ko[2], Ya.Ya. Khomutnyk[2], L.S. Lysyuk[1],
V.M. Ogenko[1], S.V. Volkov[1]

[1]*Institute of General and Inorganic Chemistry, National Academy of Sciences of Ukraine, 32/34 Palladina ave., Kyiv 03142, Ukraine*
Email lyusharanda@yahoo.com

[2] *Institute of Organic Chemistry, National Academy of Sciences of Ukraine, 5 Murmans'ka str., Kyiv 02660, Ukraine*
email onysko_@ukr.net

Abstract. *Novel nanostructured bi- and three- metallic Ni- or Fe-containing catalytic systems were prepared by incorporation of carbon nanotubes, modified with diamine ligand, in silica matrix with the using sol-gel method. Ni-containing catalysts proved to be effective for conversion of nitroarenes into anilines by transfer hydrogenation method with the use of hydrazine hydrate as hydrogen donor.*

Keywords: *bi-, three-metallic nanomaterials, heterogeneous catalysis, nitroarenes, hydrogenation, hydrazine hydrate*

Introduction. One of the most important principles embodied in the concept of "green chemistry" is application a highly efficient, highly selective catalytic systems [1,2]. Design of highly efficient and selective catalysts will allow efficient use of natural resources and energy and thus contribute to environmental preservation and increasing quality of life in human society. Nanomaterials have emerged as green catalysts that offer new opportunities for the development of a sustainable chemical industry. In the last decades there is a standing interest in development of well-defined catalysts, which may include both metal nanoparticles and a nanomaterial as support. Specific reactivity can be anticipated due to the nanodimension (quantum size effect) that can afford their unique electronic, optical, magnetic and catalytic properties which cannot be achieved with regular, non-nanomaterials that render them very promising candidates for various applications, including catalysis [3-7].

Carbon nanoparticles are well-known materials for the solution of various energy problems and environmental problems. There is a growing interest in the application of carbon nanotubes as supports for catalysts since the nanostructure of these materials offers a unique combination of the electronic properties because of curvature of the graphene sheets and concave (internal) surfaces. For instance, it has been shown that hematites located inside the carbon nanotubes inner cavity are more easily reduced (1073°C) on the support than those on the outer surface (1273°C) [8].

Significant progress has recently been made towards the catalytic applications of bimetallic nanomaterials, which show unique properties that are superior to those of the ordinary materials, and therefore provide an opportunity for the development of novel catalysts with enhanced activity, selectivity, and stability [9-11]. Müslehiddinoğlu et al. [12] developed a Pd−Cu/C catalyst as an alternative to Raney nickel for the highly diastereoselective hydrogenation of imines prepared from prochiral ketones and α-phenylethylamines. Chiral amines were obtained with diastereomeric excess (de) up to 94% using Pd−Cu/C, while conventional Pd−C catalysts afforded only 72% de. Recent research has led to development of efficient a magnetically recyclable Pt/C(Ni) catalysts which consisted of Pt nanoparticles on the surface of flower-like C(Ni) nanocomposite. The Pt/C(Ni) catalysts show higher selectivity towards o-chloroaniline than the Pt/C catalyst due to the synergistic effect between Pt and Ni species. Compared with Raney Ni, the key advantages of this bimetallic Pd-Cu/C system include improved safety, no issues with catalyst suspension, and enhanced operational scalability [13]. However, uses of carbon nanomaterials, as support for metallic nanoparticles have some disadvantage because of tend of carbon to agglomerate due to van der Waals forces.

In the present paper we report on elaboration of $Ni(M)/SiO_2$, $Ni(M_1)/SiO_2$, $Fe(M)/SiO_2$, $Fe(M_1)/SiO_2$ and $Ni(M)/(M_1)/SiO_2$, $Fe(M)/(M_1)/SiO_2$ (M =Pd; M_1 = Ce, Y) catalysts by introduction of carbon nanotubes modified with diamine ligand as metallic nanoparticles stabilizers with subsequent incorporation in silica matrix and their application for the reduction of nitroarenes with hydrazine hydrate by catalytic transfer hydrogenation method.

Experimental. *Preparation of catalysts.* Preparation of catalysts was performed by the sol-gel method. Typically, to a tetraethoxysilane (12.55 mmol) and methyltriethoxysilane (12.55 mmol) were added a water solution of maleic acid (1.39 g, 1.5 mmol), water (27.8 mmol). The reaction mixture was stirred vigorously at 20 °C for 2 hours to complete hydrolysis. To obtained sol were added consecutively with constant stirring $Y(ac)_3$ (0.57 mmol) or $Ce(ac)_3$ (0.36 mmol), cetyltrimethylammonium bromide (2.74 mmol), and multiwalled carbone nanotubes (0.5g) mixed with *N*-[3-(trimethoxysilyl)propyl]-ethylenediamine (3.0 mmol), $Ni(OAc)_2\cdot$(1.35 mmol) or $FeCl_3$ (1.42 mmol), $PdCl_2$ (0.15 mmol). Stirring was continued for additional 1 hour. After completion of sol-gel conversion (2-4 weeks) reaction mass was heated on air (300°C, 4 hrs) and reduced by heating in flow of hydrogen (for Ni- and Fe-based catalysts at 400 and 700°C, 2 hrs, respectively). The resulting solid was crushed and sieved to give 1-3 μm fraction.

Catalytic tests. In a typical procedure, to a mixture of respective nitrobenzene **1** (0.25 mmol) and methanol-water 9:1 (3 mL), were added 10 mol% of the catalyst and 100 μl of 100% hydrazine hydrate. The mixture was stirred at 80 °C for a given time. The mixture was quantitatively analyzed by liquid chromatography (HPLC). In preparative procedures, after completion of the reaction (1-3 h, monitored by TLC), the catalyst was filtered off; the filtrate was concentrated under reduced pressure. The residue was subjected to silica-gel column chromatography using petroleum ether-ethyl acetate as an eluent to give analytically pure product.

Results and discussion. *X-ray Diffraction Spectra.* The X-ray diffraction (XRD) patterns were obtained in a diffractometer (DRON-3M), using Cu-K_α mono-chromatized radiation (λ=1.54178Å).

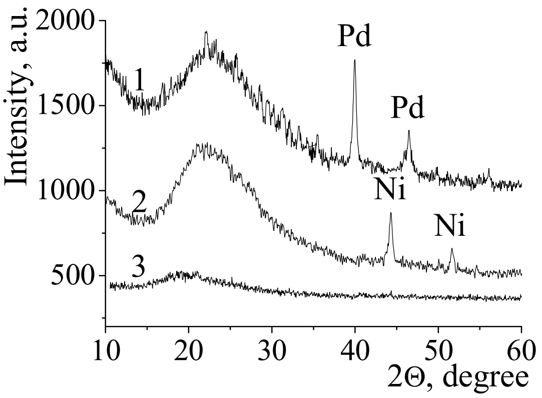

Fig. 1. *XRD Patterns of Pd/SiO_2/CNT (1), Ni/SiO_2/CNT (2), PdNi/SiO_2/CNT (3) Samples Calcined at 400 °C.*

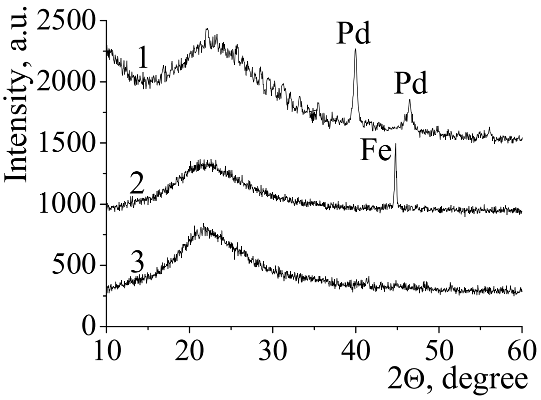

Fig. 2. *XRD Patterns of Pd/SiO_2/CNT (1), Fe/SiO_2/CNT (2), PdFe/SiO_2/CNT (3) Samples Calcined at 700 °C.*

X-ray diffractograms of Pd/SiO_2/CNT (1) sample arrow intense diffraction maxima at 2θ = 39.95°, 46.5° and 68.2°corresponding to the cubic structure of metallic Pd (JCPDS card: 05-0681) (fig. 1 (1)). Further, it is observed that for Ni/SiO_2/CNT sample ((Fig. 1 (2)) display the three characteristic peaks for the lines of the cubic structure of metallic nickel (JCPDS card: 99-101-3059).

It was interesting that for bimetallic PdNi/SiO_2/CNT catalyst intense peaks of pure Ni or Pd has not been observed in XRD patterns. As can be seen in fig.1(3), the diffraction patterns of catalysts characterized by broad diffuse maximum with low intensive peak in the region 2θ = 41.0° indicating on the formation of Pd_xNi_y bimetallic particles or cluster. Besides a significant decrease in intensity of the diffraction peaks may be associated with the formation of the amorphous and/or crystalline nickel or palladium particles with a size <10 nm [14].

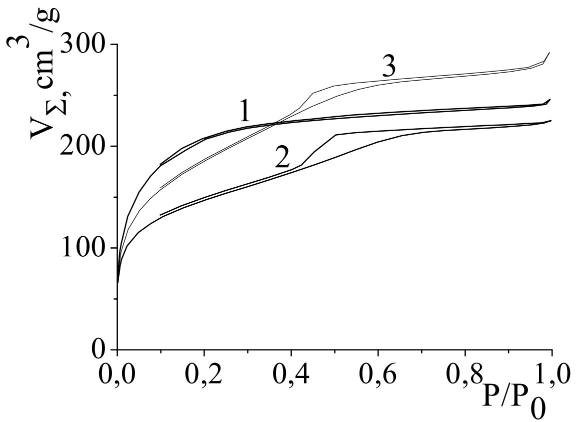

Fig. 3. *Nitrogen Adsorption-Desorption Isotherms for Pd/SiO_2/CNT (1), Ni/SiO_2/CNT (2), PdNi/SiO_2/CNT (3) Samples Calcined at 400°C.*

Intense peaks observed at 2θ = 44.8° correspond to the iron metallic particles (fig.2(2)). It may be also noted that addition of Pd in Fe/SiO_2/CNT catalyst as in the case for the Ni/SiO_2/CNT sample changes the XRD significantly (fig.2(3)): the diffraction patterns of catalysts characterized low intensive peaks at 2θ = 41.2° and 2θ = 44.8°, that can due to formation of Pd_xFei_y bimetallic particles or/and iron and palladium nanoparticles.

BET specific surface area determinations were made using N_2 gas adsorption/desorption an Quantachrome ASIQwin^{TM} micromeitics apparatus. Figure 3(1) presents the adsorption-desorption isotherm N_2 of Pd/SiO_2/CNT sample. As can be seen the hysteresis loop is slightly visible and the isotherm can be assigned to supermicropores. The shape of adsorption-desorption isotherm of Ni-containing catalysts shows biporous (micro- and mesoporous) structure and isotherm adsorption IV+I type with the shape hysteresis loop of H2 type inherent for materials with mesoporous of bottle type, according to the IUPAC classification. The surface areas, total pore volums and average pore radius for all catalysts are shown in Table 1. It shows, that Ni-containing catalysts have high surface area (527-768 m^2/g) and pore volume (V_{total}=0.348-0.476 cm^3/g; V_{mic}=0.206-0.247 cm^3/g) are nearly same. In contrast, the Fe-containing catalysts shows a significantly decreased surface area (52-258 m^2/g) and pore volume (V_{total}=0.048-0.219 cm^3/g; V_{mic}=0.017-0.079 cm^3/g).

Table 1: Surface and Porosity Characteristic of Catalysts

Catalyst	**Surface area, m^2/g**		**Pore volume, cm^3/g**		**Pore radius, Å**	
	S_{BET}	S_{DFT}	V_{total}	$V_{mic, DR}$	R_{DR}	$R_{cep.}$
Ni/CNT/SiO_2	595	530	0.401	0.218	8.90	13.47
Pd/CNT/SiO_2	768	585	0.380	0.247	9.26	9.912
Pd/Ni/CNT/SiO_2	662	525	0.452	0.229	9.34	13.65
Y-Ni/CNT/SiO_2	694	597	0.476	0.242	8.77	13.72
Pd-Y-Ni/CNT/SiO_2	527	518	0.348	0.206	9.11	13.22
Fe/CNT/SiO_2	258	201	0.219	0.079	8.13	16.99
Pd-Fe/CNT/SiO_2	54	60	0.160	0.019	8.77	58.95
Y-Fe/CNT/SiO_2	169	155	0.112	0.056	7.89	13.26
Pd-Y-Fe/CNT/SiO_2	118	118	0.082	0.043	7.93	13.77
Ce-Fe/CNT/SiO_2	141	127	0.112	0.047	8.02	15.84
Pd-Ce-Fe/CNT/SiO_2	52	42	0.048	0.017	8.19	18.31

To ensure the efficiency of our catalytic system as a general methodology for catalytic transfer hydrogenation reduction of nitrobenzenes we subjected a series of substituted nitrobenzenes **1** (Scheme 1) to reduction under the optimized conditions. Excellent results for Ni-containing catalysts were obtained in all cases. For instance, the results are summarized in Table 2 for Pd/Ni/CNT/SiO_2 catalyst.

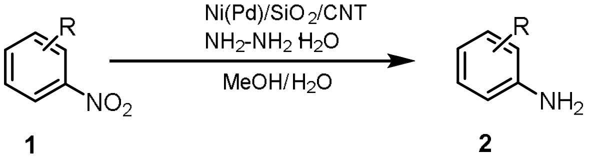

R = 3-CF_3 (**a**), H (b), 3-NH_2 (**c**), 3-OH (**d**), 4-NH_2 (**e**), 4-OH (**f**)

Scheme 1

The isolated yields of substituted anilines 1a-f are close to quantitative. As shown in Table 2, nitrobenzenes with electron-donating and electron-withdrawing groups underwent successful catalytic transfer hydrogenation reduction with hydrazine hydrate to afford substituted anilines 1a-f with almost quantitative isolated yields. The catalyst is compatible with functional groups, such as amino and hydroxy. Therefore our approach can be regarded as general methodology for reduction of nitrobenzenes. Fe/CNT/SiO_2 and Pd-Fe/CNT/SiO_2 catalysts shows a slightly less activity in the reduction of nitrobenzenes with hydrazine hydrate. Important advantage of elaborated nanostructured catalysts is the possibility to reuse them without essential loss in activity. Simple workup of reaction mixture with easy mechanical (filtration, centrifugation) or magnetic separation of catalyst after completion of the process is very convenient and advantageous from experimental point of view.

Table 2. Catalytic Transfer Hydrogenation Reduction of Substituted Nitrobenzenes **1**[a]

Entry	Substrate	Reaction time (h)	Yield of 2,%
1	1a	1	99
2	1b	1	99
3	1c	2	97
4	1d	2	97
5	1e	1.5	95
6	1f	1.5	96

[a] Conditions: **1**, 25 mmol; NiPd/SiO_2/CNT–ED2, 10 mol%; $N_2H_4 \cdot H_2O$, 5 equiv; MeOH–H_2O 9:1, 30 mL; 80 °C

Conclusions. In summary, we have developed a highly efficient, eco-friendly Ni- or Fe-containing nano-structured catalysts for the CTH reduction of nitrobenzenes into corresponding anilines with hydrazine hydrate.

Acknowledgements. The work was supported by the National Academy of Sciences of Ukraine in the framework of target comprehensive program for the Basic Research "Fundamentals for creating new substances and materials" (grant No. 10-16).

References

1. *Anastas, P. T., Warner, J. C.* Green Chemistry: Theory and Practice; Oxford University Press: New York, 1998.
2. *Beletskaya I.P., Kustov L.M.* Catalysis as an important tool of green chemistry // *Usp. Khim.* 2010. V. 79. P. 493–515.
3. *Astruc D.* Nanoparticles and Catalysis. Weinheim: Wiley-VCH Verlag GmbH & Co. KGaA, 2008.
4. *Bell A.T.* The impact of nanoscience on heterogeneous catalysis. // Science. 2003. V. 299. P. 1688–1691.
5. *Zaera, F.* Nanostructured Materials for Applications in Heterogeneous Catalysis. // Chem. Soc. Rev. 2013, V. 42. P. 2746–2762.
6. *Campbell C.T., Parker S.C., Starr D.E.* The effect of size –dependent nanoparticles energetic on catalyst Sintering. // Scince. 2002. V.29. P. 811–814.

7. *Koch, C. C.,* Ed. Nanostructured Materials, Processing, Properties and Applications; Noyes Publications: Norwich, New York, 2002.
8. *Chen W., Pan X., Bao X.* Tuning of Redox Properties of Iron and Iron Oxides via Encapsulation within Carbon Nanotubes // J. Am. Chem. Soc., 2007. V. 129 (23). P. 7421–7426.
9. *Sarno M., Ponticorvo E. , Cirillo C., Ciambelli P.* Magnetic Nanoparticles for PAHs Solid Phase Extraction // Chem. Eng. Trans. 2016. V. 47. P. 313–318.
10. *Gan N., Zhang J., Lin Sh., Long N., Li T. and Cao Yu.* A Novel Magnetic Graphene Oxide Composite Absorbent for Removing Trace Residues of Polybrominated Diphenyl Ethers in Water // Materials 2014**.** V. 7. P. 6028–6044.
11. *Changotra, A.; Gupta, R.; Paul, S.* Pd and Au Immobilized On Amine-Functionalized Magnetite Nanoparticles: A Novel and Highly Active Bimetallic Catalyst for Hydrogenation. // Inter. J. of Sci. and Res. (IJSR), 2014. V. *3(5).* P. 453–458.
12. Jale Müslehiddinoğlu, Jun Li, Srinivas Tummala and Rajendra Deshpande. Highly Diastereoselective Hydrogenation of Imines by a Bimetallic Pd−Cu Heterogeneous Catalyst // Org. Process Res. Dev. 2010. V. 14 (4). P. 890–894.
13. *Xie,Y., Xiao,N., Yu, C., Qiu, J.* Magnetically recyclable Pt/C(Ni) nanocatalysts with improved selectivity for hydrogenation of o-chloronitrobenzene. Catal. Commun., 2012, V. *28*, P. 69–72.
14. *Alonso, F.; Riente, P.; Sirvent, J. A.; Yus, M.* Nickel Nanoparticles in Hydrogen-Transfer Reductions: Characterisation and Nature of the Catalyst. Appl. Catal. A Gen. 2010. V. 378. P. 42–51.

УДК 544.478-03;546824-31

НОВІ, ЕФЕКТИВНІ, ЕКОЛОГІЧНО-БЕЗПЕЧНІ, НАНОРОЗМІРНІ ГЕТЕРОГЕННІ КАТАЛІТИЧНІ СИСТЕМИ ДЛЯ ВІДНОВЛЕННЯ НІТРОАРЕНІВ ГІДРАЗИН ГІДРАТОМ

Л.Ф. Шаранда[1], П.П Онисько[2], Я.Я. Хомутник[2], Л.С. Лисюк[1],
В.М. Огенко[1], С.В. Волков[1]

[1]Інститут загальної та неорганічної хімії ім. В.І. Вернадського НАН України
проспект Академіка Палладіна, 32/34, Київ 03142, Україна
Email lyusharanda@yahoo.com
[2]Інститут органічної хімії НАН України, вул. Мурманська, 5, Київ 02660, Україна
email onysko_@ukr.net

Резюме. *Синтезовано нові наноструктуровані бі-, триметалічні Ni- або Fe- вмісні каталітичні системи шляхом введення модифікованих аміногрупами вуглецевих нанотрубок в кремнеземну матрицю з використанням золь-гель методу. Ni-вмісні каталізатори виявилися ефективними в реакціях перетворення нітроаренів до відповідних анілінів каталітичним гідруванням з використанням гідразин гідрату як джерела водню.*

Ключові слова: *бі-, триметалічні наноматеріали, гетерогенний каталізатор, нітроарени, гідрування, гідразин гідрат.*

UDC 544.726.3 + 546.824-31 + 546.714-31

LITHIUM-SELECTIVE COMPOSITE MATERIALS BASED ON TiO_2 AND MnO_2

L.M. Rozhdestvenska, M.O. Chaban, V.N. Belyakov
V.I. Vernadskii Institute of General and Inorganic chemistry of National Academy of Sciences of Ukraine, 32/24 Paladin av., Kyiv 03142, Ukraine
e-mail: ludar777@ukr.net

Abstract. *Ion-exchange materials based on titanium dioxide-manganese dioxide composite were synthesized by template method. It was proved that sorption characteristics of the obtained materials depend of rate of heat treatment during the synthesis. Higher temperatures promote agglomeration of sorbent and decrease in its kinetic characteristics. But more lithium-selective sorption centers are formed and the selectivity of sorption increases.*

Keywords: *titanium dioxide, manganese dioxide, lithium, ion exchange selectivity*

Introduction. The need of lithium recovery from waste and search of new sources of this element (including brines and ocean water) causes the need to create new sorption materials for targeted removal of lithium ions from liquids. The basic requirements for such materials are the high selectivity and absorption rate. Known lithium-selective ion exchangers are spinels based on manganese oxide [1]. The synthesis of lithium manganese spinels is traditionally carried out by solid phase sintering of $LiCO_3$ with Mn_3O_4 [2], or LiOH with Mn_3O_4 [3]. The main reason that slows widespread commercial use of these materials is a significant loss of manganese in the process of extracting lithium ions with acids, low particle size and low absorption rate.

To improve the abovementioned characteristics selective introduction of lithium-manganese spinel into matrix of more resistant material that also exhibits absorption capacity on lithium iones was proposed. Ion exchanger based on hydrated titanium dioxide can be considered as such inorganic matrix [4]. This material has high sorption capacity, resistance to aggressive media, and it can be obtained in the form of pellets. In the heat treatment of these materials take on ion-sieve properties because of aimed structuring during condensation processes

Experimental. Synthesis of titanium-manganese composite sorbents was performed through a redox reaction between titanium chloride and potassium permanganate in aqueous solution. In this process solid potassium permanganate was gradually added to 1 M solution of titanium chloride until a molar ratio $TiCl_4$: $KMnO_4$ = 1:1, 1:2, 2:1. Obtained gel material was treated with 12% aqueous ammonia, washed with deionized water and dried in air. Upon that the granulated sorbent was treated with 1 M LiOH solution for 48 hours with the volume ratio of sorbent to solution 1:100, washed from the hydroxide with excess of water, air dried, heat treated at various temperatures (in the range of 300-700 ^{0}C), then washed with 1 M HNO_3 solution, and dried in air.

X-ray studies of samples were conducted on diffractometer DRON-2 using CuK_{α}- radiation. Scanning Electron Microscope Tescan Mira 3 LMU was used to determine the structure of the materials and the elemental composition (Ti, Mn).

Study of Li^+ ions selective absorption was carried from solutions containing different amounts of LiCl with 0.5 M NaCl as background in static and dynamic conditions. Sorption kinetics was studied using a limited volume method with sample fractions of 0.16-0.25 mm. After certain time the contact of the solution with the ion exchanger was interrupted, adsorbed ions where desorbed with acid, and the eluate was analyzed by atomic absorption method.

Results and discussion. The synthesized titanium-manganese composite ionites, unlike obtained by solid-phase sintering lithium-manganese spinels, are mechanically stable granules with an average size 0.25-0.5 mm and metallic luster (Figure 1 a). Increasing the content of manganese in the final product causes deterioration of mechanical properties - significantly increases the content of fine fractions.

The results of SEM study show the presence of nanoscale material particles that are agglomerated during the heat treatment process. The sorbent treated at higher temperature is characterized by tighter structure of the aggregates due to structural rebuild with formation of spinel structure.

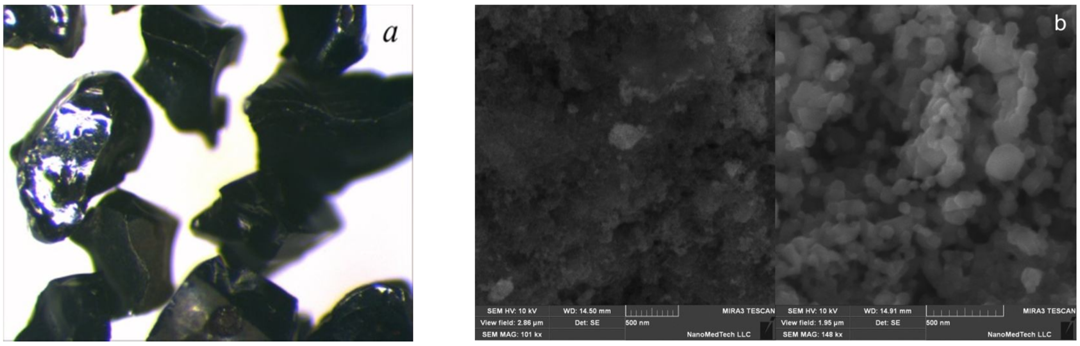

Fig. 1. *Microphoto (a) and SEM Photos (b) of Ion Exchange Materials Based on TiO_2 - MnO_2, Calcinated at 500 ^oC (on the Left), 700 ^oC (on the Right)*

Heat treatment promotes strengthening of sorbents, accompanied by shrinkage and compaction of oxyhydrate materials. In the temperature range 100-400 ^oC samples are X-ray amorphous. It is known that at 400-500 ^oC in titanium dioxide anatase structure is formed that transfers to the form of rutile at temperatures above 700 ^oC [5]. Along with dehydration, crystallization of samples and forming of lithium-containing phase (space group Fd3m) occurs. The presence of manganese dioxide in titanium dioxide leads to a shift of polymorphic transformations to high temperatures. According to X-ray analysis (Table 1) for a sample calcined at 500 ˚C, rutile phase is formed and lithium-manganese-titanium spinel $(Li_{0.989}Mn_{0.01})[Mn_{0.876}\ Ti_{0.124}]O_4$. At calcination temperature of 700 ^oC the largest reflexes correspond to rutile and lithium-manganese-titanium spinel $(LiMn_{1.6})Ti_{0.4}O_4$. Increasing calcination temperature increases content of lithium-containing phase and, therefore, the total content of lithium ions. Thus there is an increase in the crystal lattice constant (a), unit cell volume (V), and average particle size, confirming the structural data, according to which with the increase of calcination temperature particles consolidate and agglomerated during the heat treatment process.

Table 1: Composition of Lithium-Containing Samples of TiO_2-MnO_2 According to X-ray Analysis

Material	TiO_2-MnO_2 (500 ˚C)		TiO_2-MnO_2 (700 ˚C)	
Composition	TiO_2	$(Li_{0.989}Mn_{0.01})[Mn_{0.876}Ti_{0.124}]O_4$	TiO_2	$Li(Mn_{0,8}Ti_{0.2})_2O_4$
Content, %	78,2	21.8	59,3	40,7
Li, mmol/g	-	2,02	-	2,28
a	4.6396	8.1868	4.5935	8.2878
c	2.9575	-	2.9592	
V	63.665	548.701	62.440	569.276
Average particle size, nm	20	9	34	26

Ion exchange on ionites of MnO_2 type is caused by OH groups, which are distributed in the volume of substance: $(MnO_x)_2OH + Li^+ = (MnO_x)_2OLi + H^+$. Oxyhydrate sorbents of TiO_2 type are weakly acidic cation exchangers and exchange capacity depends on solution acidity as: $TiO_m(OH)_{p-1}O^-H^+ + Li^+ \leftrightarrow TiO_m(OH)_{p-1}OLi + H^+$. Thus, for composite TiO_2-MnO_2 similar dependence is observed - absorption capacity increases in an alkaline environment.

Sorption of sodium ions caused only by dissociation of ion exchange groups at higher pH, and lithium ions are also adsorbed due to localization in octahedral cavities that are unavailable for sodium ions. Selectivity of lithium ions adsorption in the presence of background ions (Li/Na = 1/25) increases with treatment temperature growth due to large number of selective sorption centers formed, while the total ion exchange capacity of the material decreases. Reduced capacity of the sorbent with increasing synthesis temperature is explained by sintering of the material and increasing amount of non-exchange lithium left in the bulk of the sorbent (Table 2).

The efficiency of composite materials use was studied with ion exchange in dynamic conditions from solution containing both Na^+ and Li^+ with concentration ratio of 50:1 respectively. This proved that synthetized material TiO_2-MnO_2 500 ^oC is extremely selective to sorption of lithium ions as after the experiment concentration ratio of Na^+/Li^+ in the ion exchanger was 0,55:1.

Table 2: Sorption Properties of TiO_2-MnO_2 Composite Materials

Ion exchanger	A_{Li}, mmol/g	Ks	Kd	D_{Li}, m^2/s.
TiO_2-MnO_2 500 °C	1,352	40	216	$1.5*10^{-12}$
TiO_2-MnO_2 600 °C	1,187	684	180	$3.9*10^{-13}$
TiO_2-MnO_2 700 °C	0,961	990	136	$5.8*10^{-14}$

A_{Li} – adsorption capacity , Ks^* - selectivity coefficient, Kd – distribution coefficient , D_{Li} – diffusion coefficient (all the values are obtained at pH=8)

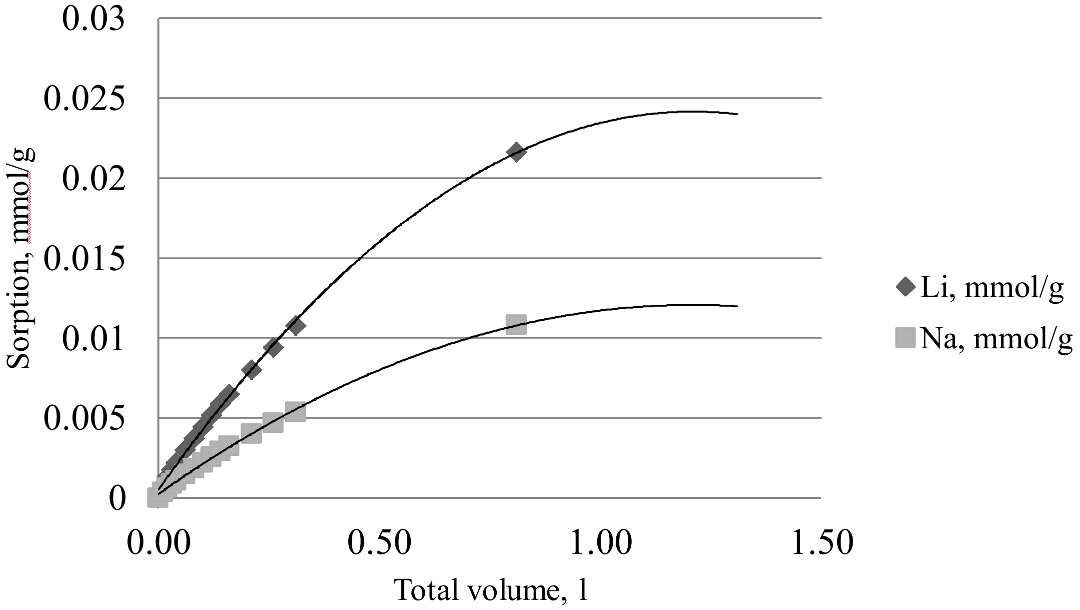

Fig. 2. *Ion Exchange from Mixed Solution of LiCl and NaCl under Dynamic Conditions*

Conclusions. Although increasing treatment temperature increases the synthesis of the total content of lithium ions, but this lithium is not available for ion exchange after washing of applicative ion. Thus optimal conditions to obtain ion exchange materials based on TiO_2-MnO_2 is thermal modification of lithium-substituted samples at 500-600 °C and equimolar ratio of the components in which the selectivity and rate of absorption are combined. . This synthesis method allows us to obtain mesoporous materials with high distribution coefficients of lithium. Diffusion coefficients calculated for ionites synthesized at 500-600 °C correlate with the values of diffusion coefficients in the lithium compounds $LiM_yMn_{2-y}O_4$ with spinel structure [6].

References

1. *Vol'khin V., Pogodina O., Leont'eva G.* Nonstoichiometric compounds based on manganese (III, IV) oxides with the birnessite structure// Russian journal of general chemistry. 2002. V.72. No. 2. P. 173-177.
2. *Vol'khin V., Pogodina O., Leont'eva G.* Nonstoichiometric compounds based on manganese (III, IV) oxides with the birnessite structure // Russ. J. Gen. Chem. 2002.V.72. P. 173-177.
3. *Leont'eva G. V.* Synthesis of lithium-manganese spinel for inorganic ion-exchange materials // J. Inorg. Chem.(in Russian). 1988. V. 33. P. 2196-2199.
4. *Kitajou A., Suzuki T., Nishihama S., Yoshizuka K.* Selective recovery of lithium from seawater using a novel MnO_2 type adsorbent II-Enhancement of lithium ion selectivity of the adsorbent // Ars, Sep. Acta 2003. V. 2. P. 97-106.
5. *Hodyashev N.B.* Ion-exchange properties and structural characteristics of the nano-sized lithium-cation phase based on titanium dioxide // Chemistry and Chemical Engineering (in Russian). 2007. V.50. P. 112-115.
6. *Khazin L.G.* Titanium dioxide (in Russian), Leningrad,1970.
7. *Churikov A.V., Sychev V.O.* Determination of the diffusion coefficient of lithium in the spinel $LiM_YMn_{2-Y}O_4$ by galvanostatic intermittent titration // Electrochimiya (in Russian). 2012. V.48. P. 120-126.

UDC 544.726.3 + 546.824-31 + 546.714-31

ЛІТІЙ-СЕЛЕКТИВНІ КОМПОЗИТИ НА ОСНОВІ ОКСИДІВ TiO_2-MnO_2

Л.М. Рождественська, М.О. Чабан, В.Н. Беляков
Інститут загальної та неорганічної хімії ім. В.І. Вернадського Національної академії наук України, пр. акад. Палладіна, 32/34, Київ 03680, Україна
e-mail: ludar777@ukr.net

Резюме. *Синтезовані комопозиційні іонообмінні матеріали на основі гідратованих оксидів титану та мангану темплатним методом. Показано, що сорбційні характеристики отриманих матеріалів визначаються умовами термічної обробки на стадії синтезу. Вищі температури синтезу призводять до агломерації сорбента та зниження його кінетичних характеристик, але водночас утворюється більша кількість літій-селективних центрів і вибірковість сорбції зростає.*

Ключові слова*: діоксид титану, діоксид мангану, літій, іонообмінна селективніть*

UDC [628.161.2:546.19] 66.081.63

REMOVAL OF As(V) COMPOUNDS FROM WATER USING OPMN-P NANOFILTRATION MEMBRANE

L. O. Melnyk

A.V. Dumansky Institute of Colloid and Water Chemistry of NAS of Ukraine,
Vernadsky blvd., 42, 03142, Kyiv, Ukraine
e-mail: lumel2903@gmail.com

Abstract. *High efficiency of removal of As(V) compounds from water with nanofiltration technique was shown. OPMN-P nanofiltration membrane was involved to investigations, which were performed within a wide range of pH, concentration of background electrolyte, operating pressure and permeate recovery (25-90%). The rejection has been found to reach 93-98%. As shown, the membrane is promising for water purification from arsenic, the maximal contaminant level is 10 µg/dm^3. As(III) has to be oxidized preliminarily down to As (V) using photocatalysis.*

Keywords: *arsenate, removal, drinking water, nanofiltration, membrane.*

Introduction. Arsenic compounds are often found in natural waters, owing to both natural factors and human impact. However, the content of As-containing ions in water sources can be higher than the maximal allowable concentration. Thus, the development of efficient and low-cost methods for the removal of these toxic impurities is an important task.

It has been shown earlier, that reverse osmosis (RO) involving ESPA-1 membrane provides high efficiency of water purification from As(V) compounds [1].

Since the operating pressure of nanofiltration (NF) is lower than that for RO, the energy costs of NF is 21% lower. Additionally, higher output at lower operating pressure is achieved. Thus, a possibility of NF application to removal of As(V) compounds from water solutions has to be considered. The purpose of this work was to research the NF process, which involves OPMN-P nanofiltration membrane (Vladipor, RF). This type of membranes is available in the market, they are often used in Ukraine.

Experimental. The effect of pressure, permeate recovery, temperature, pH and composition of the feeding solution on As(V) rejection was studied. OPMN-P membrane was used. Model solutions contained 100 µg/dm^3 As(V), 1-3 g/dm^3 NaCl (1-3 g/dm^3 Na_2SO_4). The solution pH was varied.

Results and discussion. As shown from Table 1, no significant effect of operating pressure within the range of 0.5-1.5 MPa on As(V) removal can be found, when the temperature was kept at 15-16^o C. The rejection coefficient, *R*, decreased from 97.8 to 97.1%, the permeate recovery was 90 %.

Table 1. Removal of As(V) Compounds Using OPMN-P Nanofiltration Membrane at Different Operating Pressure and $T = 15\text{-}16^{\circ}$ C. Modeling Solution Contained Initially100 μg/dm^3 As(V), 1 g/dm^3 NaCl, the pH Was 7.5

Permeate recovery, %	**0.5 MPa**			**1.0 MPa**			**1.5 MPa**		
	$C_{\text{As,perm}}$, μg/dm^3	R_{As}, %	J, dm^3/(m^2·h)	$C_{\text{As,perm}}$, μg/dm^3	R_{As}, %	J, dm^3/(m^2·h)	$C_{\text{As,perm}}$, μg/dm^3	R_{As}, %	J, dm^3/(m^2·h)
25	1.5	98.5	15.2	-	-	28.5	2.6	97.4	40.5
50	1.8	98.2	15.1	1.8	98.2	27.8	2.5	97.5	39.8
75	1.6	98.4	15.1	1.9	98.1	27.7	2.4	97.6	39.8
90	2.2	97.8	14.9	2.3	97.7	27.1	2.9	97.1	39.1

However, the rejection coefficient for As(V) reduces significantly, when the pressure increases to 1,5 MPa at 20-22° C (Table 2). This may be caused by growing influence of concentration polarization on the process. When the temperature increases, the output (J) of the OPMN-P membrane shows a growth (Tables 1, 2).

Table 2 Removal of As(V) Compounds Using OPMN-P Nanofiltration Membrane at 20-22°C and under Different Pressure. Modeling Solution Contained Initially 100 μg/dm^3 As(V), 1 g/dm^3 NaCl, the pH Was 7.8

Permeate recovery, %	**0,75 MPa**			**1,0 MPa**			**1,5 MPa**		
	$C_{\text{As, perm}}$, μg/dm^3	R_{As}, %	J, dm^3 (m^2·h)	$C_{\text{As, perm}}$, μg/dm^3	R_{As}, %	J, dm^3/(m^2·h)	$C_{\text{As.perm}}$, μg/dm^3	R_{As}, %	J, dm^3/(m^2·h)
25	1.2	98.8	24.5	1.7	98.3	31.7	14.0	86.0	40.9
50	1.5	98.5	24.3	1.9	98.1	31.7	16.5	83.5	40.6
75	2.5	97.5	24.3	3.2	96.8	31.7	17.2	82.8	40.5
90	2.8	97.2	24.1	3.3	96.7	31.2	18.9	81.1	40.5

The effect of increase of the permeate recovery from 25 to 90% on As(V) removal is inconsiderable. Nevertheless, the rejection of sodium chloride decreases from 55.1 to 30.4% ($P = 1.0$ MPa, $T = 22$ °C).

Table 3 shows that the change of the pH within the range of 4.0-9.3 does not affect As(V) rejection. Slightly higher rejection of arsenate (99,7-99,8%) at pH of 4.0-4.9 is probably due to lower temperature of the process (the research at these pH values was performed at 12-13° C, the separation processes at the pH of 5.9-9.3 was carried out at 15-16°C).

According to [2], As(V) rejection by NF270 and TFC-SR-2 nanofiltration membranes increases dramatically (from 51-54% to 89%) with the pH growth from 4.0 to 6.7. Further increasing of the pH (up to pH 10) causes insignificant change of As(V) rejection (91-93%). These data are in agreement with of [3], where the similar effect is reported for N30F and NE90 nanofiltration membranes. It is noted in [2], that the similar dependence of As(V) rejection on pH is observed only for the membrane with a relatively large pore sizes. These membranes reject As mainly according to the charge repulsion mechanism.

When the solution pH increases, monovalent arsenate anions transforms into divalent one (a sharp transition at pH 6-7), which causes the improvement of arsenic rejection by negatively charged membranes. Membranes with much smaller pore sizes (e.g, NF70 membrane) reject As mainly due to the steric factor (size exclusion), thus, with the change of pH the As(V) rejection of such membranes virtually remains the same [2].

Table 3: Effect of pH and Permeate Recovery on Rejection of As(V) compounds with OPMN-P Nanofiltration Membrane. $P = 1.0$ MPa, $T = 12\text{-}16^{o}$C. Modeling Solution Contained 100 µg/dm^3 As(V) and 1 g/dm^3 NaCl

pH	**Permeate recovery, %**							
	25		50		75		90	
	$C_{\text{As,perm}}$, µg/dm^3	R_{As}, %	$C_{\text{As, perm}}$, µg/dm^3	R_{As}, %	$C_{\text{As, perm}}$, µg/dm^3	R_{As}, %	$C_{\text{As, perm}}$, µg/dm^3	R_{As}, %
4.0	0.3	99.7	0.3	99.7	0.4	99.6	-	-
4.9	0.2	99.8	0.5	99.5	0.5	99.5	1.0	99.0
5.9	1.7	98.3	2.1	97.9	2.4	97.6	2.8	97.2
6.9	1.8	98.2	1.9	98.1	2.0	98.0	2.3	97.7
9.3	2.4	97.6	2.5	97.5	2.6	97.4	2.8	97.2

Comparison of the results obtained by the author and other researchers shows domination of steric factor for NF of As(V)-containing solutions using OPMN-P membrane. Nature of background electrolyte (NaCl or Na_2SO_4) and increasing in its concentrations up to 3 g/dm^3 slightly affect As(V) rejection.

The results of NF treatment of ground water are shown in Table. 4. As(V) compounds (Na_3AsO_4) were added preliminarily to natural water.

Table 4. Rejection of As(V) Compounds with OPMN-P Nanofiltration Membrane. Ground Water Is from Artesian Well (Kyiv, Irpenska str., 76) was treated. P=1 MPa, T=16-17° C.

Permeate recovery, %	**$C_{\text{As(V),feed}}$, µg/dm^3**							
	116				220			
	$C_{\text{As, perm}}$, µg/dm^3	R_{As}, %	R_{salt}, %	J, dm^3/(m^2·h)	$C_{\text{As, perm}}$, µg/dm^3	R_{As}, %	R_{salt}, %	J, dm^3/(m^2·h)
25	4.9	95.8	85.6	84.3	4.1	98.1	85.4	75.7
50	6.5	94.4	84.3	82.4	6.9	96.9	83.8	74.2
75	7.0	94.0	81.9	79.8	8.4	96.2	81.7	74.1
90	7.7	93.3	79.7	77.8	9.4	95.7	79.3	72.9

As seen from Table 4, the rejection coefficient of As(V) compounds is 93.3 and 95.7%, when the concentration of these components in the feeding solution was 116 and 220 mg/dm^3 respectively (the permeate recovery was 90%). This gives a possibility to obtain permeate, in which the content of As corresponds to standards for drinking water.

Conclusions. NF processes, which involve OPMN-P membrane allow us to reach high efficiency of removal of As(V) compounds from water. The process can be performed within a wide ranges of the solution pH, concentration of background electrolyte and pressure at 90% permeate recovery. The membrane is promising for purification of water from arsenic compounds (including the As (III) with its previous photocatalytic oxidation [1]), concentration of the toxic component decreases down to the maximal allowable level of 10 μg/dm^3.

References

1. *Babak Yu.V., Melnik L.A., Goncharuk V.V.* Removal of arsenic compounds from natural waters using a hybrid system (photocatalysis-reverse osmosis) // Journal of Water Chemistry and Technology. 2014. Volume 36. P. 296-302.
2. *Fang J., Deng B.* Arsenic rejection by nanofiltration membranes: effect of operating parameters and model analysis // Environmental Engineering Science. 2014. V. 31. P. 495-506.
3. *Nguyen C.M., Bang S., Cho J., Kim K.-W.* Performance and mechanism of arsenic removal from water by a nanofiltration membrane // Desalination. 2009. V. 245. P. 82-94.

УДК [628.161.2:546.19] 66.081.63

ВИДАЛЕННЯ As(V) ІЗ ВОДИ МЕТОДОМ НАНОФІЛЬТРАЦІЇ З ВИКОРИСТАННЯМ МЕМБРАНИ ОПМН-П

Мельник Л.О.
Інститут колоїдної хімії та хімії води ім. А.В. Думанського НАН України,
просп. Вернадського, 42, 13142Б м. Київ, Україна
E-mail: lumel2903@gmail.com

Резюме. *Показано високу ефективність затримки сполук As(V) нанофільтраційною мембраною ОПМН-П в широкому діапазоні pH розчину, концентрації фонового електроліту, робочого тиску при ступені відбору пермеату до 90%. Вказана мембрана є перспективною для очистки води від сполук арсену до гранично допустимої концентрації 10 мкг/дм^3 (в тому числі і від As(III)) при попередньому його фотокаталітичному окисненні.*

Ключові слова: *арсенати, видалення, питна вода, нанофільтрація, мембрана*

UDC 66.081.63

APPLICATION OF MEMBRANE FILTRATION PROCESSES IN WHEY PROCESSING

İ. Özdemir[1,2], Y.A. Jarma[1], E. Altıok[1], N. Kabay[1*], S. Ötleş[2*], M.Yüksel[1]
[1]*Ege University, Faculty of Engineering, Chemical Engineering Department, Izmir/Bornova Turkey*
[2]*Ege University, Faculty of Engineering, Food Engineering Department, Izmir/Bornova Turkey*
e-mail: nalan.kabay@ege.edu.tr, semih.otles@ege.edu.tr

Abstract. *Membrane separation techniques are extensively used in the dairy industry, especially in cheese whey processing. In this study, the potential of an integrated membrane process based on ultrafiltration (UF) and nanofiltration (NF) was investigated for fractionation of whey components, such as proteins, fat, lactose and mineral salts.*

Keywords: *whey, nanofiltration, ultrafiltration, integrated membrane process, whey processing*

Introduction. Whey is the main by-product obtained from cheese production. It contains high concentrations of organic matters, mainly proteins and lactose, and also mineral salts. Even some applications of whey already exist, it is still considered as a waste product of the cheese industry. Nowadays, the utilization of minor whey components represents a big challenge for whey processing. Usually, the pre-treated whey is discharged into sewer together with the other liquids effluents of the dairy industry. However, the increasingly stringent legal standards for wastewaters in contrast with the high COD and BOD of whey have entailed a change in the approach to whey management [1,2]. Whey also contains minerals such as sodium, potassium and chloride in large quantities. Demineralization processes (including ultrafiltration (UF), nanofiltration (NF), reverse osmosis (RO), electrodialysis (ED) and ion exchange (IE)) have been used to remove mineral components from whey [3]. Desalination of whey is necessary for further use of it as a raw material for other valuable products such as baby food or for the recovery of proteins. Most often used processes for the desalination of whey are IE and ED [4]. With these methods, cheese production can be re-designed to a more environmentally friendly and efficient process. Also, other membrane filtration processes such as UF, NF and RO are used to find the potential applications of membrane systems for whey recycling and utilization [5].

Experimental. Sweet whey powder is supplied by Malkara Birlik Dairy Products Co. (Maybi), Turkey. The composition of sweet whey powder was given in Table 1.

Table 1: Composition of Sweet Whey Powder

Parameters	Amounts(%)
Protein	11,55
Lactose	78.82
Fat	0,33
Salt	Not informed
pH	6,48

The whey powder was used to prepare a 6% of whey solution in ultrapure water. In the experimental studies, a cross-flow flat sheet membrane test unit (SEPA CF II GE Osmonics) was used. For membrane tests, Osmonics – JW membranes for UF and NF-90 membrane for NF tests were employed. The properties of the membranes used are given in Tables 2 and 3. Flow scheme of the integrated membrane method for whey processing was given in Figure 1.

Table 2: The Properties of NF-90 Membrane (Dow Water & Process Solutions, 2014)

Membrane Type	NF-90
Producer	DOW FİLMTEC
Material	Thin Film Composite
Maximum Temperature	45^{o}C
Maximum Operating Pressure	41 bar
pH Range	2-11
Free Chlorine Tolerance	< 0.1 ppm
Stabilise Salt Removal	> % 97.0
Permeate Flow Rate	16 gpm

Table 3: The Properties of JW-UF Membrane (GE Osmonics Water & Process Technologies, 2014)

Membrane Type	JW
Producer	GE Osmonics
Material	Polyvinylidene floride
Maximum Temperature	50^{o}C
Typical Operating Pressure	5.55-9.31 bar
Maximum Operating Pressure	7 bar
Typical Operating Flux	5-20 gfd
pH Range	2-10

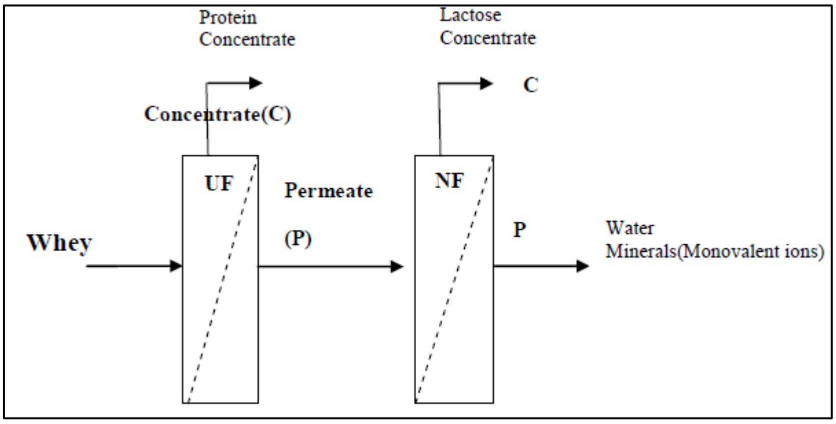

Fig. 1. *Separation of Whey Components by Integrated UF-NF Process*

The experiment was carried out at 7 bar of pressure for UF operation. The permeate was collected as a feed solution for NF process in the next step. The NF process was performed at an applied pressure of 10 bar. During NF test, permeate and concentrate streams are fed back to the feed tank with a constant flow rate 96 L/h. Samples were taken from both permeate and concentrate streams with certain time intervals in order to measure temperature, flow rate, conductivity, total dissolved solids (TDS), salinity and pH. The protein, lactose, fat and mineral analyses of samples were performed using standard methods.

Results and discussion. The protein contents of feed and concentrate samples obtained during UF operation were summarized in Table 4. It was possible to concentrate the protein with more than 20% in the concentrate stream of cheese whey solution by single step UF operation. Next, the permeate of UF process was employed as the feed solution for NF process. The permeate flux of NF membrane versus time was shown in Figure 2. The average permeate flux value was about 22.5 L/m^2 h for NF-90 membrane at 10 bar of pressure. The qualities of permeate and concentrate samples of NF membrane in terms of TDS, pH, conductivity and salinity were illustrated in Figure 3.

Table 4: The Protein Contents of UF Membrane Feed and Concentrate Samples

Sample	**Protein (%)**	**C/Co**
UF-Feed	0.92	-
UF-Concentrate (Average)	1.12	1.22

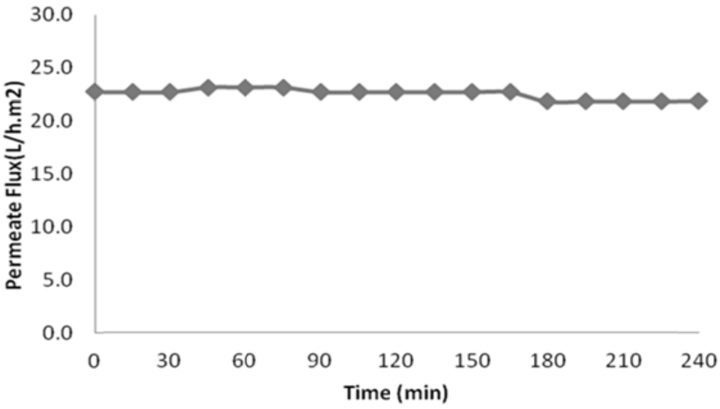

Fig.2. *Permeate Flux versus Time for NF-90 Membrane*

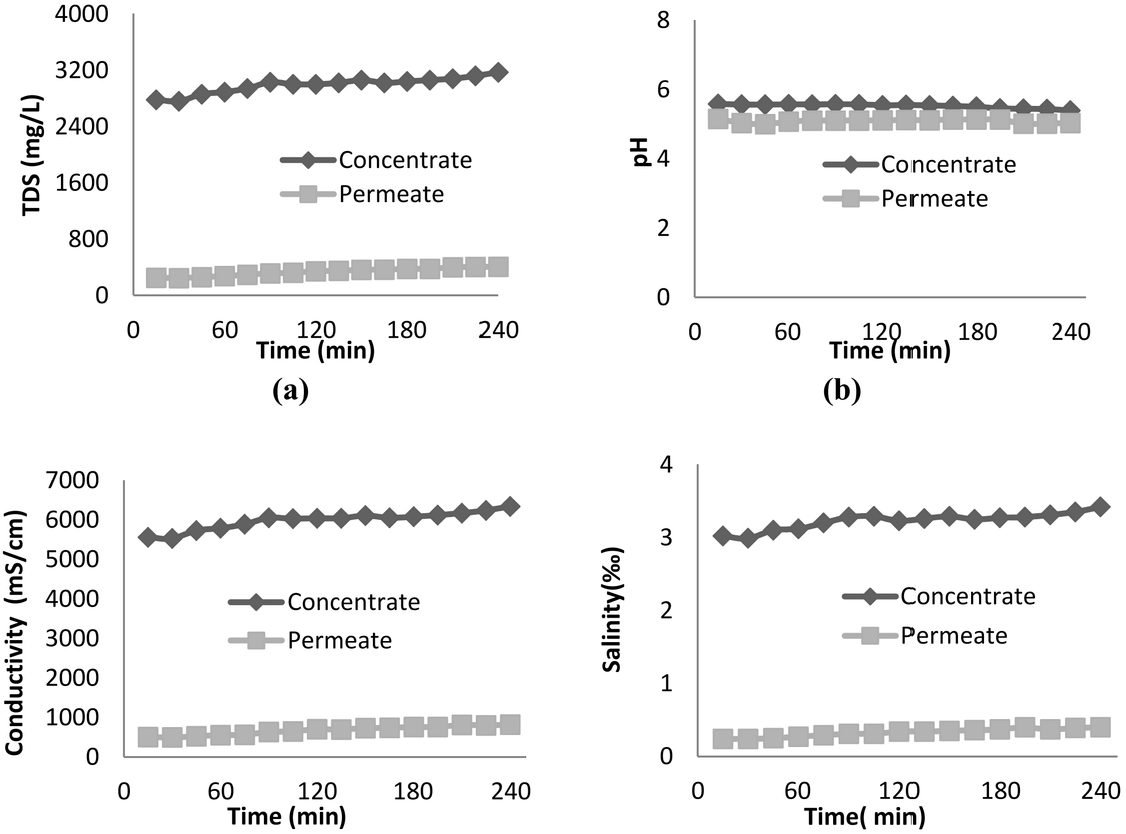

(a) **(b)**

(c) **(d)**

Fig. 3. *TDS (a), pH (b), Conductivity (c) and Salinity (d) of Permeate and Concentrate Streams of NF-90 Membrane*

Figure 4 exhibits the conductivity rejection of NF-90 membrane versus time from UF permeate. Average conductivity rejection obtained by NF-90 membrane was around 90% while average TDD rejection was 86%.

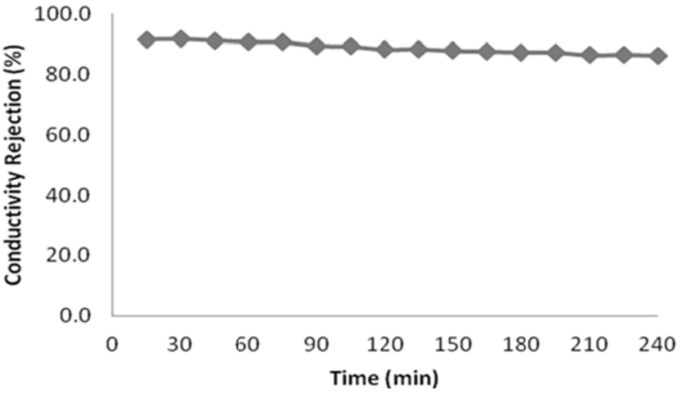

Fig. 4. *Conductivity Rejection of NF-90 Membrane vs. Time*

Average lactose contents of feed and concentrate streams of NF-90 membrane were given in Table 5. According to Table 5, it was possible to concentrate the lactose in the concentrate of NF by 29% with a single NF operation.

Table 5: The Lactose Contents of NF-90 Feed and Concentrate Samples

Samples	**Lactose (%)**
NF-90 Feed (UF Permeate)	56
NF-90 Concentrate (Average)	72

Conclusions. According to the obtained results, protein in cheese whey solution was collected in the concentrate stream of UF membrane while lactose passed through the UF membrane and collected in the permeate stream of UF membrane. Thus, it was possible to separate protein from lactose using UF process. Also, demineralization of cheese whey concentrate will be possible since the mineral ions will be collected in the permeate side of UF membrane.
On the other hand, lactose in the UF permeate was mostly rejected by NF membrane along with mineral ions. Future study will focus on demineralization of lactose as well.

Acknowledgements. This research was supported by TUBITAK (Project no: 114M551). We thank Malkara Birlik Dairy Products Co. (Maybi), Turkey for the kind support to send us cheese whey samples. The authors thank C.Kartal, B.Erdoğan, Food Engineering Department of Ege University for technical support.

References

1. *Cuartas-Uribe B., Alcaina-Miranda M.I, Soriano-Costa E., Mendoza-Roca J.A., Iborra-Clar M.I., Lora-García J.* A study of the separation of lactose from whey ultrafiltration permeate using nanofiltration // Desalination. 2009. V. 241. P. 244-255.
2. *Hinkova A., Zidova P., Pour V., Bubnik Z., Henke S., Salova A., Kadlec P.* Potential of membrane separation processes in cheese whey fractionation and separation // Procedia Engineering. 2012. V. 42. P. 1425-1436.
3. *Diblíková L., Curda L., Kincl J.* The effect of dry matter and salt addition on cheese whey demineralisation // International Dairy Journal. 2013. V.31. P. 29-33.
4. *Greiter M., Novalin S., Vendland M., Kulbe K.D., Fischer J.* Desalination of whey by electrodialysis and ion exchance resins // J.Membrane Sci. 2002. V. 210. P. 91-102.
5. *Rektor A., Vatai G.* Membrane filtration of Mozzarella whey // Desalination. 2004. V. 162. P. 279-286.

UDC 66.081.63

ЗАСТОСУВАННЯ МЕМБРАННОЇ ФІЛЬТРАЦІЇ ДЛЯ ПЕРЕРОБКИ СИРОВАТКИ

İ. Özdemir[1,2], Ya.A. Jarma[1], E. Altıok[1], N. Kabay[1*], S. Ötleş[2*], M. Yüksel[1]

[1]Егейський університет, факультет машинобудування, хіміко-технологічний факультет, Ізмір, Борнова Туреччина

[2]Егейський університет, інженерний факультет, кафедра харчової інженерії, Ізмір, Борнова Туреччина

*E-mail: nalan.kabay@ege.edu.tr, semih.otles@ege.edu.tr

Резюме. *Методи мембранного розділення широко використовуються у молочній промисловості, особливо при переробці пдсирної сироватки. У даній роботі досліджено потенціальні можливості інтегрованого мембранного процесу ультрафільтрації (УФ) та нанофільтрації (НФ) для фракціонування компонентів сироватки, таких як білки, жири, лактоза та мінеральні солі.*

Ключові слова: *сироватка, нанофільтрація, ультрафільтрація, інтегрований мембранний процес, переробка молочної сироватки*

UDC 544.23.022+544.726

ION EXCHANGE MEMBRANES AND ACTIVATED CARBON

Yu. M. Volfkovich[1], V. E. Sosenkin[1], Yu. S. Dzyazko[2]

[1]A.N. Frumkin Institute of Physical Chemistry and Electrochemistry of the RAS,
Leninskii pr. 31, 119071, Moscow, RF
e-mail: yuvolf40@mail.ru
[2]V.I. Vernadskii Institute of General and Inorganic Chemistry, Palladin Ave.
32/34, 03680, Kyiv, Ukraine
e-mail: dzyazko@gmail.com

Abstract. *Application of standard contact porosimetry to investigations of activated carbon, polymer ion exchange membranes and composites based on them is considered. The method allows us to research porous structure of swollen materials in a wide diapason of pore radii (from 1 nm to 100 μm), to recognize mechanism of composite formation, to find location of inorganic particles in one or other type of pores of the polymers, to estimate hydrophilic and hydrophobic porosity.*

Keywords: *ion exchange membranes, organic-inorganic composites, activated carbon, standard contact porosimetry, hydrophilic and hydrophobic pores.*

Introduction. Functional properties of ion exchange membranes (IEMs) and activated carbon (AC) are determined, particularly, by their porous structure, which can be investigated with various methods [1-5]. The information content of widespread porosimetry techniques is limited. Regarding polymer IEMs, their structure is labile, it is formed mainly during swelling and strongly depends on liquid or temperature. This makes it impossible the application of mercury porosimetry, BET and microscopy methods. No swelling is characteristic for AC, but these materials contain both hydrophilic and hydrophobic pores, which cannot be recognized with the mentioned methods. These two types of pores affect functional properties of AC. Moreover, the pore size is within a very wide diapason (4-5 orders) for IEMs and AC.

Experimental. Such untraditional method as standard contact porosimetry (MSCP) is the most informative and correct technique for investigations of IEMs and AC [1-5]. MSCP gives a possibility to keep temperature, which is equal to that in fuel cells or electrodialysis cells. Similar working liquid (electrolyte solution or water) can be also used [2, 3]. Thus, porous structure that is realized under the real operating conditions can be determined. The MSCP allows us to obtain pore size distributions in the maximal diapason: from 1 nm to $3x10^5$ nm (five orders of magnitude).

Results and discussion. *Homogeneous ion exchange membranes*. These materials can be considered as solid polymer electrolytes containing only one phase (ion-exchanger). As shown in example of MA-100 anion exchange membrane, very insignificant swelling occurs in octane (Fig. 1, [3]). It means practically mo porosity in this medium similarly to air-dry state. In aqueous medium, considerable porosity is formed in the region of pores, a radius of which is less than 10 nm. The most known homogeneous materials are proton conductive perfluorinated membranes of Nafion type containing sulfo groups. Porous structure of these materials is formed only in water or in water vapour due to hydration of functional groups [6]. Water molecules move apart the polymer chains producing pores.

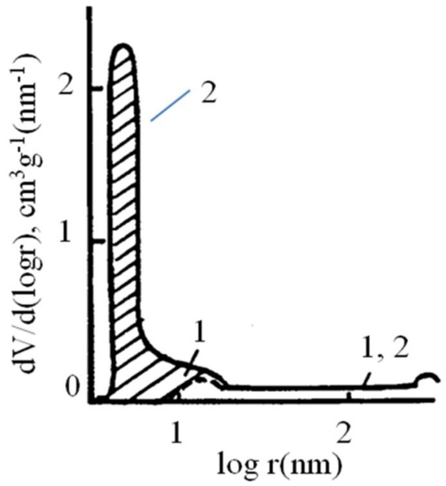

Fig. 1. *Differential Pore Size Distributions for Homogeneous MA-100 Membranes (Adapted from [3]). Working Liquids Are Water (1) and Octane (2).*

Pore size distributions have been also obtained for Nafion 112, Nafion 115, Nafion 117 as well as for Russian analogue of these membranes (MF-4SK), water was used as a working liquid [6]. Porosity of these IEMs was shown to be provided mainly by micro- and mesopores, a radius (*r*) of which is less than 10 nm. This structure is so-called as "nanostructure" or "ion exchanger phase". The curves of pore size distribution for all mentioned membranes are close to each other in the nanostructure region. It is assumed that the nanostructure is determined by similar chemical nature of the membranes. Based on the investigations of other IEMs, this conclusion can be related for all ion exchange membranes. The pore size distributions are rather different in the region of *r*=10-500 nm. These pores are evidently affected by the procedures of membrane preparation, which are different for various type of IEMs.

Any change of the synthesis procedure affects porous structure of IEMs [7]. For instance, increasing in ion exchange capacity of the MF-4SK membrane from 0.71 to 1.02 mg-eq g^{-1} causes almost doubling porosity value. The cumulative volume of micro- and mesopores in ethanol is higher in two times than that in water. Macropores are practically absent in two cases. The information about the membrane structure is important for methanol-air fuel cell. The swelling degree of the membranes depends also on nature of counter-ions. The MF-4SK membrane shows a decrease of porosity (about 30%) after loading with Na$^+$. The volume of pores decreases sufficiently, when inorganic counter-ions are substituted by organic species [3].

Heterogeneous membranes. These IEMs contain not only ion-exchanger but also inert components. For example, Fig. 2 illustrates differential pore size distributions for the MC-40 membranes containing different amount of divinylbenzene (DVB) and polyethylene particles as a binder [8]. The curves are characterized by two maxima: the first peak is in the region of micro- and mesopores (from <1 nm to 100 nm), the second one is attributed to macropores (r=300-3000 nm). Pores of the first type are formed due to swelling of ion exchanger phase, voids of the second type are due to inert polyethylene phase. As seen, a growth of DVB content causes an increase of the second maximum, the first peak becomes smaller.

Organic-inorganic membranes. These membranes are probably the widespread type of composite IEMs. One way to prepare them is to insert inorganic particles into preliminarily formed polymer membranes. Since porous structure of ion exchange polymers are complex, the incorporated particles can be precipitated in one or other types of pores depending on their size. The particle size is determined by Ostwald-Freundlich equation [9]:

$$\ln\frac{C}{C_\infty}=\frac{\beta v_m \sigma\cos\varphi}{RTr}. \qquad (1)$$

Here C is the compound concentration in the solution, C_∞ is the concentration of saturated solution, β is the shape factor of particles, v_m is the molar volume of the compound, σ is the surface tension of the solvent, φ is the wetting angle, R is the gas constant, T is the temperature, r is the particle radius. The particles, a radius of which is less than the r value, are dissolved and reprecipitated as larger formations. This thermodynamic equation allows us to control the modification conditions and to form purposefully smaller or larger particles of the modifier (usually it is inorganic ion-exchanger) [10]. The equation was adapted taking into consideration ion exchange properties of the polymer [11].

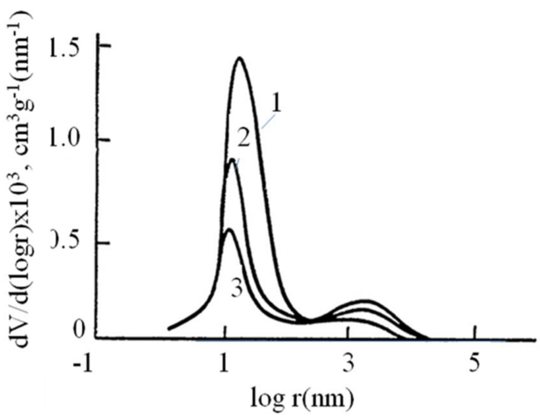

Fig. 2. *Differential Pore Size Distributions for Heterogeneous MK-40 Membranes Obtained by Copolimerization of Styrene with DVB (Adapted from [8]). The Content of DVB: 2 % (1), 4 % (2) and 8 % (3).*

The composite IEMs were obtained by modification of heterogeneous membranes with zirconium hydrophosphate (MC-40 cation exchange membrane) and hydrated zirconium dioxide (MA-40 anion exchange material). In order to establish the interrelation between structure of the modified polymers and their functional properties, following parameters have been introduced: (i) a ratio of volumes of pores of the first and the second type (α), (ii) a ratio of volumes of micro- and mesopores of the first type (γ) [12]. A change of these parameters, which is caused by the inorganic particles, has been found to reflect ion movement through the composites. Primary nanoparticles in pores of the first type improve ion transport due to additional counter-ions. Small aggregates (up to 200-300 nm) in pores of the second type are filters against co-ions and uncharged particles (for instance, organics). Large agglomerates can be also formed in pores of the second type, a size of which is several microns. They deteriorate functional properties of IEMs. Thus, the modification procedure has to provide no agglomerate formation.

The modification procedure [12] allows us to precipitate only primary nanoparticles and their small aggregates inside heterogeneous IEMs (Table 1). The primary particles cause a decrease of α and γ parameters indicating location inside pores of the first type. The inorganic cation-exchanger, such as zirconium hydrophosphate, increases the membrane potential in neutral media. Amphoteric hydrated zirconium dioxide deteriorates charge selectivity under these conditions. Thus, at least one side of the composite ion-exchange membrane has to be in a contact with acidic solution. It is necessary to provide anion exchange ability of the modifier. Lower electrical conductivity of the composite IEMs than that of the pristine membranes is due to barrier function of the aggregates in pores of the second type.

Table 1: Characteristics of IEMs (Adapted from [12])

Membrane	α	γ	**Potentiometric transport number (0.5 M/1 M NaCl)**	**Electrical conductivity, mOhm^{-1} m^{-1} (0.5 M NaCl)**
MK-40, pristine	1.85	1.59	0.92	160
MK-40, composite	1.76	1.50	0.94	30
MA-40, pristine	1.35	0.98	0.96	27
MA-40, composite	1.11	0.91	0.92	22

The membranes were applied to desalination of biological liquids, for instance, milky whey. The advantages of organic-inorganic membranes over polymer IEMs are no concentration polarization, when the current is lower than the limiting value [12], higher desalination degree [13] and current efficiency [12, 13], faster removal of hardness, hydrophosphate and dihydrophosphate ions than cations of alkaline metals and chloride anions [13]. At last, organic-inorganic IEMs are stable against fouling with organics.

Composite polymer membranes. Polymer fibrous composites are relatively new IEMs. Combination of different fibrous fillers and ion exchangers allows us to obtain materials with a wide diapason of properties. Cation exchange materials of Polycon type are obtained with a polycondensation method: strongly acidic ion-exchanger is formed between the fibers as well on outer surface of the fibrous membranes (Fig. 3). Synthesis procedure involves impregnation of the membrane with a solution of monomer followed by pressing. Exothermic heating of the material occurs during pressing, this affects structure of the membrane being formed.

Hydrophilic and hydrophobic pores of composite membranes, which are determined by pressure during synthesis, were investigated in [14] using octane and water. The method of standard contact porosimetry allows us to determine a wetting angle for water (θ) [1-4]. As shown, porous structure of swollen Polycon-type membranes involves pores due to fibers and ion exchange filler. In general, fibers contain hydrophilic micropores ($\theta \approx 0^{o}$), hydrophilic-hydrophobic mesopores ($\theta < 90^{o}$) and hydrophobic meso- and macropores ($\theta > 90^{o}$) [14]. The ion exchange filler contains only completely hydrophilic micro- and mesopores. The values of specific surface area are different (70-480 m^2 g^{-1}) for various Polycon membranes containing an equal amount of the ion-exchanger (90 mass %). However, exchange capacity is similar for all samples (2.6-2.8 mg-eq g^{-1}). This is explained by different orientation of functional groups relatively to polymer chains. The orientation provides different distributions of water molecules and different nanostructure of the filler.

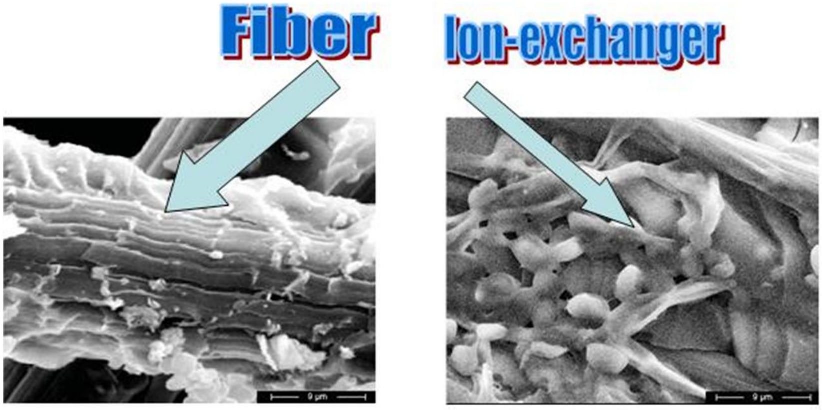

Fig. 3. *SEM Images of Polycon Membrane (Adapted from [14]).*

Pore corrugation. The method of standard contact porosimetry allow us to recognize pore corrugation: this feature of porous structure of the IEMs affects their electrical conductivity [15]. Homogeneous MA-100 anion exchange membrane and home-made heterogeneous cation exchange membranes were investigated [16]. The last samples were produced by copolymerization of methacrylic acid with DVB in a solution of polyethylene (a binder) in m-xylene.

Fig. 4a illustrates integral energetic adsorption-desorption isotherms measured in water for the MA-100 membrane, integral pore size distributions obtained during evaporation of water or decane and the difference between these curves. A change of the membrane volume, which was measured with a micrometer during water evaporation, is also given. During swelling in water, the pore volume increases in 9 times mainly due to pores of the first type attributed to nanostructure. The volumes of pores of the second type are practically similar, when water or decane are used as working liquids. The main important result is a coincidence of the curves in the region of nanostructure and small hysteresis in the region of macropores.

Similar family of curves are given in Fig. 4b for the home-made membrane. The curves for water adsorption and desorption also coincide in the region of nanostructure, however, the hysteresis is much significant comparing with homogeneous MA-100 membrane. Thus, pores of the first type, which are formed in water, are not corrugated. At the same time, macropores are corrugated. Since corrugation means also pore tortuosity, the highest values uf electrical conductivity and diffusion coefficients should be found for homogeneous membranes, in which macropores are practically absent. This conclusion is assumed to be common for all ion exchange membranes. Particularly this assumption explains very high conductivity of Nafion membranes, which are used in low-temperature fuel cells.

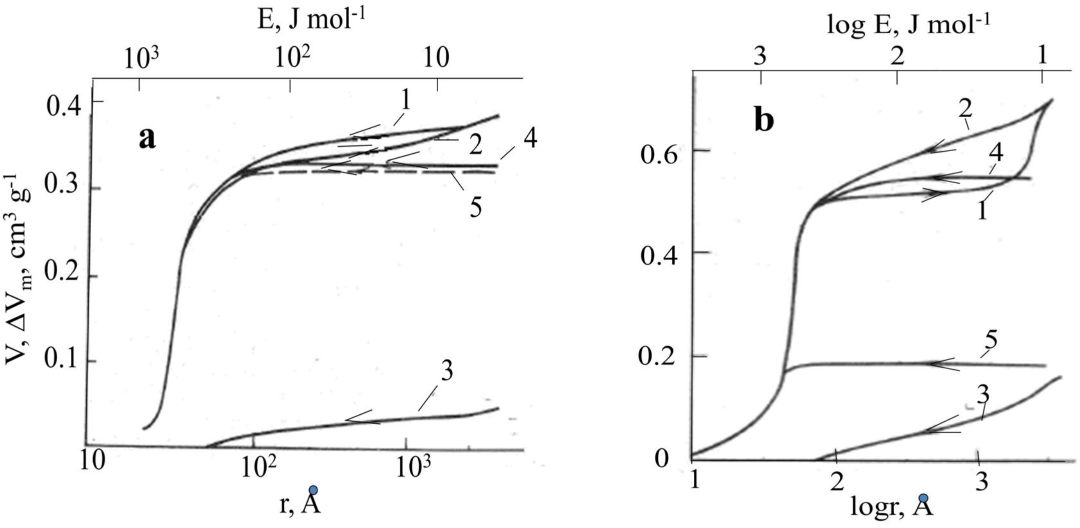

Fig. 4. *Integral Energetic Isotherms of Water Adsorption (1) and Desorption (2), Integral Pore Size Distributions Measured in Water (2) or Decane (3) during Evaporation. The Curve (4) Is the Difference of Curves (2) and (3), the Curve (5) Is a Change of the Membrane Volume during Release of Water from Pores. The Data Are Given for the MA-100 Anion Exchange Membrane (a) and for the Membrane Produced by Copolymerization of Methacrylic Acid with DVB (b). Adapted from [16].*

Activated carbon. These sorbents are applied to solution of following tasks: prevention of emission of harmful gases into the atmosphere, purification of waste waters, production of pure water using capacitive deionization (CDI) etc. The CDI method requires the most hydrophilic electrodes, this property can be estimated with a method of standard contact porosimetry. Here the results of investigations of porous structure and hydrophilic-hydrophobic properties of following AC are given: CH900 (Curaray Co, Japan), VISKUMAK (Neorganica LTD, RF), SAIT (SAIT Co, South Korea). The first two samples are textiles, the electrode of SAIT type was produced by pressing of powder of activated carbon with a binder (polytetrafluorethylene).

Integral and differential pore size distributions for the carbon materials were obtained using water or octane (Fig. 5a-c). These distributions are plotted *vs* effective pore radius ($r*$) that is determined as [2– 5]:

$$r^* = \frac{r}{\cos\theta} \tag{2}$$

where r is the true value of pore radius. The $\theta - \log r$ curves were also plotted (Fig. 5d). Since octane wets all materials almost perfectly, $r^* \approx r$ for this liquid. The difference between the maximal content of octane and water corresponds to hydrophobic pores. All investigated carbon electrodes were found to include both hydrophilic and hydrophobic pore volumes (hydrophilic and hydrophobic specific surface area, Table 2). The wetting angle distributions show hydrophobicity for all electrodes, especially for the SAIT material containing particles of hydrophobic binder. Moreover, complex $\theta - \log r$ dependences are due to inhomogeneous distribution of surface groups in pores of different size.

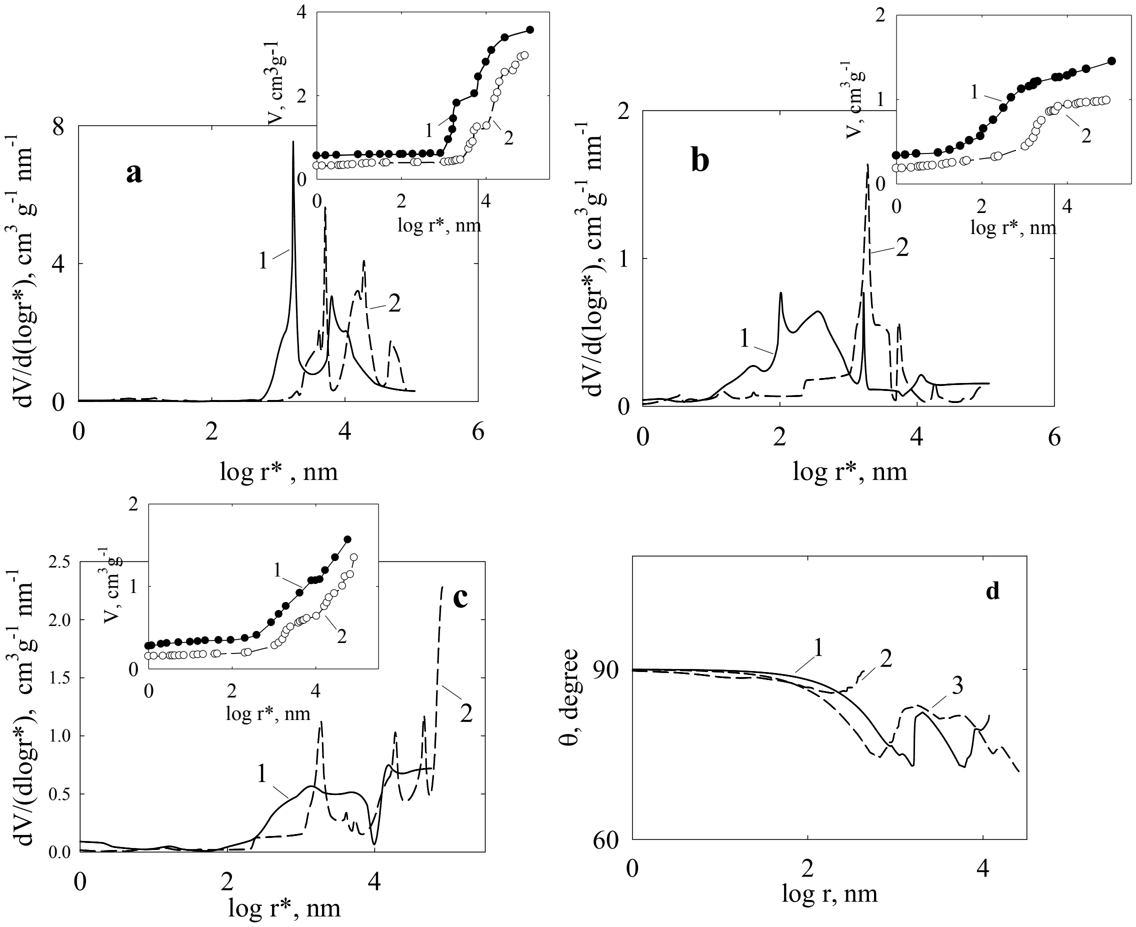

Fig. 5. Differential Pore Size (a-c) and Wetting Angle (d) Distributions Measured in Octane (a-c, 1) and Water (a-c, 2) for the CH900 (a, d1), SAIT (b, d2) and VISKUMAK (c, d3) Electrodes. Insertions: Integral Pore Size Distributions (a-c).

A very wide diapason of pore size is characteristic for the electrodes (from $r < 1$ nm to 100 μm), pores are both hydrophilic and hydrophobic. The values of specific surface area are rather high, they are sufficiently different from each other. The magnitudes of hydrophilic and hydrophobic porosity are also various.

The data obtained in octane media allow us to make main conclusions. A total diapason of pore size is very wide: the r values are less than 1 nm for the smallest pores and larger than 100 μm for the largest voids. Micropores

(r<1nm) as well as large macropores (r>100 μm) are attributed for all materials. Pores, a radius of which is 1-100 nm, are practically absent in the CH900 and VISKUMAK textiles. All types of pores have been found for the SAIT electrode.

Table 2. Characteristics of Porous Structure of Carbon Electrodes

Electrode	**Specific surface area (m^{2}g^{-1})**		**Ratio of hydrophilic and total surface areas**	**Porosity (cm^3 cm^{-3})**		
	Total	Hydrophilic		Total	Hydrophilic	Hydrophobic
CH900	1520	850	0.56	0.850	0.786	0.064
VISKUMAK	600	416	0.70	0.729	0.623	0.106
SAIT	940	520	0.55	0.715	0.490	0.225

Total porosity is rather high for all electrodes. A comparison of the data, which were obtained in water and octane media, shows higher volume of hydrophilic pores than that for hydrophobic voids. The magnitudes of total specific surface are 600-1520 m^2 g^{-1}, particularly the values of 42**0**-850 m^2 g^{-1} are due to hydrophilic pores. The last values are very important, since electric double layer, which determines main characteristics of CDI processes, is realized in these pores. The largest contribution of hydrophilic regions into total surface area has been found for the VISKUMAK textile. Regarding the CH900 ACT textile and the SAIT composite, the ratios of hydrophilic and total surface areas are sufficiently lower and close to each other.

Conclusions. The MSCP allows us to investigate porous structure of polymer IEMs in a very wide diapason of pore radius unlike, for instance, a method of water adsorption-desorption isotherms. In opposite to mercury porosimetry, this method can be applied to swollen materials, i.e. they can be researched under real conditions. Inert voids and pores that are responsible for ion exchange are recognized by this manner. The information about the influence of synthesis conditions on structure of IEMs and composites based on them can be obtained. Particularly inversion of polymer chains in polymer composite membranes and location of inorganic particles in one or other types of pores of the polymers have been found. The method also allows us to research hydrophilic-hydrophobic properties of AC, this is especially important for CDI processes.

Acknowledgements. The work was supported by the project of the Russian Foundation of Basic Research “Fundamental aspects of capacitive deionization of aqueous solutions” (grant № 14-03-00082) and also by the project “Fundamental problems of creation of new materials for chemical industry” (grant N 49/12) of the National Academy of Science of Ukraine within the framework of the program “Fundamental problems of development of new materials for chemical industry”.

References

1. *Volfkovich Yu. M., Bagotzky V. S.* The method of standard porosimetry: 1. Principles and possibilities // J. Power Sources. 1994. V. 48. P. 327–338.
2. *Volfkovich Yu. M., Bagotzky V. S., Sosenkin V. E., Blinov I. A.* The standard contact porosimetry // Colloids Surf. A. Physicochem. Eng. Asp. 2001. V. 187. P. 349–365.
3. *Volfkovich Yu. M., Sosenkin V. E. Bagotzky V. S.* Structural and wetting properties of fuel cell components // J. Power Sources. 2010. V. 195. P. 5429–5441.
4. *Volfkovich Yu. M., Filippov A. N., Bagotzky V. S.* Structural properties of porous materials and powders used in different fields of science and technology. Springer-Verlag, London, Heidelberg, New York, Dordrecht, 2014.
5. *Kononenko N. A., Fomenko M, A., Volfkovich Yu. M.* Structure of perfluorinated membranes investigated by method of standard contact porosimetry // Adv. Colloid Interface Sci. 2015. V. 222. P. 425–435.
6. *Divisek J., Eikerling M., Mazin V. M., Schmitz H., Stimming U., Volfkovich Yu. M.* A Study of Capillary Porous Structure and Sorption Properties of Nafion Proton□Exchange Membranes Swollen in Water // J. Electrochem. Soc. 1998. V. 145. P. 2677 -2683.
7. *Volfkovich Yu. M., Drejman N. A., Belyaeva O. N., Blinov I. A.* Standard porosimetry study of perfluorinated cation-exchange membranes // Soviet Electrochem. 1988. V. 24. P. 324-330.
8. *Berezina N. P., Volfkovich Yu. M., Kononenko N. A., Blinov I. A.* Water distributiion studies in heterogeneous ion exchange membranes by standard porosimetry // Soviet Electrochem. 1987, V. 23. P. 858-862.
9. *Myerson A. S.*, Handbook of Industrial Crystallization, Butterworth-Heinemann, Woburn, 2002.
10. *Dzyazko Yu. S., Volfkovich Y. M., Ponomaryova L. N., Sosenkin V. E., Trachevskii V. V., Belyakov V. N.* Composite ion-exchangers based on flexible resin containing zirconium hydrophosphate for electromembrane separation / /J. Nanosci.Technol. 2016. V. 2. P. 43-49.
11. *Dzyazko Yu. S., Perlova N. A., Perlova O. V., Sazonova V. F., Ponomareva L. N., Volfkovich Yu. M., Palchik A. V., Trachevskii V. V., Belyakov V. N.* Organic-inorganic ion-exchanger containing zirconium hydrophosphate for removal of uranium(VI) compounds from aqueous solutions // Chemistry, Physics and Technology of Surface. 2016. V.7. P. 119-132.
12. *Dzyazko Yu., Rozhdestveskaya L., Zmievskii Yu., Volfkovich Yu., Sosenkin V., Nikolskaya N., Vasilyuk S., Myronchuk V., Belyakov V.* Heterogeneous Membranes Modified with Nanoparticles of Inorganic Ion-Exchangers for Whey Demineralization // Materials Today: Proceedings. 2015. V. 2. P. 3864-3873.
13. *Dzyazko Yu. S., Rozhdestvenskaya L. M., Zmievskii Yu. G., Volfkovich Yu. M., Sosenkin V. E., Zakharov V. V., Myronchuk V. G., Belyakov V. N., Palchik A.V.* Electromembrane recycling of liquid wastes of dairy industry using organic-inorganic membranes // ssues of Chemistry and Chemical Technology. 2015. V. 6 (104). P. 40-46.
14. *Volfkovich Yu. M., Kononenko N. A., Chernyaeva M. A., Kardash M. M., Shkabara A. I., Pavlov A. V.* Study of porous structure, hydrophilic-hydrophobic and sorption properties of fibrous ion exchange Polycon membranes and their influence on ionic selectivity // Criticheskie Tekhnologii. Membrani. 2008. N 3. P. 8-19 (*in Russian*).
15. *Eikerling M., Kharkats Yu. I., Kornyshev A. I., Volfkovich Yu. M.* Phenomenological theory of electro-osmotic effect and water management in polymer electrolyte Proton-conducting membranes // J. Electrochem. Soc. 1998. V.45. P. 2684-2699.
16. *Volfkovich Yu. M., Luzhin V. K., Vanyulin A. N., Shkolnikov E. I., Blinov I. A.* Application of the method of calibrated porosimetry to investigation of the porous structure of ion exchange membranes // Soviet Electrochem. 1984. V. 20. P. 613-621.

УДК 544.23.022+544.726

ІОНООБМІННІ МЕМБРАНИ ТА АКТИВОВАНЕ ВУГІЛЛЯ

Ю. М. Вольфкович[1], В. Е. Сосєнкін[1], Ю.С. Дзязько[2]

[1]Інститут фізичної хімії та електрохімії ім. О.Н. Фрумкіна РАН, Ленінський пр. 31, 119071, Москва, РФ

e-mail: yuvolf40@mail.ru

[2]Інститут загальної та неорганічної хімії ім. В.І. Вернадського НАН України.

пр. акад. Палладіна 32/34, 03680, Київ, Україна

e-mail: dzyazko@gmail.com

Резюме. *Розглянуто застосування методу еталонної контактної порометрії для дослідження активованого вугілля, полімерних іонообмінних мембран та композитів на їх основі. Метод дозволяє вивчати пористу структуру у широкому діапазоні радіусів пор (від 1 нм до 100 мкм), встановлювати механізм формування композитів, ідентифікувати неорганічні частинки у тих або інших порах полімерів, оцінювати гідрофільну та гідрофобну пористість.*

Ключові слова: *іонообмінні мембрани, органо-неорганічні композити, активоване вугілля, еталонна контактна порометрія, гідрофільні та гідрофобні пори.*

UDC 66.081

PHOSPHORUS-CONTAINING CARBONS – A NEW TYPE OF CARBONACEOUS ADSORBENTS

A.M. Puziy, O.I. Poddubnaya
Institute for Sorption and Problems of Endoecology, NAS of Ukraine, Naumov Str. 13, 03164, Kyiv, Ukraine,
e-mail: alexander.puziy@gmail.com

Abstract. *Recent studies of phosphorus-containing carbons are reviewed. Characteristic feature of phosphorus-containing carbons is acidic surface groups like phosphates, which determines their adsorption, catalytic and electrochemical properties. Phosphorus-containing carbons offer a great promise for water treatment, in catalysis and as electrode material for electrical double layer capacitors.*

Keywords: *phosphorus-containing carbon, porous structure, surface chemistry, electrochemical properties, catalytic properties*

Introduction. Activated carbons are the most widely used general-purpose adsorbents that have been in service for almost four millennia. Up to now, new applications of carbon adsorbents arise, and the potential of carbons is far from exhausted. The properties of carbon adsorbents are determined both by their porous structure and by the chemical nature of their surface [1][2].

The effect of oxygen and nitrogen heteroatoms on the chemical nature of the surface of carbon materials has received the most study. It has been shown that a relatively small amount of oxygen-containing surface groups gives the carbon materials such characteristics as hydrophilicity and the ability to absorb cations from aqueous solutions and catalytic activity in acid-catalyzed reactions. The inclusion of nitrogen in the structure of the carbon increases the amount of basic groups and changes the charge in the graphene layers, increases anion-exchange capacity and catalytic activity in redox reactions.

Phosphorus heteroatom has received much less attention. The purpose of the present communication is review recent advances in phosphorus-containing carbons [3,4].

Experimental. Phosphorus-containing carbons were obtained by (i) carbonization of phosphorus-containing copolymer [5]; (ii) by phosphoric acid activation of polymer [6–10], lignocellulosic [11,12] or lignin [13] precursor; or (iii) by heat treatment of ready-made activated carbon impregnated with phosphoric acid [14].

Results and discussion. Phosphorus-containing carbons show developed porous structure with different pore-size distributions depending on the precursor. BET surface area range from 625 to 2070 m^2/g (Table 1.). Total pore volume is almost equally distributed between micro and mesopores. The most developed porous structure in biomass-derived carbons - fruit-stone-based carbon APP400 and corncob-based carbon CCP400.

Table 1. Parameters of Porous Structure of Phosphorus-Containing Carbons Obtained from Polymer (SP900 [15], BMP600 [7]), Biomass (APP400 [12] and CCP400 [16]) and Lignin (LSP400 [13]) Precursors

Carbon	**A_{BET} m^2/g**	**V_{tot} cm^3/g**	**V_{mi} cm^3/g**	**V_{me} cm^3/g**
SP900	625.2	0.44	0.20 (46%)	0.24 (54%)
BMP600	891.1	0.45	0.26 (57%)	0.20 (43%)
APP400	1750	0.90	0.47 (53%)	0.42 (47%)
CCP400	2071	1.13	0.55 (49%)	0.58 (51%)
LSP400	1018	0.76	0.31 (41%)	0.45 (59%)

The procedure used for preparation yielded carbons with high amount of phosphorus [6,7,10–13]. With increasing carbonization temperature up to 800 °C, the amount of phosphorus increases for all carbons while at higher temperatures phosphorus content decreases. This fact is due to simultaneously occurring two processes. One is enhancing the intensity of the reaction between phosphoric acid and carbonaceous matter with increasing temperature. The other is destruction of phosphorus-containing compounds with formation of volatile products. Thermodynamic calculations show that volatilization of phosphorus compounds is favored at temperatures higher than 750 °C.

Some information about the chemical structure of phosphorus species in the structure of carbons can be obtained from elemental analysis [6,7,10–13]. Oxygen to phosphorus atomic ratio decreases with increasing carbonization temperature reaching a value between 3 and 4, which is between monophosphates, as in phosphoric acid (n=4), and polyphosphates (n=3). This fact allows ascribing phosphorus species in carbon structure to polyphosphates.

FTIR investigation confirms existence of polyphosphates (P-O-P symmetric 1070 cm^{-1}, P-O-P asymmetric 990 cm^{-1}) bound to carbon lattice via C-O-P bonding (C-O-P and P=O 1230 cm^{-1}) [6].

The existence of polyphosphates is corroborated by XPS experiments, which show a single state of phosphorus atom like in phosphates structure [17,18].

In addition to the above studies, ^{31}P-NMR shows the existence of phosphonate structures (C-P bonding) at 500-600 °C which disappears at higher temperatures [18].

Direct evidence of polyphosphates on carbon surface was obtained by laser desorption/ionization time-of-flight mass spectrometry [19]. LDI-ToF mass-spectra revealed polyphosphates fragments with polymerization degree up to 4.

Analysis of LDI ToF mass-spectra allows putting forward fragmentation scheme of phosphorus species during acquisition of LDI ToF mas-spectra [19].

Characteristic feature of phosphorus-containing carbons is acidic character of surface with significant cation exchange capacity (CEC) [6,10–12]. This feature may be compared to that of oxidized carbons obtained by treating carbonaceous adsorbents with oxidizing agents like HNO_3, H_2O_2, HClO etc.

Potentiometric titration revealed the difference between surface group composition in phosphorus-containing and oxidized carbons. Phosphorus-containing carbons contain much more acidic phosphate groups (pK ~2) while most acidic groups in oxidized carbons are carboxylic (pK ~3).

Significant amount of acid surface groups determines the metal ion binding properties of phosphorus-containing carbons. Adsorption of heavy metal ions is much higher on phosphorus-containing carbons, especially in acid solutions, due to binding to very acidic phosphate groups which are absent in oxidized carbons [6,20].

Column adsorption experiments shows 1.5-4 times higher breakthrough volume and saturated capacity even over synthetic ion exchange resins like carboxylic KB-4 (Amberlite IRC-50 analog) and sulfonic KU-23 (Amberlyst-15 analog).

Very acidic surface groups imparts catalytic activity of phosphorus-containing carbons in acid-catalyzed reactions like synthesis of ethyl-tert-butyl ether [21], butyl acetate and hydrolysis of ethyl acetate [22]. Catalytic activity of phosphorus-containing carbons is proportional to the content of phosphate groups.

Phosphorus-containing carbons show high electrical capacity 192-220 F/g in aqueous (1 M H_2SO_4) electrolyte [23,24]. Phosphorus imparts carbon adsorbents high electrochemical stability, which allows operating at high potentials up to 1.3 V for 15000 cycles with very small loss of capacitance. Widening operating voltage window greatly increases the energy stored in electrochemical double layer capacitor. Statistical analysis reveals than the most influential factors for high electrical capacity are phosphorus content and surface area of pores with 0.65-0.83 nm (determined from CO_2 adsorption data).

Conclusions. Recent studies show that phosphorus-containing carbons are a new type of carbonaceous adsorbents. Phosphorus-containing carbons show high cation exchange capacity and offer a great promise for removal of heavy metal ions from aqueous solutions (water treatment) or for metal ion concentration (recovery). Phosphorus-containing carbons show high catalytic activity in acid-catalyzed reactions (etherification, esterification, and hydrolysis). Phosphorus-containing carbons have great potential as electrode material for EDLC.

References

1. *Marsh H., Rodríguez-Reinoso F.* Activated Carbon, Elsevier Ltd., Oxford, 2006.
2. *Bandosz T.J. (Ed.)* Activated Carbon Surfaces in Environmental Remediation, Academic Press, Amsterdam, 2006.
3. *Puzii A.M.* Methods of production, structure, and physicochemical characteristics of phosphorylated carbon adsorbents // Theor. Exp. Chem. 2011. V. 47. P. 277–291.
4. *Puziy A.M., Tascón J.M.D.* Adsorption by phosphorus-containing carbons, in *Novel Carbon Adsorbents*, ed. Tascón, J.M.D., Elsevier, Amsterdam, 2012, pp. 245–267.

5. *Puziy A.M., Poddubnaya O.I.* The properties of synthetic carbon derived from nitrogen- and phosphorus-containing polymer // Carbon 1998. V. 36. P. 45–50.
6. *Puziy A.M., Poddubnaya O.I., Martínez-Alonso A., Suárez-García F., Tascón J.M.D.* Synthetic carbons activated with phosphoric acid I. Surface chemistry and ion binding properties // Carbon 2002. V. 40. P. 1493–1505.
7. *Puziy A.M., Poddubnaya O.I., Sobiesiak M., Gawdzik B.* Structural and surface heterogeneity of phosphorus-containing polyimide-derived carbons: effect of heat treatment temperature // Adsorption 2013. V. 19. P. 717–722.
8. *Puziy A.M., Poddubnaya O.I., Gawdzik B., Sobiesiak M., Tsyba M.M.* Phosphoric acid activation - functionalization and porosity modification // Appl. Surf. Sci. 2007. V. 253. P. 5736–5740.
9. *Puziy A.M., Poddubnaya O.I., Gawdzik B., Sobiesiak M., Tsyba M.M.* Functionalization of carbon and silica gel by phosphoric acid // Adsorpt. Sci. Technol. 2007. V. 25. P. 531–542.
10. *Puziy A.M., Poddubnaya O.I., Martínez-Alonso A., Suárez-García F., Tascón J.M.D.* Synthetic carbons activated with phosphoric acid. III. Carbons prepared in air // Carbon 2003. V. 41. P. 1181–1191.
11. *Puziy A.M., Poddubnaya O.I., Martínez-Alonso A., Suárez-García F., Tascón J.M.D.* Surface chemistry of phosphorus-containing carbons of lignocellulosic origin // Carbon 2005. V. 43. P. 2857–2868.
12. *Puziy A.M., Poddubnaya O.I., Martínez-Alonso A., Castro-Muñiz A., Suárez-García F., Tascón J.M.D.* Oxygen and phosphorus enriched carbons from lignocellulosic material // Carbon 2007. V. 45. P. 1941–1950.
13. *Myglovets M., Poddubnaya O.I., Sevastyanova O., Lindström M.E., Gawdzik B., Sobiesiak M., et al.* Preparation of carbon adsorbents from lignosulfonate by phosphoric acid activation for the adsorption of metal ions // Carbon 2014. V. 80. P. 771–783.
14. *Puzii A.M., Stavitskaya S.S., Poddubnaya O.I., Vikarchuk V.M., Tsyba N.N.* Structural and adsorption properties of active carbon from coconut shells modified with phosphorus heteroatoms // Theor. Exp. Chem. 2012. V. 48. P. 272–277.
15. *Puziy A.M., Poddubnaya O.I., Martínez-Alonso A., Suárez-García F., Tascón J.M.D.* Synthetic carbons activated with phosphoric acid. II. Porous structure // Carbon 2002. V. 40. P. 1507–1519.
16. *Sych N.V., Trofymenko S.I., Poddubnaya O.I., Tsyba M.M., Sapsay V.I., Klymchuk D.O., et al.* Porous structure and surface chemistry of phosphoric acid activated carbon from corncob // Appl. Surf. Sci. 2012. V. 261. P. 75–82.
17. *Puziy A.M., Poddubnaya O.I., Ziatdinov A.M.* On the chemical structure of phosphorus compounds in phosphoric acid-activated carbon // Appl. Surf. Sci. 2006. V. 252. P. 8036–8038.
18. *Puziy A.M., Poddubnaya O.I., Socha R.P., Gurgul J., Wiśniewski M.* XPS and NMR studies of phosphoric acid activated carbons // Carbon 2008. V. 46. P. 2113–2123.
19. *Puziy A.M., Poddubnaya O.I., Gromovoy T.Y.* Laser desorption/ionization time of flight mass spectrometry of phosphorus-containing carbons // Carbon 2013. V. 53. P. 405–408.
20. *Puziy A.M., Poddubnaya O.I., Zaitsev V.N., Konoplitska O.P.* Modeling of heavy metal ion binding by phosphoric acid activated carbon // Appl. Surf. Sci. 2004. V. 221. P. 421–429.
21. *Puziy A.M., Poddubnaya O.I., Kochkin Y.N., Vlasenko N.V., Tsyba M.M.* Acid properties of phosphoric acid activated carbons and their catalytic behavior in ethyl-tert-butyl ether synthesis // Carbon 2010. V. 48. P. 706–713.
22. *Stavitskaya S.S., Poddubnaya O.I., Tsyba N.N., Puziy A.M.* Catalytic Properties of

Phosphorus-Containing Charcoals in Ethyl Acetate Hydrolysis // Theor. Exp. Chem. 2014. V. 50. P. 187–190.

23. *Hulicova-Jurcakova D., Puziy A.M., Poddubnaya O.I., Suárez-García F., Tascón J.M.D., Lu G.Q.* Highly stable performance of supercapacitors from phosphorus-enriched carbons. // J. Am. Chem. Soc. 2009. V. 131. P. 5026–5027.
24. *Huang C., Puziy A.M., Sun T., Poddubnaya O.I., Suárez-García F., Tascón J.M.D., et al.* Capacitive Behaviours of Phosphorus-Rich Carbons Derived from Lignocelluloses // Electrochim. Acta 2014. V. 137. P. 219–227.

УДК 66.081

ФОСФОРОВМІСНЕ ВУГІЛЛЯ – НОВИЙ ТИП ВУГЛЕЦЕВИХ АДСОРБЕНТІВ

О.М. Пузій, О.І. Піддубна

Інститут сорбції та проблем ендоекології НАН України, вул. Наумова 13,
03164, Київ, Україна,
e-mail: alexander.puziy@gmail.com

Резюме. *Наведено огляд нещодавніх досліджень фосфоровмісного вугілля. Показано, що характерною рисою фосфоровмісного угілля є кислі поверхневі групи типу фосфатів, які визначають адсорбційні, каталітичні та електрохімічні властивості. Фосфоровмісне вугілля є перспективним для водопідготовки, у каталізі та як електродний матеріал для конденсаторів подвійного шару.*

Ключові слова*: фосфоровмісне вугілля, порувата структура, хімія поверхні, електрохімічні властивості, каталітичні властивості.*

UDK 544.723:634.747:631.577:666.322

ADSORPTION KINETICS OF ANTHOCYANINS FROM ELDERBERRY EXTRACTS ON BENTONITE

L.M. Soldatkina, V.O. Novotna
Odessa I.I. Mechnikov National University, Dvoryanskaya Str. 2, 65082, Odessa, Ukraine
e-mail: soldatkina@onu.edu.ua

Abstract. *Adsorption kinetics of anthocyanins from aqueous extracts of elderberries on bentonite at various concentrations of anthocyanins, mass of bentonite, and temperature was investigated in this work. It was found that the equilibrium adsorption capacities and correlation coefficients for pseudo-second order model are much more reasonable than that of the pseudo-first order model.*

Keywords: *adsorption kinetics, anthocynians, bentonite, pseudo-first order, pseudo-second order*

Introduction. In recent years there is an increasing interest in anthocyanins as natural food colorants [1] and as substances with strong therapeutic effects (anti-inflammatory, anti-cardiovascular, anti-diabetic, anti-cancer) [2]. Anthocyanins are widely distributed in berries, flowers, fruits, vegetables, leaves, and roots. Among all fruits and vegetables, especially berries of dark red or dark blue colours have a very high content of anthocyanins. For example, total anthocyanin content in elderberries is between 2000-15600 mg/kg [3]. This makes the elderberries suitable raw material for extraction of anthocyanins on industrial scale.

Adsorption is one of the most effective methods of concentration, removal and purification of anthocyanins from plant extracts. However, data of anthocyanin adsorption on cheap adsorbents (for example, natural clay minerals) are extremely rare [4, 5].

The aim of this study was to get the kinetic curves of adsorption of anthocyanins from elderberry aqueous extracts using bentonite at various initial concentrations of anthocyanins, mass of bentonite, and temperature of extracts, in order to evaluate the capacity of bentonite to efficiently adsorb the anthocyanins and carry out mathematical modeling of adsorption using kinetic equations of pseudo-first and pseudo-second order.

Experimental. Fully ripe elderberries were harvested in Zhmerynka district of Vinnitsa region (Ukraine) in 2015. Berries were immediately frozen and kept at almost 20^{o}C prior to tests.

Extraction was carried out by adding the berries in 0.1M HCl (as 1:2=w:v) for 24 hours at 20^{o}C in the dark. Then the extracts of berries were separated from the berries by filtration through filter paper. Extracts of the berries were stored at 4^{o}C.

Bentonite ($Al_2O_3 \cdot 4SiO_2 \cdot H_2O$) was employed as the adsorbent obtained from Dashukovsky deposit (Ukraine). Before adsorption studies bentonite was pounded in a porcelain mortar and mixed with distilled water at 20°C. The resulting suspension of bentonite was maintained for 2 hours, and then the top layer of suspension was separated by decanting. The washed precipitate was then dried at 95°C.

Adsorption of anthocyanins was carried out in static conditions, shaking mixtures of anthocyanin extracts with bentonite at a agitation speed of 150 rpm. After adsorption, these mixtures were filtered out and total anthocyanin concentrations in extracts were determined by pH-differential method as mg cyanidin-3-glucoside per litre extract.

Results and discussion. The adsorption kinetics of anthocyanins from elderberry extracts on bentonite is shown in Fig.1. The equilibrium time of adsorption was approximately obtained at 150 min. The rates of adsorption removal of anthocyanins increased rapidly in the first 100 min, and then slowly increased, finally reaching equilibrium after 150 min.

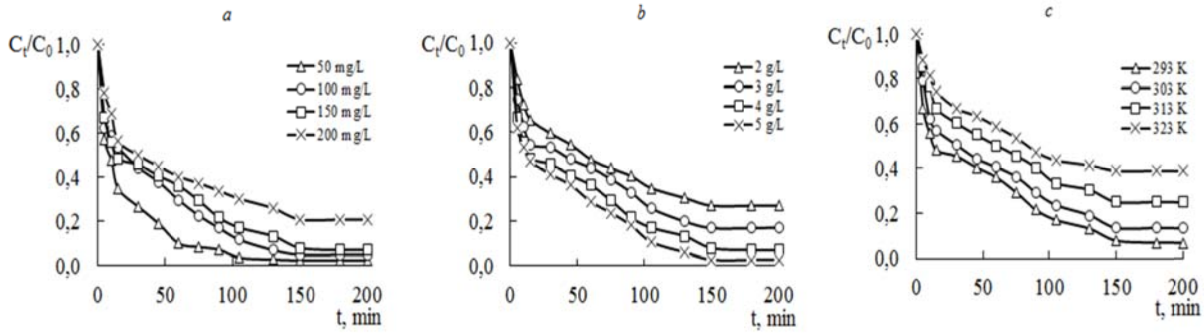

Fig.1. *Kinetic Adsorption Curves of Anthocyanines on Bentonite at Various: a - Initial Concentrations of Anthocyanins; b - Mass of Adsorbent; c - Temperature.*

Adsorption removal of anthocyanins decreased with increasing of temperature in the interval of 293–323 K as well as with increasing the initial dye concentration increases from 50 to 200 mg/L (Figs.1a and c). The adsorption at the all temperatures studied usually completed when the surface of clay is covered with a monolayer of anthocynians. After the equilibrium, the decrease in anthocyanin removal in the interval 293–323 K indicates the exothermic nature of adsorption. The adsorption capacity decreases with increasing temperature indicates that the adsorption process occurs through physical interactions. As seen from Fig.1b, removal of anthocyanins increased with increasing adsorbent mass from 2 to 5 g/L . This imply that the number of active sites of the adsorbent increase as parallel to increasing adsorbent mass.

It is known that bentonite carries a negative charge arising from isomorphous substitutions of certain atoms in their structure for other atoms of a different valence. For example, in the tetrahedral sheet, Si(IV) may be replaced by trivalent cations, or divalent cations may replace with Al(III) in the octahedral sheet. The negative potential of the adsorbent is compensated by the adsorption of anthocynian cations on its surface.

Two commonly well-known kinetic models (pseudo-first and pseudo-second order) were applied to the experimental kinetics data in order to investigate the behavior of elderberry anthocyanins on bentonite. According to the results, the theoretical values of equilibrium adsorption capacities of anthocyanins on bentonite calculated using pseudo-second order kinetic model were found to be the closest to the experimentally found values of equilibrium adsorption capacities (Table 1). The data shows that the regression coefficients for the linear plots of the pseudo-second order equation were higher than 0.98. It is clear that the equilibrium adsorption capacities and correlation coefficients for the pseudo-second order model are much more reasonable when compared with experimental results than that of the first pseudo-order model.

Table 1. Kinetic Parameters of Anthocyanin Adsorption from Elderberry Extracts on Bentonite

Parameter	**A_p^{exp}, mg/g**	**Pseudo-first order model**			**Pseudo-second order model**			
		A_p^{theor} mg/g	**$k_1 \cdot 10^2$, min^{-1}**	**R^2**	**A_p^{theor}, mg/g**	**$k_2 \cdot 10^3$, $\frac{g}{mg \cdot \text{min}}$**	**V_0, $\frac{мг}{г \cdot хв}$**	**R^2**
C, mg/L								
50	12.2	8.8	3.61	0.9722	12.9	8.33	1.3	0.9994
100	23.8	19.9	2.36	0.9496	26.4	1.77	1.2	0.9908
150	34.9	23.8	2.26	0.8506	38.9	1.09	1.6	0.9848
200	39.7	27.0	1.68	0.9825	43.5	1.07	2.1	0.9933
q, g/L								
2.0	55.9	39.5	1.64	0.9754	61.0	0.68	2.6	0.9872
3.0	41.5	33.5	1.97	0.9021	46.3	0.86	1.9	0.9809
4.0	34.9	23.8	1.64	0.9676	38.2	1.17	1.6	0.9848
5.0	29.2	35.8	3.34	0.7325	32.1	1.52	1.5	0.9887
T, K								
293	34.9	30,1	2.26	0.8506	38.2	1.17	1.5	0.9848
313	32.5	24.5	1.69	0.9696	36.3	1.04	1.3	0.9859
323	28.1	23.2	1.67	0.9575	32.8	0.89	0.9	0.9864
333	22.9	21.7	2.20	0.9529	27.0	1.11	0.8	0.9904

Conclusions. According to the results, bentonite is a suitable adsorbent for the removal of anthocyanins from elderberry acid aqueous extract. It was shown that rates of adsorption removal of anthocyanins increased rapidly in the first 100 min, and then slowly increased, finally, reaching equilibrium after 150 min. It was found that the pseudo-second order model appeared to be more promising than the pseudo-first order in describing the adsorption kinetics of anthocyanins from elderberry extracst on bentonite at various conditions.

References

1. *Delgado-Vargas F., Paredes-López O.* Natural Colourants for Food and Nutraceutical Uses, Boca Raton, CRC Press LLC, 2003.
2. *Denev P., Ciz M., Ambrozova G., Kratchanova M.* Solid-phase extraction of berries' anthocyanins and evaluation of their antioxidative properties // Food Chemistry. 2010. V. 123. P.1055–1061.
3. *Clifford M.* Anthocyanins – nature, occurrence and dietary burden// J. Sci. Food Agric. 2000. V. 80. P.1063-1072.
4. *Lopes T., Yaginuma S., Novy Quadri M., Quadri M.* Evaluation of Red Cabbage Anthocyanins after Partial Purification on Clay // Braz. Archives of Biology and Technol. 2011. V.54, № 6. P.1349-1356.
5. *Lopes T., Quadri M., Quadri M.* Recovery of anthocyanins from red cabbage using sandy porous medium enriched with clay// Appl. Clay Sci. 2007. V. 37. P. 97–106.

УДК 544.723:634.747:631.577:666.322

КІНЕТИКА АДСОРБЦІЇ АНТОЦІАНІВ З ЕКСТРАКТІВ БУЗИНИ НА БЕНТОНІТІ

Л.М. Солдаткіна, В.О. Новотна
Одеський національний університет імені І.І.Мечникова, вул. Дворянська, 2, 65082, Одеса, Україна,,
e-mail: soldatkina@onu.edu.ua

Резюме. *Досліджена кінетика адсорбції антоціанів з водних екстрактів бузини на бентоніті при різних умовах проведення експерименту (при зміні концентрації антоціанів, маси бентоніту, температури). Встановлено, що рівняння псевдо другого порядку краще описує експериментальні кінетичні криві адсорбції антоціанів на бентоніті, ніж рівняння псевдо першого порядку.*

Ключові слова: *кінетика адсорбції, антоціани, бентоніт, псевдо перший порядок, псевдо другий порядок*

UDC 637.142.2

WHEY AND WHEY PROCESSING

İ. Özdemir[1,2], S. Ötleş[2*], N. Kabay[1*], M. Yüksel[1]
[1]*Ege University, Faculty of Engineering, Chemical Engineering Department,*
Izmir, Bornova Turkey
e-mail: nalan.kabay@ege.edu.tr
[2]*Ege University, Faculty of Engineering, Food Engineering Department,*
Izmir, Bornova Turkey
**e-mail: semih.otles@ege.edu.tr*

Abstract. *Whey is a liquid by-product of the dairy industry produced during the manufacture of cheese and it contains more than half of the solids present in the original whole milk, including whey proteins (20% of the total protein) and most of the lactose, minerals, water-soluble vitamins and minerals. In recent years, whey has been recognized as a major source of nutritional and functional ingredients for the food industry. Commercial whey products include various powders, whey protein concentrates and isolates, and fractionated proteins, such as a-lactalbumin and b-lactoglobulin. The increased interest in separation and fractionation of whey proteins arises from the differences in their functional, biological and nutritional properties. For this reason, the aim of this work is first to put together all the necessary information about whey, its composition, properties, potential usages and describe the common methods of whey processing.*

Keywords: *whey, type of whey, whey composition, whey valorization, whey processing.*

Introduction. Whey is the liquid substance obtained by separating the coagulum from milk, cream, or skim milk in cheese making. Whey could be also obtained from curd formation by the direct acidification of milk. The whey stream contains approximately 6% of solids, mainly lactose, minerals, whey proteins, fat, and by-products of cheese (or casein) manufacture. The quality and compositions of the whey vary depending on the type of cheese (or casein) being produced and manufacturing practices [1-3].

Whey is used mainly as animal feed or discharged into the wastewater treatment plants, although it is rich in valuable components. It contains lactose, minerals (e.g., calcium, magnesium, phosphorus), vitamins, non-casein protein (except glycomacropeptide), and traces of milk fat. Because of its content of organic compounds, whey cannot be discharged to receiving environments. Therefore, it is necessary to process the whey even it may not be economic. Also, when its considered that on cheese making about half of the total milk finds its way into the whey, it is more understandable that the processing of whey and in particular its organic constituents are considered very important. Thus, recovery of valuable compounds such as protein and lactose from whey has received intense attention recently.

Worldwide whey production is estimated at around 180 to 190×10^6 ton/year; of this amount only 50% is processed. The whey can be considered as a valuable by-product with several applications in the food and pharmaceutical industries; however, it is often treated as a dairy wastewater. The treatment of whey represents a serious problem due to its high organic load, which can reach a chemical oxygen demand (COD) of 100,000 mg O_2 L^{-1} [4].

In Turkey, 5 major dairy companies that process 19% of Turkish raw milk are present, whereas there are hundreds of so called "mandras" possessing small traditional dairy processors which generate huge amounts of whey. Whey treatment processes include traditional techniques such as evaporating and drying which are widely employed in Turkish companies. These processes do not contribute to recovery of valuable products in whey. These methods are used to remove some part of the water in whey to diminish the volume and to enhance the keeping quality. Anaerobic treatment is another process employed for organics removal from whey. This process is preferred instead of conventional aerobic wastewater treatment since cheese whey has a very high organics content (60–80 g COD/L) and may impair biomass granulation during biological treatment. This would in turn result in biomass wash-out [5]. Further purification of whey can be achieved via ion exchange, affinity chromatography and selective precipitation. Recent developments in membrane filtration have provided exciting new opportunities for large-scale whey treatment to produce cleaner discharge as well as protein and lactose fractionation [6,7].

Type and Forms of Whey. The traditional whey is produced as a result of processes aimed at recovering casein, the principal protein of milk. Separation of casein from the rest of the milk (as in cheese making or production of industrial casein and caseinates) is usually accomplished by acidification to pH 4.5-4.8 or through the action of rennet, a casein-coagulating enzyme preparation. In acid coagulation, the pH is lowered either by microbial fermentation of the milk sugar lactose into lactic acid or by direct addition of a mineral (phosphoric, hydrochloric, sulfuric, etc.) or an organic (lactic, citric) acids. The fermentation route is most often used in the production of fresh cheeses, while the direct acidification is typical for production of industrial casein and caseinate products; in both cases, the resulting why is referred to as *acid whey*. In contrast, *sweet wheys* are obtained in manufacture of most hard and semihard cheeses for which the rennet coagulation principle is employed, as well as in production of industrial rennet casein. Since enzymatic clotting of milk by rennet occurs at pH 6.0 or higher, the lactic acid content of freshly obtained sweet whey is very low but may increase quickly if subsequent bacterial fermentation is not controlled by rapid pasteurization and/or by deep cooling [8,9].

*Whey Composition***.** Whey is a fairly dilute product with a total solids of about 6.5%. As mentioned before the solids are basically lactose, whey protein, ash, lactic acid and fat (Table 1).

Table 1. Whey Composition

Constituent	**Sweet Whey (%)**	**Acid Whey (%)**
Water	93-94	94-95
Dry matter	6-6.5	5-6
Lactose	4.5-5	3.8-4.3
Lactic acid	Traces	Up to 0.8
Total protein	0.8-1	0.8-1
Whey protein	0.6-0.65	0.6-0.65
Citric acid	0.1	0.1
Minerals	0.5-0,7	0.5-0.7
pH	6.4-6.2	5-4.6

***Source:** *www.dairyforall.com*

Possibilities of Whey Utilization. The whey can be considered a valuable by-product with several applications in the food and pharmaceutical industries.

From a valorization point of view, two different options in cheese whey (CW) management can be considered: the first one is based on the application of technologies to recover valuable compounds such as proteins and lactose. Currently, valorization processes applied to CW constitute the preferential option to treat this by-product, only exceeded by the production of powdered CW. The second option relies on the application of fermentation processes to obtain value added products such as: organic acids (e.g. lactic, succinic and propionic), single cell proteins and oils, biopolymers (enzymes, polyhydroxyalkanoates, exopolysaccharides) and bacteriocins. Sometimes whey permeate, obtained from ultrafiltration (UF) step, has been used as fermentation medium; in this case, both management options are applied.

The UF process produces a whey permeate rich in lactose (about 80% of the original lactose in milk) and nanofiltration (NF) or reverse osmosis (RO) processes can be applied for concentration of the lactose which can be applied in the sweet industry or in pharmaceutical fermentation procedures.

In addition to lactose, whey permeate containing other nutrients essential for microbial growth; so the possibility to use it as a fermentation medium to obtain high value products represents an interesting opportunity which must not be neglected. Moreover, whey permeate is an attractive source of oligosaccharides for potential application in human nutrition [10].

Among the different possibility of whey valorization, reported in Figure 1, individual whey protein purification and application of fermentation technology on whey permeate could be also considered [11].

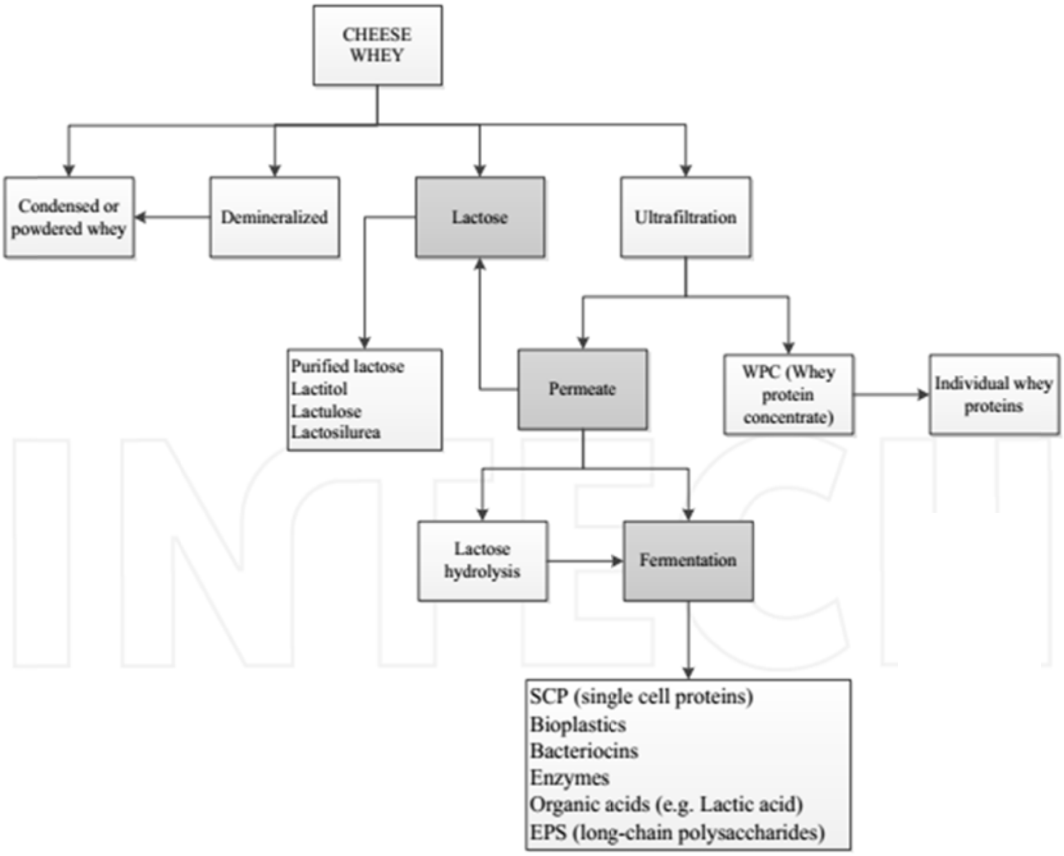

Fig. 1. *Scheme of Current Possibility of Whey Valorization [11].*

Industrial Processing of Whey. Processing of cheese whey was the first successful commercial application with several research initiatives underway to find uses of whey-waste. Since whey disposal is costly and problematic for cheese manufacturers; the focus is on techniques to convert this waste product into valuable functional components [12].

Whey processing is one of the most successful industrial membrane applications. For reasons of simplicity, urgency and the economics of disposal problem solution, UF of whey was the first application of membrane fractionation to reach a full commercial scale. The membranes used should be high yielding, resistant to physical, chemical and microbiological agents, unaffected by cleaning and disinfection materials [4,12]. Figure 2 shows a general scheme of possible membrane applications in whey treatment [13].

Applications of membranes in whey processing include **a)** concentration of whey 3 folds (24%) with RO and NF prior to evaporation and drying, **b)** manufacture of whey protein isolate (WPI) (90%), **c)** production of whey protein concentrate (WPC) (35-80% protein), **d)** converting the lactose to higher-value products by fermentation (e.g., ethanol or lactic acid) or by enzyme hydrolysis in continuous membrane reactors, **e)** fractionation of whey to value-added nutraceuticals, **f)** Microfiltration (MF) of whey as a pre-treatment for UF, and **g)** concentration and demineralization of whey and UF permeate with NF [10,13].

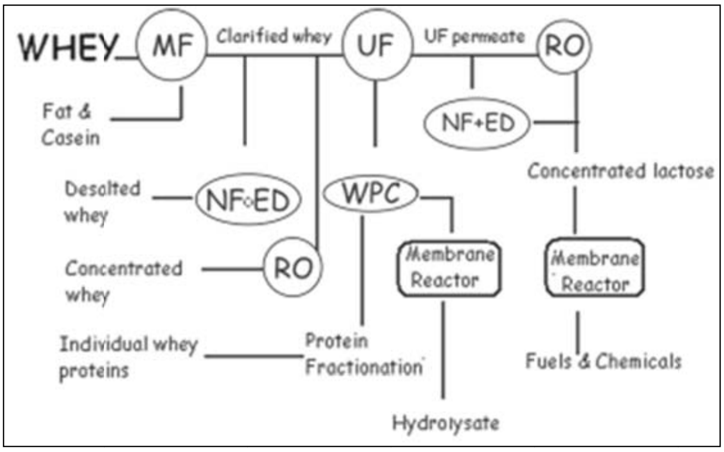

Fig.2. *Membrane Applications Used in Whey Processing [13]*

Conclusions. Whey is a very interesting by-product due to its components. Their properties, functions and chemistry structure make whey a great base for the creation of a series of new products or an ideal alternative compound to more traditional ones.

Membrane technologies have been commercially integrated in dairy industry and recently the new applications exist for extending their uses. Challenging developments in membrane processes should focus on efficient fractionation of minor whey components with desired biological and nutraceutical properties.

Acknowledgements. This research was supported by TUBITAK (Project no: 114M551).

References

1. *Patel M.T., Kilara A., Huffman L.M., Hewitt S.A. and Houlihan A.V.* Studies on whey protein concentrates: 1. Composition and thermal properties // Journal of Dairy Science. 1990. V. 73. P. 1434 – 1449.
2. *De la Fuente M.A., Hemar Y., Tamehana M., Munro P., Singh H.* Process - induced change in whey proteins during the manufacture of whey protein concentrates // International Dairy Journal. 2002a. V. 12 P. 361 – 369.
3. *De la Fuente M.A., Singh H., Hemar Y.* Recent advances in the characterization of heat - induced aggregates and intermediates of whey proteins // Trends Food Science and Technolology. 2002b. V. 13. P. 262 – 274.
4. *Yorgun M.S., Akmehmet Balcioglu I., Saygin O.* Performance comparison of ultrafiltration, nanofiltration and reverse osmosis on whey treatment // Desalination. 2008. V. 229. P. 204–216.
5. *Mockaitis G., Ratusznei S.M., Rodrigues J.A.D., Zaiat M., Forest E.* Anaerobic whey treatment by a stirred sequencing batch reactor (ASBR): effects of organic loading and supplemented alkalinity // J. Environ. Manage. 2006. V. 79. P. 198–206.
6. *Brans G., Schroen C.G.P.H., Van der Sman R.G.M., Boom R.M.* Membrane fractionation of milk: state of the art and challenges // J. Membr. Sci. 2004. V. 243. P. 263– 272.
7. *Zydney A.,* Protein separations using membrane filtration: New opportunities for whey fractionation // Int. Dairy J. 1998. V. 8. P. 243–250.

8. *Sheth H., Jelen P., Ozimek L., Sauer W.* Yield, Sensory Properties and Nutritive Qualities of Quarg Produced from Lactose—Hydrolyzed and High Heated Milk // J. Dairy Sci. 1988. V. 71, 2891.
9. *Jelen P., Renz-Schauen A.* Quarg Manufacturing Innovations and Their Effect on Quality, Nutritive Value and Consumer Acceptance // Food Techonol. 1989. V. 43. P. 74.
10. *Atra R., Vatai R.G., Bekassy-Molnar E., Balint A.* Investigation of Ultra- and Nanofiltration for utilization of whey protein and lactose // Journal of Food Engineering. 2005. V. 67. P. 325-332.
11. *Mollea C., Marmo L., Bosco F.* Valorisation of Cheese Whey, a By-Product from the Dairy Industry // Food Industry, Dr. Innocenzo Muzzalupo (Ed.), InTech, DOI, 10.5772/53159.
12. *Cuartas-Uribe B., Alcaina-Miranda M.I, Soriano-Costa E., Mendoza-Roca J.A., Iborra-Clar M.I., Lora-García J.* A study of the separation of lactose from whey ultrafiltration permeate using nanofiltration // Desalination. 2009. V.241. P. 244-255.
13. *Cheryan M.* Ultrafiltration and Microfiltration Handbook, Technomic Publishing Company, Lancaster PA., 1998. P. 527.

УДК 637.142.2

СИРОВАТКА ТА ЇЇ ПЕРЕРОБКА

İ. Özdemir[1,2], S. Ötleş[2*], N. Kabay[1*], M. Yüksel[1]

[1] *Егейський університет, факультет машинобудування, хіміко-технологічний факультет, Ізмір, Борнова Туреччина*
e-mail: nalan.kabay@ege.edu.tr
[2] *Егейський університет, інженерний факультет, кафедра харчової інженерії, Ізмір, Борнова Туреччина*
**e-mail: semih.otles@ege.edu.tr*

Резюме. Сироватка являє собою рідкий побічний продукт, який утворюється при виробництві сиру. У сироватці міститься більше половини твердих речовин, які є наявними у вихідному незбираному молоці, зокрема білки молочної сироватки (20% від загального білка), більша частина лактози, мінеральні речовини, водорозчинні вітаміни та мінерали. В останні роки, сироватка була визнана основним джерелом поживних речовин та функціональних інгредієнтів серед відходів харчової промисловості. Комерційні продукти, які виробляють із сироватки, – концентрати та ізоляти білків, а також фракціоновані білки, такі як α-лактальбумін і β-лактоглобулін. Підвищений інтерес до поділу і фракціонування сироваткових білків зумовлений відмінностями їх функціональних, біологічних та поживних властивостей. З цієї причини, метою даної роботи є, передусім, систематизація всієї необхідної інформації щодо сироватки, її складу, властивостей та потенціальних можливостей використання, а також огляд загальних методів переробки сироватки.

***Ключові слова**: сироватка, тип сироватки, склад сироватки, ревалоризація, переробка молочної сироватки.*

UDC 544.018.2: 544.472.3

INTERACTIONS IN THE SYSTEM AIR – WATER - NATURAL ALUMOSILICATES AND TECHNOLOGY FOR THE ACCELERATION OF SELF- REMEDIATION IN NATURAL WATER BASINS

K. Pershina, K. Kazdobin
V.I. Vernadsky Institute of General & Inorganic Chemistry NAS Ukraine, Kiev
Palladin Avenue, 32-34, 03680 Kiev, Ukraine
e-mail: kazdobin@ionc.kiev.ua

Abstract. *Mechanochemical origin of H_2O_2 formation in natural water basins due to interactions between water structures, air and minerals under dynamic conditions is discussed. Obtained results are proposed for design of the technology of water remediation using minerals with pre-assigned properties.*

Keywords: *water, air, mineral, hydrogen peroxide, remediation*

Introduction. Acceleration of self-remediation in natural water basins is aimed on pre-purification of water for its further utilization. Total water pollution stipulates the need to find competitive methods of water remediation in open basins. To realize these approaches it is necessary to study the mechanism of self-remediation of waters.

A common scheme of water remediation in natural basins is shown below. The scheme involves interaction of active oxygen forms with abiotic sources, such as minerals containing “life” redox- couples, biota and sunlight.

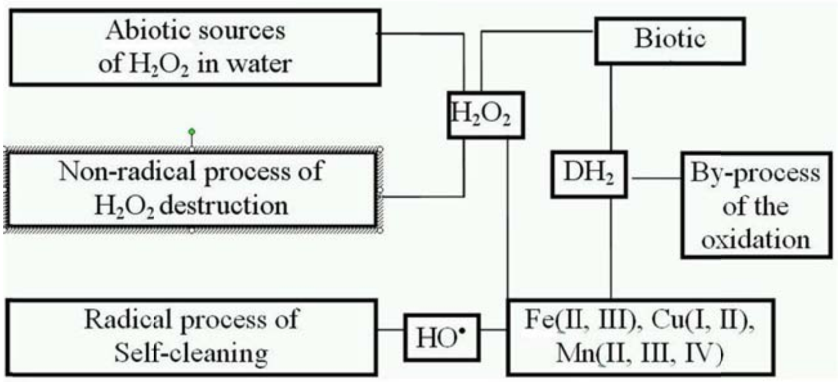

Fig.1. *Common Scheme of Water Remediation in Natural Basins*

The main oxidant in these processes is hydrogen peroxide, H_2O_2. This substance strongly affects lifetimes of many biogenic and anthropogenic trace pollutants. Hydrogen peroxide is produced in natural water, very low concentrations of this compound is found there [1, 2]. The highest H_2O_2 concentration is detected in rain waters, it reaches 5×10^{-5} M [2, 3]. Main amount of H_2O_2 is concentrated in ocean water. The concentration varies from 10^{-9} M near the coast and up to 5×10^{-7} M in coastal areas [3-5]. “Healthy” water basin needs $\approx10^{-6}$ M H_2O_2. Atmospheric processes are considered to be the main source of H_2O_2. Appearance of H_2O_2 in athnospheric condensation is explained as a result of photolysis of water vapor according to Fenton mechanism under the influence of short-wave radiation [6].

This approach has lots of contradictions. Self- remediation of water basin is the most efficient in winter (lack of light) and slows down at high temperatures. Fenton’s mechanism is offered for atmospheric redox reactions, it is realized under conditions of far ultraviolet (UV). Analysis of radical equilibriums (1-5) [7] shows decomposition of all water on the Earth. Really, the concentration of radicals in natural water is 10^{-25}-10^{-35} M [8].

$$Fe^{2+} + \bullet OH \rightarrow Fe^{3+} + OH- \tag{1}$$

$$E_0\,(\bullet OH/OH-) = 2.0\ V \tag{2}$$

$$H_2O_2 + \bullet OH \rightarrow HO_2\bullet + H_2O \tag{3}$$

$$E_0(HO_2\bullet/H_2O_2) = 1.44\ V \tag{4}$$

$$2H_2O \rightarrow 2\,H_2 + O_2 \quad E_o = 1{,}23\ V \tag{5}$$

Thus, UV-radiation plays only minor role in remediation of natural waters.

Other mechanism of remediation is mechanochemical decomposition of liquid water, which is assumed to be a dynamical polymer system. In other words, complex heterogeneous structure is characteristic for liquid water. This system is unstable under the influence of strain and stress vibrations.

Here, similarly to photolysis, the appearance of H_2O_2 in water is due to radical dissociation of water. In general, the mechanochemical transformations of water may be arranged [9] in the form of:

$$(H_2O)_n\left(H_2O_{\dots}H - \int -OH\right)(H_2O)_m \xrightarrow{+D_1(H-O)_{aq}} (H_2O)_{(n+1)}(H^+)+(OH^-)(H_2O)_m \tag{6}$$

Nowadays water is considered as a multiphase system [10]. Cluster structure of water is discussed now: it can be formed on supramolecular level [11] or as a result of bubble formation [12], Dynamic methods of water purification (so called "microbubble technologies") become more and more popular, since they are easy and free from chemical reagents. The aim of the work is quantitative determination of H_2O_2 concentration in the dynamic systems of water – air – mineral, establishment of the mechanisms of H_2O_2 generation *in vivo* in water, electrolyte solutions and minerals (solids are in a form of suspensions and coarse particles). These are necessary for further improvement of dynamic technologies for purification of water and self- remediation of natural water basins.

Experimental. Following liquids were used: pure water, 0.01 M Na_2SO_4 (hard water in the west of Ukraine) and modeling marine water. The modeling solution was prepared using dry marine salt, which was dissolved in distilled water. The salt content was 1.25, 2.50 or 3.75 mass %, respectively, it corresponds to water composition for the different Mediterranean areas. Mineral suspensions containing

0.1 - 0.5% of bentonite clays (Dashukovka deposit, Ukraine) were used, a particle size was less than 0.05 mm. River sand (Dnipro, 99.8% SiO_2) was also applied to investigations. Dynamic conditions were provided by stirring and fluidization [13]. A flow rate of the electrolyte or suspension through the measuring cell was ≈6 cm/s providing turbulent flow conditions.

The red-ox potential Eh was controlled with an ORP-200 portable Red-ox-meter HM Digital Inc. Experimental technique of cyclic voltammetry (CVA) and electrochemical impedance spectroscopy (EIS) was used for studies of red-ox properties of waters and slurries. The cyclic voltammograms were registered in a cell containing composite probe described elsewhere [14]. The sweep rate was 10 mV/s in the range of 1.8-0.5 V. The flow rate along the indicator spherical electrode was $1{,}28\times10^{-3}$ m/s. These hydrodynamical conditions provided turbulent flow through the sphere. Electrochemical impedance spectra (EIS) were measured using a two-electrode cell. An area of each platinum electrode was 1 cm^2, a distance between them was 1 cm. The measurements were carried out using an Autolab 30 electrochemical module (PGSTAT302N Metrohm Autolab) equipped with an FRA (Frequency Response Analyzer) assembly unit. The EIS were obtained within the frequency range from 10^{-2} to 10^6 Hz. The module was controlled by Autolab 4.9 according to the standard procedure with post-processing using Zview 2.1 program. Electrochemical phenomena were simulated by the equivalent circuit method.

The measurements were carried out in the temperature range of 16 - 36^0 C.

Results and discussion. Systematic voltammetric studies have shown that the wave of formation is observed in the anodic area [14-17]. This corresponds to the electrochemical reaction:

$$H_2O_2 - 2e \Rightarrow O_2 + 2H^+ \qquad (7)$$

Its value depends on flow velocity and the presence of minerals both in form of slurries and particulate beds. Concentrations of H_2O_2 were calculated from the value of this reproducible wave (Table 1). Table 1 show that under dynamic conditions the maximum conversion of oxygen dissolved in the water to its active form, from 10 to 13% is achieved in saline waters and in the presence of suspensions of alumosilicates. Its conversion in stagnant water is only 0.001%, and in moving water - about 0.01%. To explain obtained results, let’s consider the structure of different waters as electrolytes.

The EIS data for pure and saline water are represented at Figs 2. Obviously both pure and saline water (mixture of inorganic electrolytes) have heterogeneous structure in contrary to well organized 1:1 electrolyte, such as KCl (curve 4, fig. 1,b). The mechanisms of H_2O_2 generation in clusters are quite different. Regarding weakly saline water, dissolved oxygen molecule forms a cluster containing 22÷26 molecules of H_2O over it. Mechanical disturbance of such cluster yields H_2O_2:

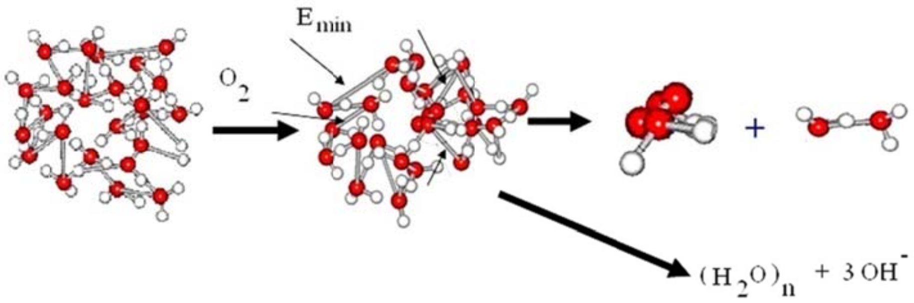

Table 1. H_2O_2 Content in Different Water Systems under Dynamic Conditions

System	**$[H_2O_2]$, M**
Water, stirring	1.7×10^{-6}
0.01 M Na_2SO_4, static (potable water)	$\approx10^{-8}$
0.01 M Na_2SO_4 stirring	$\approx8\times10^{-7}$
0.1% Bentonite C4T2k, 0,01 M Na_2SO_4 stirring	$1,7\times10^{-5}$
0.5% Bentonite C4T2k (H^+ form), 0.01 M Na_2SO_4 stirring	5.5×10^{-5}
Marine water, 1.25%	1.2×10^{-5}
Marine water, 2.50%	1.5×10^{-5}
Marine water, 3.75%	1.7×10^{-5}
Marine water, 1.25%, fluidized bed	2.3×10^{-5}
Marine water, 2.50%, fluidized bed	2.5×10^{-5}
Marine water, 3.75%, fluidized bed	4.1×10^{-5}

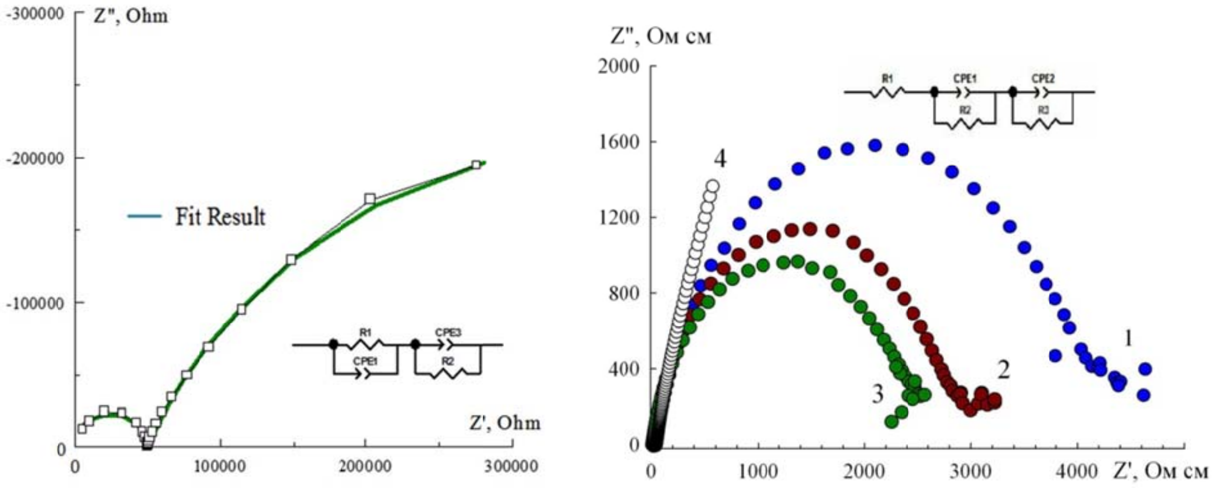

a b

Fig. 2. *EIS Spectra as Nyquist Plots and Equivalent Circuits for Electrolyte Solutions Simulating: a – Water after Reverse Osmosis; b - Marine Water of Concentration (%) 1 - 1.25; 2 - 2.5; 3 - 3.75, 4 - 0.1 M KCl, t=20 ^{0}C*

In marine water, dissolved gases form microbubbles (≈1 μm) [12]. Hydrogen peroxide is generated at multiple interfaces providing enhancement of mechanochemical reaction. In suspensions, dissolved oxygen is adsorbed on multiple interfaces of mineral particles forming multiple double electric layers [15]. Generation of H_2O_2 takes place in the sum of DLs.

Catalytic activity can be realized, when proton and electron are present simultaneously at the reactive site. Structure of minerals based on natural aluminosilicates involves ion channels, where transport of proton or electron is realized [18]. Clay minerals contain these channels, which also could be modified chemically. In addition, usually the measured redox potential (Eh = 0.6-0.8 V) in prevalent majority of natural waters. It coincides with redox potentials of H_2O_2 and minerals containing redox couples of Fe, Cu, Mn (Table 2).

Table 2. Electrochemical Potentials of Some Minerals in Water

Equilibrium	**E_{st} V**	**Processes or components**
$O_{2(s)} + 2H^+ + 2e(solv.) \rightarrow H_2O_2\ (aq)$	0.6824	Hydrogen peroxide formation
$2\ H_2O - 4\ e \rightarrow O_2\ (g) + 4H^+$ $E_a = 1.229 - 0.059\ pH$	1.229	Oxygen evolution (acid or neutral media)
$Fe_2O_3 + 6H^+ + 2e = 2Fe^{2+} + 3H_2O$	0,74	Mineral slurries
$Fe^{3+} + 1{,}5O_2 - 3e = FeO$	0,82	Mineral slurries
$Fe_2O_3 + 2H^+ + 2e = 2Fe_3O_4 + H_2O$	0,58	Mineral slurries
$2CuO - 2H^+ + 2e = Cu_2O + H_2O$	0,669	Mineral slurries
$CuO + H_2O + e = Cu(OH)_2$	<0,8	Mineral slurries
$2MnO_2 + 2H^+ + 2\ e = Mn_2O_3 + H_2O$	0,98	Mineral slurries

So, such ions as Fe, Cu, Mn in the structure of chemically modified clay enhance mechanochemical generation of H_2O_2.

Conclusions. Obtained results allow one to develop the technology for acceleration of self- remediation in natural water basins/ This technology should involve clay minerals with pre-assigned properties.

References

1. *Schumb W.C., Satterfield C.N., Wentworth R.L.* Hydrogen Peroxide, Reinhold Publ. Corp., NY, 1955.
2. *Cooper, W.J., Sulzman, E.S., Zika, R.G.* The contribution of rainwater to variability in surface ocean hydrogen peroxide //J. Geoph. Res.1987. V. 92.P. 2970 - 2978.
3. *Zika R.G., Saltzman E.S., Chameides W.L., Davis D.D.* H_2O_2levels in rainwater collected in South Florida and Bahama Islands //J. Geophys. Res.1982. V. 87.P. 5015-5017.
4. *Clark C.D., De Bruyn W.J., Hirsch C. M., Aiona P.*, Diel cycles of hydrogen peroxide in marine bathing waters in Southern California, USA //*Marine Pollution Bull.*, 2010. V. 60 P. 2284-2288.
5. *Clark C.D., De Bruyn W.J., Jakubowski S.D., Grant S.B.* Hydrogen peroxide production in marine bathing waters: Implications for fecal indicator bacteria mortality // Marine Pollution Bull., 2008. V. 56.P. 397-401.

6. *Gunz D.W., Hoffmann M.R.* Atmospheric chemistry of peroxides: a review // Atmospheric Environment. Part A. General Topics, 1990, V. 24. P. 1601-1633.
7. *Bard A.J., Faulkner L.R.* Electrochemical methods. Fundamentals and applications,N.-Y.: Willey. 2001.
8. *Duca Gh.*Ed.Ecological Chemistry: Latest Advances. Proceedings Ed.Gh.Duca.Cishinau.,2006.
9. *Gulyaev Yu., Yeremin S.M., Markov I.A. et al.* Chemical free modified water // Russ. J. Radioelectronics.2005. V. 11.
10. *Goncharuk V.V., Smirnov V.N., Syroyeshkin A.V., Malyarenko V.V.,*Clustersandgiganticheterophasewaterclusters //J. Water Chem. and Tech. 2007. V. 29. P. 3-17.
11. *Galashev A.E., Chukanov V.N., Galasheva O.A.*Dielectric Characteristics of O_2 $(H_2O)_i$and $(O_2)_2(H_2O)_i$Clusters. Computer-Aided Experiment // ColloidJournal.2006.V.68, P. 131-136.
12. *Bunkin N.F., Ninham B.W., Ignatiev P.S., et al.*Long-living nanobubbles of dissolved gas in aqueous solutions of salts and erythrocyte suspensions. // J. Biophotonics.2011. V.4, P. 150-164.
13. *Kazdobin, K., Shvab, N., Tsapakh, S.*Scaling-up ofFluidized Bed Electrochemical Reactors// J.Chem. Engineering. 2000.V. 79.P. 203-209.
14. *Pershina K.D., Kazdobin K.A., Poliichuk A.A., Kokhanenko V.V.* Electrochemical methods of hydrogen peroxide control in aqueous media under dynamic conditions // J. Water Chem.& Tech. 2016. V. 38. P. 71-76.
15. *Pershina K.D., Kokhanenko V.V., Masluk L.N., Kazdobin K.A.* Conductivity of aqueous Suspensions of Alumosilicates // J. Surf. Eng.& Appl. Electrochem. 2011. V. 47. P. 441-445.
16. *Pershina, K.D., Kokhanenko V.V., Masluk L.N., Kazdobin K.A*., Energy transformation in water and electrolytes containing oxygen // J. Surf.Eng.& Appl. Electrochem.2012. V.48.P. 90-96.
17. *Kazdobin K.A., Pershina K.D., Klyashtornaya O.S.* Generation of hydrogen peroxide in the seawater-air-mineral dynamic system // J. Water Chem.& Tech. 2015. V. 37.P. 242-247.
18. *Pershina K.D.* Heterogeneous redox - interactions in aqueous suspensions of natural alumosilicates, Thesis for a degree of Doctor in Physical Chemistry,Vernadsky Institute of General & Inorganic Chemistry NAS Ukraine, 2014.

УДК 544.018.2: 544.472.3

Взаємодії в системі повітря – вода – мінерал та технологія посилення самоочищення природних водоймищ

К.Д. Першина, К.О. Каздобін

Інститут загальної і неорганічної хімії ім. В.І. Вернадського НАН України.
пр. акад. Палладіна 32/34, 03680, Київ, Україна
e-mail: kazdobin@ionc.kiev.ua

Резюме. *Обговорюється природа механохімічної генерації пероксиду водню у природних водах, зумовлена взаємодією структури води з повітрям та частками мінералів в динамічних умовах. Отримані результати пропонуються для розробки технологій самовідновлення природних водойм.*

Ключові слова*: вода, мінерал, пероксид водню, самовідновлення*

UDC 544.725

NANOCOMPOSITE POLYSULFONE MEMBRANES WITH IMPROVED ANTIFOULING PROPERTIES

O. Dzhodzhyk, I. Kolesnyk, V. Konovalova, A. Burban

Department of Chemistry, National University of Kyiv-Mohyla Academy,
Skovoroda str. 2, 04655 Kyiv, Ukraine
e-mail: vita@ukma.kiev.ua

Abstract. The immobilization methods of nanoparticles of magnetite and tin oxide on membrane surface have been developed for improving the stability of polysulfone membrane to fouling. SnO_2 nanoparticles were deposited on the membrane by the method of "layer-by-layer" with using polyelectrolyte complexes of polyethyleneimine and carboxymethyl cellulose to provide them photocatalytic properties. Fe_3O_4 nanoparticles were covalently immobilized on the membrane using polyethyleneimine as a polymer spacer. It has been shown that the resulting nanocomposite membranes were characterized by improved transport properties in the ultrafiltration of protein solutions. Membrane resistance to fouling increased by reducing the effect of concentration polarization and increasing mass transfer coefficient.

Keywords: *nanocomposite membrane, membrane fouling, membrane modification.*

Introduction. Surface modification is an effective approach to obtain fouling-resistant membranes [1-5]. Numerous modification methods have been adopted to improve the antifouling properties of polymer membranes [2-3]. Hydrophilic moieties can be introduced on the membrane surface through covalent bonding via grafting or through physical interaction via coating [2]. The grafting method requires caustic chemical treatment or special equipment, which decreases the ease of membrane preparation. In the coating method, the stability of the coated hydrophilic layer on the membrane surface depends strongly on the physical affinity of the coating material with the membrane surface. The coated layer can easily be detached from the membrane surface by changes in the solution pH or by the application of back flushing during the filtration process [3-4]. Blending modification also can avoid the difficulties and short comings mentioned above and provide the ease of one-step modification.

In this work two different approaches were applied to modified polysulfone membrane with improved antifouling resistance. Firstly, photocatalytic membranes were developed by immobilization of SnO_2 nanoparticles (NP) on the polyethersulfone ultrafiltration membranes with “layer-by-layer” (LbL) technic. LbL assembly exploits the surface charge of polyelectrolytes to adhere suspended catalytic nanoparticles to a surface. This process includes two steps: i) applying polyelectrolytes (PE) on the surface, and then ii) exposing the polyelectrolyte-modified surface to a nanoparticle suspension to enable particle adhesion to the polyelectrolyte-coated surface. We have investigated the effect of SnO_2 nanocomposites on membrane performance, morphology, and antifouling properties during milk filtration without UV irradiation applying.

And secondly radically new method of suppressing fouling during ultrafiltration was developed by grafting a magnetically responsive nanolayer, consisting of hydrophilic polyelectrolyte chains grown from the surface of a thin film composite membrane. The magnetic nanoparticles were attached to the chain ends. In an oscillating magnetic field the chains oscillate. Movement of the magnetically responsive nanobrushes leads to mixing at low Reynolds number at the membrane surface and reduces concentration polarization effect [5].

Experimental. *Membrane modification by "layer-by-layer" method.* For membrane modification polyelectrolyte solutions were alternately deposited on the membranes for 15 min each with a water rinse between layers. Sodium polystyrene sulfonate (0.02 $mol \cdot L^{-1}$) was used as the first layer because it adsorbs well to polysulfone surface by hydrophobic interactions. Next layers were assembled of PEI (MW 750 kDa) as a positively charged polyelectrolyte and carboxymethyl cellulose (CMC) as negatively charged ones. They adsorbed to the previous layer via electrostatic interactions and van der Waals forces. The sonicated SnO_2 nanoparticles were used as the top layer, because they had negative charge at pH 6.5 and adsorbed to PEI layer, thus resulting in 3.5 layers.

*Membrane modification by magnetite nanoparticles***.** In the first step of the modification sequence, PES membrane disc were modified by reacting terminal hydroxyl groups with diepoxide EGDGE. The samples were placed into 50 mL of a 0.3 M EGDGE solution in the isopropanol–water azeotrope. After 15 min of incubation (wetting the pore surfaces) the reaction was catalyzed with 50 µL of 1 M KOH solution. The samples were incubated at room temperature for 15 h and then washed five times with deionized water. In the second step the epoxidized PES membranes were modified by polyethyleneimine as a nucleophilic reagent. Membranes were incubated in 0.5 % water solution of PEI for 1 h at room temperature. Nanoparticles were attached to the membrane surface by reacting carboxyl groups on the nanoparticle surface to the primary amine at the PEI chain via an amide linkage. Carbodiimide activated amide formation was used. 10 mg of 1-ethyl-3-(3-dimethylaminopropyl) carbodiimide was added to 10 mL of water and pour into a plastic jar containing a membrane disk for 10 min. Next, 5 mL of carboxyl shell Fe_3O_4 nanoparticles (4 g/L) were added and incubated in the dark for 4 h. Then, the membrane was removed, washed in water for 15 h.

Filtration studies. A dead-end stirred cell (Amicon-8050, MA) with a total cell volume of 50 ml and effective membrane area of 13.4 cm^2 was used for filtration experiments. The permeation flux of the membranes was determined by the volume of the permeate during a certain period of time. BSA water solutions with concentration from 0.1 to 5 % were used to study transport properties.

Results and discussion. Ultrafiltration experiments of BSA solutions at different concentrations have been carried out to determine the mass transfer coefficient for unmodified pristine membrane and membrane with immobilized nanoparticles. Fig. 1 shows the mass transfer coefficient for membrane with immobilized magnetic nanoparticles is $12.3 \cdot 10^{-6}$ m/s, which is a 1.64 times higher than for control membrane without nanoparticles. Mass transfer coefficient is the ratio of solute diffusion coefficient in our case to the BSA diffusion to bounding layer thickness. Since the diffusion coefficient under these conditions does not change, it is obvious that increase of the mass transfer coefficient occurs by reducing the thickness of the diffusion layer, which in turn depends on the criterion of turbulence Reynolds. And, therefore, the movement of magnetic nanoparticles in membranous layer creates additional turbulence, which reduces concentration polarization.

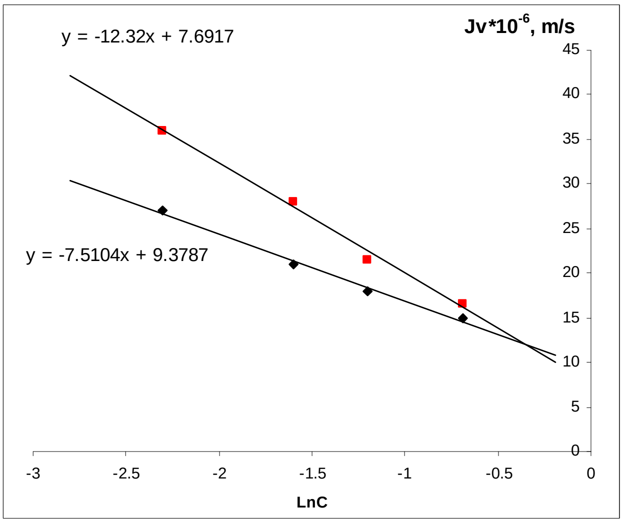

Fig. 1. *Determination of mass transfer coefficient by linearization of the concentration polarization equation for control membranes (●) and the membranes with immobilized magnetic NP (■).*

The permeate fluxes *vs.* applied pressure data obtained in the ultrafiltration experiments are shown in Fig. 2.

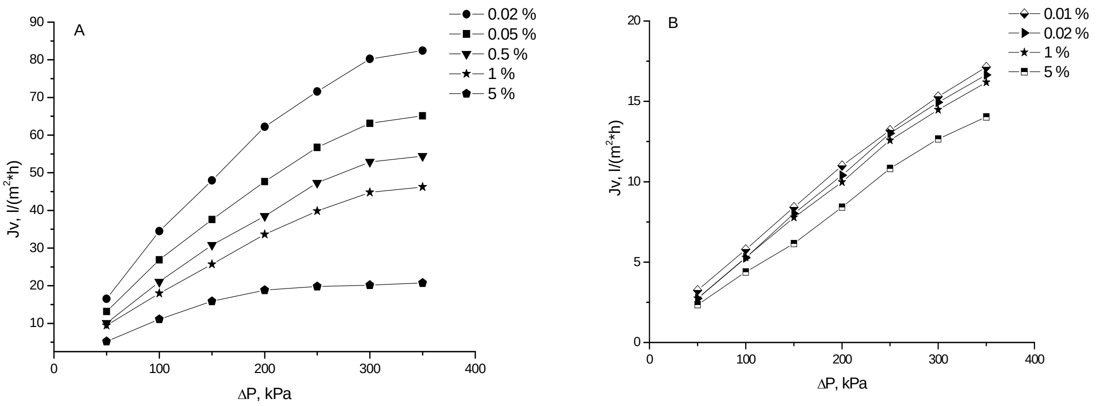

Fig. 2. *Permeate flux through (A) unmodified membrane, and (B) membrane with immobilized SnO_2 nanoparticles as function of the applied pressure and different BSA concentrations.*

For unmodified polysulfone membrane the permeate fluxes *vs.* applied pressure have well-known shapes. Permeate flux does not increases and the maximum flux is achieved at pressure equal to ca. 200 kPa (Fig. 2A) due to the formation of a concentration polarization boundary layer. Additionally, the maximum permeate flux decreases with an increase of bulk BSA concentration.

It is interesting, that for membranes with the immobilized SnO_2 NP the flux dependencies on applied pressure have different shape than for the unmodified membrane (Fig. 2B). It can be observed that membrane flux increased almost linearly with increasing pressure. It can be also noticed that for membrane with immobilized NP, the maximum permeate flux J_∞ is not achieved and does not depend on BSA concentration. It can be concluded, that the immobilization NP on the membrane surface reduces the concentration polarization effect due to photocatalytic reaction on the membrane surface.

References

1. *Wang P., Tan K.L., Kang E.T., Neoh K.G.* Synthesis, characterization and antifouling properties of poly(ethyleneglycol)grafted poly(vinylidene fluoride) copolymer membranes // J. Mater. Chem. 2001. V. 11. P. 783–789.
2. *Liu J., Shen X., Zhao Y.P., Chen L.* Acryloylmorpholine-Grafted PVDF Membrane with Improved Protein Fouling Resistance // Ind. Eng. Chem. Res. 2013. V. 52. P. 18392–18400.
3. *Kochkodan V., Johnson D.J., Hilal N.* Polymeric membranes: Surface modification for minimizing (bio)colloidal fouling // Adv. Colloid Interface Sci. 2014. V. 206. P. 116–140.
4. *Sui Y. , Wang Z.N., Gao C.J., Wan Q., Zhu L.P.* An investigation on the antifouling ability of PVDF membranes by polyDOPA coating, Desalin. Water Treat. 2012. V. 50. P. 22–33.
5. Himstedt H.H., Yang Q., Dasi L.P., Qian X., Wickramasinghe S.R. Ulbricht M. Magnetically activated micromixers for separation membranes // Langmuir. 2011. V.27. P. 5574–5581.

УДК 544.725

НАНОКОМПОЗИТНІ ПОЛІСУЛЬФОНОВІ МЕМБРАНИ З ПОКРАЩЕНОЮ СТІЙКІСТЮ ДО ЗАБРУДНЕННЯ

О.Я. Джоджик, І.С. Колесник, В.В. Коновалова, А. Ф. Бурбан
Центр мембранних досліджень, Національний університет «Києво-Могилянська академія», 04070, Київ, вул. Сковороди, 2
e-mail: vita@ukma.kiev.ua

Резюме. *З метою покращення стійкості полісульфонових мембран до забруднення розроблені методи іммобілізації наночастинок оксиду стануму та магнетиту на їх поверхні. Наночастинки SnO_2 наносили на мембрану методом "layer-by-layer" з використанням поліелектролітного комплексу поліетиленімін-карбоксиметилцелюлоза для надання їм фотокаталітичних властивостей. Наночастинки Fe_3O_4 були іммобілізовані на мембрані ковалентно за допомогою полімерного спейсеру поліетиленіміну. Показано, що отримані нанокомпозитні мембрани характеризуються покращеними транспортними властивостями у процесі ультрафільтрації білків. Стійкість мембран до забруднення збільшується за рахунок зменшення ефекту концентраційної поляризації та зростання коефіцієнту масопереносу.*

Ключові слова: *нанокомпозитні мембрани, модифікування мембран, забруднення мембран.*

UDC 66.081

CONCENTRATE MANAGEMENT FOR NF BRINE OF GROUND WATER USING ELECTROMEMBRANE (ED AND EDI) PROCESSES

E. Altıok[1], S. Bunani[1, 2, 3], D. İpekçi[1], N. Kabay[1*], M.Arda[2], M.Yüksel[1]

[1]*Ege University, Chemical Engineering Department, Faculty of Engineering, 35100, İzmir, Turkey*
[2]*Ege University, Chemistry Department, Faculty of Science, 35100 Izmir, Turkey*
[3]*Burundi University, Chemistry Department, Faculty of Science, Bujumbura, Burundi*
**e-mail: nalan.kabay@ege.edu.tr*

Abstract. *In this study, treatment of ground water used in a fruit juice company located in İzmir city by integrated nanofiltration (NF), electrodialysis (ED) and electrodeionization (EDI) methods was studied. For this purpose, the ground water obtained from the plant was treated by using two different NF membranes (NF-90 and NF-270). The brine from both NF membranes was fed to ED stack. The ED diluate was further treated by EDI process for ultrapure water production.*

Keywords: *Concentrate management, food industry, nanofiltration, electrodialysis, electrodeionization, water reuse*

Introduction. Water is generally used in food and beverage productions as direct ingredient during food production and/or cleaning. Moreover, food production and processing require large amounts of water at varying qualities. When it comes to direct ingredient, the quality of water has a significant impact on the quality and taste of food products [1].

Because of a wide gap between clean water sources and water demand, water reuse becomes a prevailing issue. The reuse of water means to valorize wastewater by increasing water supplies. Water reuse in food production will be more important by time due to increasing population [2, 3].

Generally, the water used in food industries is obtained from ground water treated by membrane filtration systems. However, membrane filtration systems produce two different streams with different water quality streams: Permeate which is clean water and concentrate (brine) that contains high level of pollutants. While permeate is used as clean water, concentrate is not even suitable to be discharged to surface water bodies [4]. Therefore, a further treatment step for concentrate management is needed [5].

In this study, application of electromembrane processes such as ED and EDI for post-treatment of NF brine of ground water was studied.

Experimental. After pre-filtration, ground water from a fruit juice plant was passed through a lab-scale cross-flow flat sheet membrane test system (SEPA CF II GE-Osmonics) by using NF membranes (Dow FilmTech NF-90 and NF-270) The flow sheet of membrane filtration system and the membrane characteristics were shown in Figure 1 and Table 1, respectively. Operation pressure was kept constant at 10 bar and the concentrate effluent was collected as ED process feed. Figure 2 and Table 2 show Tokuyama TS-1-10 model ED system and the membranes characteristics, respectively. During ED process, a 10 V of electrical potential was applied for NF brines. According to EDI feed water requirements, feed water conductivity should not be greater than 50 µS/cm, so ED process was run until the diluate compartment conductivity reached the required limit. In the following part of this work, EDI was applied at 10 V using the diluate of ED process with around 50 µs/cm of electrical conductivity. EDI flow sheet and resin characteristics were shown in Figure 3 and Table 3, respectively.

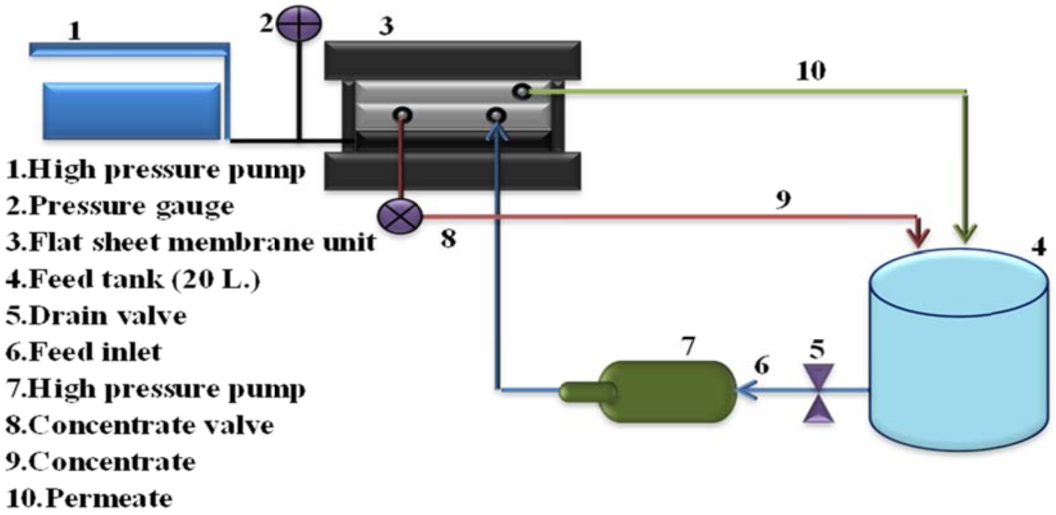

Fig. 1. *Flow Sheet of Lab-scale Cross-flow Flat Sheet Membrane Test System*

Table 1: Characteristic of NF Membranes

Membrane	NF-90	NF-270
Manufacturer	Dow FilmTech	Dow FilmTech
Membrane Type	Polyamide thin film composite	Polyamide thin film composite
Maximum Operating Pressure (bar)	41	41
Maximum Temperature (^oC)	45	45
Operating pH Range	3.0-10.0	3.0-10.0
Minimum NaCl rejection (%)	85<	97<
MWCO (Dalton)	200	400

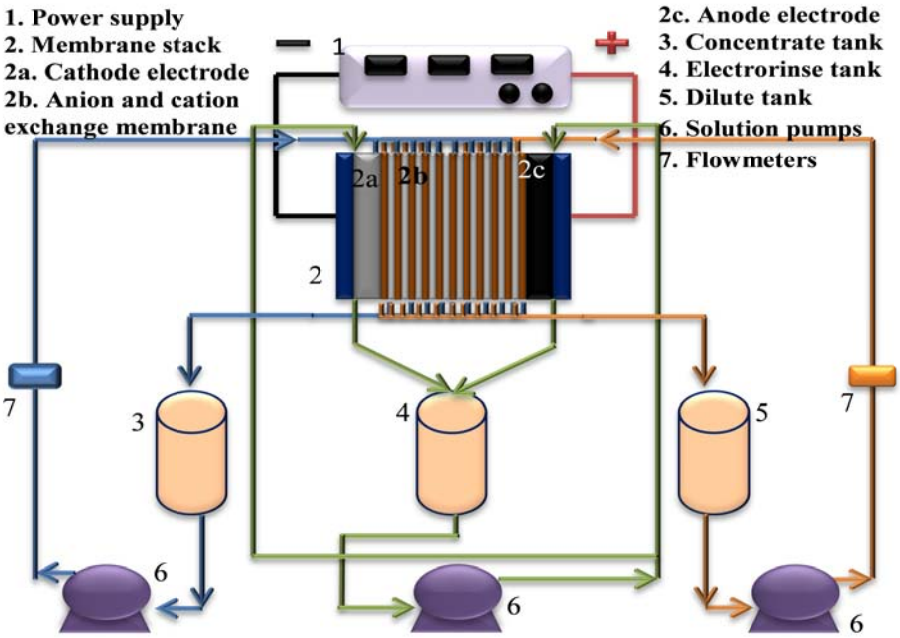

Fig. 2. *Tokuyama TS-1-10 Model Electrodialysis (ED) System*

Table 2. Properties of Ion Exchange Membranes Used in ED System

Membrane	NEOSEPTA CMX	NEOSEPTA AMX
Type	Strongly acidic cation permeable	Strongly basic anion permeable
Characteristics	High mechanical strength (Na-form)	High mechanical strength (Cl-form)
Electric Resistance (Ω -cm^2)	2.0 - 3.5	2.0 - 3.5
Burst Strength (kgf/cm^2)	3.5 - 6.0	4.5 - 5.5
Thickness (mm)	0.16 - 0.20	0.14 - 0.18
Application	Demineralization of whey, purification of organics, concentration of inorganics, demineralization of sucrose, desalination of ground water	Demineralization of whey, purification of organics, concentration of inorganics

Table 3. Properties of Ion Exchange Resins Used in EDI System

	Lewatit® UltraPure 1213 MD	Lewatit® UltraPure 1243 MD
Ionic form as shipped	H^+	OH^-
Functional group	Sulfonic acid	Quaternary amine, type I
Matrix	Crosslinked polystyrene	Crosslinked polystyrene
Structure	Gel type beads	Gel type beads
Appearance	Brown, translucent	Light brown, translucent

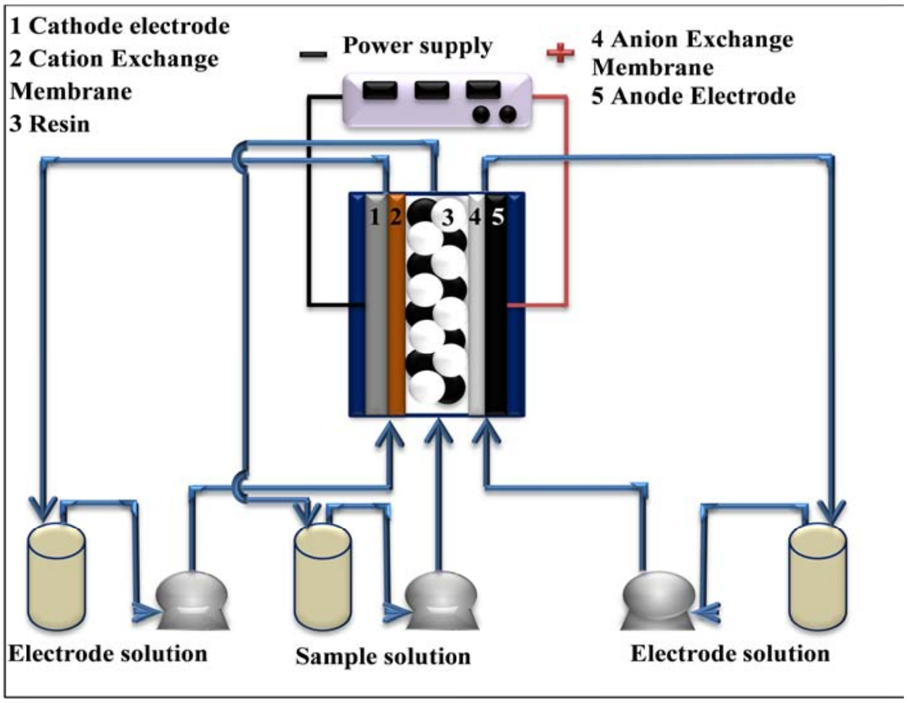

Fig.3. *Flow Scheme of Single Cell Electrodeionization (EDI) System*

Results and discussion. In this study, lab-scale cross-flow flat sheet membrane test system was used for collecting NF brine from ground water. The NF tests were performed at 10 bar and the collected brine streams are fed to ED system. In the second part of study, ED tests were carried out with brines of NF-90 and NF-270 membranes. According to the obtained results, the conductivity removals were 93% and 89% for the brines of NF-90 and NF-270 membranes, respectively in 30 min when 10 V of electrical potential was employed for ED tests (Figure 4).

In the next step of the work, EDI process was applied at 10 V using diluates of ED process with around 50 µs/cm of electrical conductivity. A 95% of conductivity rejection was obtained for ED diluate of NF-90 membrane brine in 75 min. The respective value was 78% in 105 min for ED diluate of NF-270 membrane (Figure 5).

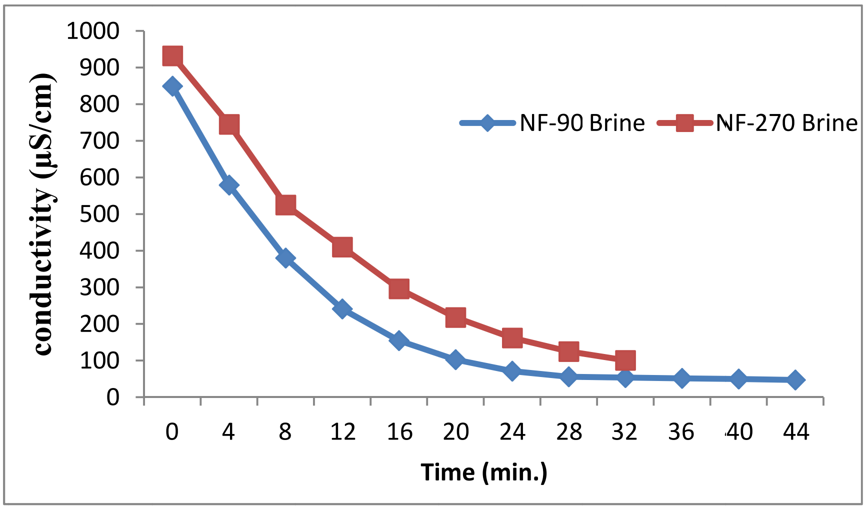

Fig. 4. *Conductivity Changes of NF Brines during ED Process*

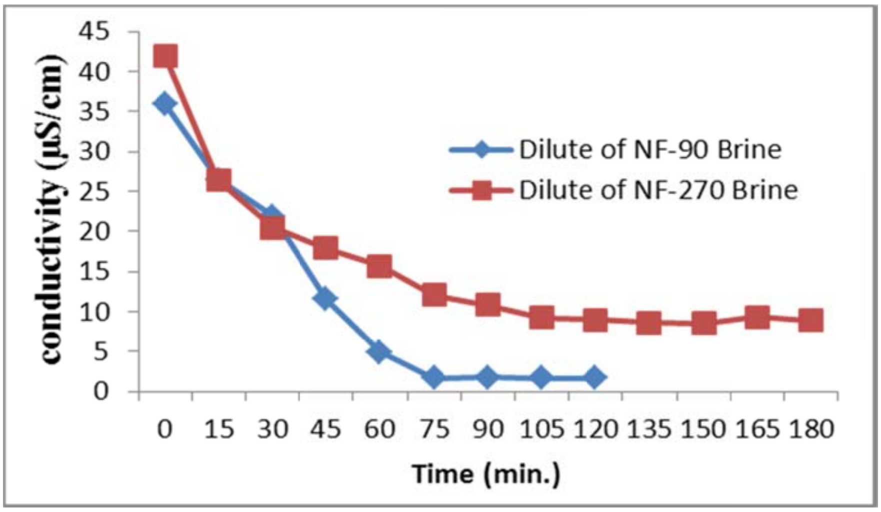

Fig. 3. *Conductivity Changes of ED Diluates of NF Membranes Brines during EDI Process*

The properties of feed, diluate and concentrate of each processes for both membranes are summarized in Tables 5 and 6.

Conclusions. The application of an integrated process based on ED and EDI processes for management of NF brines of ground water is a good strategy to decrease the amount of discharged part of water. It is possible to obtain a boiler feed water when EDI process is integrated with ED process by improving the product water quality.

Table 4: Characteristics of Water at Various Steps of Treatment of NF-90 Membrane Brine

			NF	ED		EDI	
Parameters	Unit	Ground-water	Brine	Concentrate	Diluate	Feed	Product
pH	-	7.62	8.48	7.88	4.16	8.37	6.78
Conductivity	µS/cm	771	791	1222	36.5	36.00	1.65
TDS	mg/L	377	387	606	17.6	16.92	0.78
Salinity	‰	0.38	0.39	0.61	0.02	0.02	0.00

Table 5: Characteristics of Water at Various Steps of Treatment of NF-270 Membrane Brine

			NF	ED		EDI	
Parameters	Unit	Ground-water	Brine	Concentrate	Dilute	Feed	Product
pH	-	7.82	7.89	7.44	8.09	8.31	5.54
Conductivity	µS/cm	873	888	1315	71.7	42.00	8.87
TDS	mg/L	428	436	653	33.7	19.74	4.17
Salinity	‰	0.43	0.44	0.66	0.03	0.02	0.00

Acknowledgements. This research was supported by TUBITAK (Project no: 114M551). We thank Dimes for the kind support to get ground water samples. The authors thank TUBITAK for PhD scholarship (TUBITAK-2235) for S.Bunani.

References

1. *Reynolds K.A.* The Importance of Water Quality to the Food Industry // Water Conditioning and Purification Magazine, 2002. P. 11,44.
2. International Life Sciences Institute (ILSI) Europe Expert Group on Water Safety Considering water quality for use in the food industry. Brussels, Belgium: ILSI, 2008.
3. *Kirby R.M., Bartram J., Carr R.* Water in food production and processing: quantity and quality concerns // Food Control, 2003. V. 14. P. 283–299.
4. *Van der Bruggen B.* Advances in electrodialysis for water treatment, in “Advances in Membrane Technologies for Water Treatment”, Woodhead Publishing, Elsevier Ltd, London, United Kingdom, 2015. P. 185-203.
5. *Xu P., Cath T.Y, Robertson A.P., Reinhard M., Leckie J.O., Drewes J.E.* Critical Review of Desalination Concentrate Management, Treatment and Beneficial Use // Environmental Engineering Science. 2013. V. 30. P. 502-514.

УДК 66.081

БЕЗПЕРЕРВНА ПЕРЕРОБКА РОЗСОЛУ НАНОФІЛЬТРАЦІЇ ГРУНТОВИХ ВОД З ВИКОРИСТАННЯМ ЕЛЕКТРОМЕМБРАННИХ (ЕД ТА ЕДІ) ПРОЦЕСІВ

E. Altıok[1], S. Bunani[1, 2, 3], D. İpekçi[1], N. Kabay[1*], M.Arda[2], M.Yüksel[1]

[1]Егейський університет, інженерний факультет, хіміко-технологічний факультет, Ізмір, 35100, Туреччина
**e-mail: nalan.kabay@ege.edu.tr*
[2]Егейський університет, факультет природничих наук, хімічний факультет, Ізмір, 35100, Туреччина
[3]Університет Бурунді, факультет природничих наук, Хімічний факультет, Бурунді.

Резюме. У даній роботі досліджували очищення грунтових вод, які використовуються підприємством з виробництва фруктових соків, що розташовано у місті Ізмір. Вивчали інтегровані методи нанофільтрації (НФ), електродіалізу (ЕД) та електродеіонізації (ЕДІ). Із цією метою, грунтові води, отримані із підприємства, обробляли з використанням двох різних НФ мембран (NF-90 і NF-270). Розсол з обох мембран NF подавали до ЕД установки. У подальшому, для отримання високочистої води, очищення ЕД діалізату здійснювали за допомогою ЕДІ.

Ключові слова: *безперервна переробка, харчова промисловість, нанофільтрація, електродіаліз, електродеіонізація, повторне використання води.*

UDC 544.726+546.791.6-381

SORPTION REMOVAL OF URANIUM (VI) COMPOUNDS WITH ORGANIC-INORGANIC ION-EXCHANGERS

N.O. Perlova[1], O.V. Perlova[1], I.Yu. Halutska[1], Yu.S. Dzyazko[2], A.V. Palchik[2], V.F. Sazonova[1]

[1]*I.I. Mechnikov Odesa National University, 2 Dvoryanska Str., 65082, Odesa, Ukraine,*
e-mail: n.perlova@yandex.ua

[2]*V.I. Vernadskii Institute of General and Inorganic Chemistry, NAS of Ukraine, 32/34 Palladin ave., 03142, Kyiv, Ukraine,*
e-mail: dzyazko@gmail.com

Abstract. Organic-inorganic composites based on ion exchange resins containing zirconium hydrophosphate (cation-exchanger) and hydrated zirconium dioxide (anion-exchanger) were applied to removal of soluble U(VI) compounds from modeling solutions. The advantages of the composites over the pristine resins are more significant sorption capacity, higher sorption rate and more facile regeneration.

Keywords: *organic-inorganic ion-exchangers, zirconium hydrophosphate, hydrated zirconium dioxide, uranyl ions, waste water treatment.*

Introduction. Purification of liquid wastes after processing of poor uranium-containing ores [1] is an actual ecological problem (maximal allowable concentration of soluble uranium compounds in waste waters is 0.015 – 0.6 mg dm^{-3} [2, 3]). Sorption is the most widespread method for removal of these highly toxic impurities from diluted aqueous solutions, the development of new effective sorbents is in a focus of attention. In addition to sorbents investigated earlier [4-6], organic-inorganic ion-exchangers are rather prospective [7]. These materials are characterized by higher sorption rate than the inorganic materials, moreover, they are more selective than ion exchange resins. The aim of the research is to estimate a possibility to use organic-inorganic cation- and anion-exchangers for removal of uranium (VI) compounds from modeling solutions of different composition.

Experimental. Aqueous solutions of uranium (VI) acetate were used ($2.0 \cdot 10^{-4}$ mol dm^{-3}). Additionally the solutions contained acid or salt (0.02 M H_2SO_4 or HCl or $NaHCO_3$). These reagents are used for treatment of uranium-containing minerals. Under these experimental conditions, uranium was in a form of cations in the chloride solution (98.3% of UO_2^{2+} and 1.6% of $[UO_2Cl]^+$,) [8]. The sulfate solution contained anionic and neutral complexes, such as $[UO_2(SO_4)]$ (46.3%) and $[UO_2(SO_4)_2]^{2-}$ (6.5%) and also UO_2^{2+} cations (46.3%). There were $[UO_2(CO_3)_2]^{2-}$ (87%) and $[UO_2(CO_3)_3]^{4-}$ (13%) in the carbonate solution. The modeling solutions were also used (g dm^{-3}): I – U(VI) (0.05),

$FeCl_3$ (0.25), HCl (0.73) (modeling waste waters of monazite processing), II – U(VI) (0.007), Cl^- (0.14), $NaHCO_3$ (0.46), Ca^{2+} (0.01), Mg^{2+} (0.07), SO_4^{2-} (0.04) (modeling carbonate mine waters), III – U(VI) (0.1), Ca^{2+} (0.5), Mg^{2+} (0.5), Fe^{3+} (0.5), Al^{3+} (2), SO_4^{2-} (15) (modeling technological solutions that are formed during the autopsy of poor uranium ores).

Dowex HCR-S cation exchange resin (*CR*) and EDE-10P anion exchange resin (*AR*) were applied to the investigations. Organic-inorganic sorbents, which had been obtained by modification of these resins with nanopartilces of zirconium hydrophosphate (*CR-ZHP*) or hydrated zirconium dioxide (*AR-HZD*), were also used. The synthesis conditions are given in Table 1.

Table 1. Modification Conditions and Sorption of U(VI) Compounds from Sulfate, Chloride and Carbonate Solutions (Sorbent Dosage Was 2 g dm^{-3})

Sorbent	**Reagents for modifications**	***S*, %**	**$t_{1/2}$, min**	**t_{eq}, min**	**$k \times 10^4$, s^{-1}**
Chloride solution					
CR	-	99.5±0.5	44	120	3.00
CR-ZHP-1	0.1 M $ZrOCl_2$ 1 M H_3PO_4	99.5±0.5	15	80	9.67
CR-ZHP-2	1 M $ZrOCl_2$ 1 M H_3PO_4	99.5±0.5	16	100	5.17
Carbonate solution					
AR	-	99.5±0.5	25	300	2.35
AR-HZD-1	0.1 M $ZrOCl_2$ 1 M NH_4OH	99.5±0.5	40	390	2.00
AR-HZD-2	1 M $ZrOCl_2$, 1 M NH_4OH	99.5±0.5	20	300	2.52
Sulfate solution					
AR	-	70.0±0.5	70	210	1.22
AR-HZD-1	0.1 M $ZrOCl_2$ 1 M NH_4OH	65.5±0.5	140	300	6.17
AR-HZD-2	1 M $ZrOCl_2$, 1 M NH_4OH	70.5±0.5	60	240	8.50

Sorption experiments were performed under static conditions with continuous shaking at 20±2^{0}C during 15–1800 min. The sorbent dosage was 2–10 g dm^{-3}. The solutions after sorption were analyzed with a photometric method using arsenazo III [9]. Sorption degree was calculated as:

$$S = \frac{C_0 - C}{C_0} \times 100,\% \qquad (1)$$

where C_0 and C are the initial and final concentration of uranium (VI) in the solution.

Desorption experiments were carried out by similar manner using 1 M H_2SO_4 or $NaHCO_3$ solutions. Desorption degree was determined via:

$$S_{des} = \frac{C_{des}}{C_0 - C} \times 100, \% \quad , \qquad (2)$$

where C_{des} is the concentration of uranium (VI) in the solution after desorption.

Results and discussion. Pristine ion exchange resins and organic-inorganic materials remove uranium (VI) compounds practically completely from chloride and carbonate solutions (see Table 1) as well as from the modeling solution II (Table 2), when the sorbent dosage is 2 g dm^{-3}. No additional correction of the pH is needed.

Table 2: Sorption of Uranium (VI) Compounds from Modeling Solutions

Sorbent	**Sorbent dosage, g dm^{-3}**	**pH**	***S*, %**	**$t_{1/2}$, min**	**t_{eq}, min**	**$k \times 10^4$, s^{-1}**
Modeling solution I						
CR	5	2	60.0±0.5	57	>1800	3.70
		4	99.5±0.5	20	180	4.03
	10	2	99.5±0.5	33	480	7.02
CR-ZHP-2	5	2	60.5±0.5	240	>1800	3.17
		4	99.5±0.5	28	150	5.08
	10	2	99.5±0.5	36	1440	8.67
Modeling solution II						
AR	2	8	99.5±0.5	25	120	6.58
AR-HZD-1			77.5±0.5	40	150	5.97
AR-HZD-2			99.5±0.5	25	120	5.28
Modeling solution III						
AR	5	2	79.0±0.5	35	100	4.72
AR-HZD-1			47.5±0.5	-	80	7.68
AR-HZD-2			76.5±0.5	40	120	4.55

The residual U(VI) content decreases down to maximal allowable concentration by this manner. More complete removal of U(VI) species from the model solution I requires optimization of sorption conditions: it is necessary to increase either the pH (up to 4) or the sorbent dosage. This optimization causes not only an increase of the *S* value, but also sorption acceleration. Sulfate solutions contain anionic and neutral complexes of U(VI) as well as uranyl cations. These species are not able to interact with anion exchange functional groups of the polymer constituent of the sorbents. Thus, the maximal sorption degree is not reached in the sulfate solutions, particularly from the modeling solution III.

Following kinetic characteristics for sorption of uranium (VI) compounds are given in Table 2: half-time of exchange ($t_{1/2}$), time of equilibrium (t_{eq}), constant of sorption rate (k) that was calculated using the first order equation:

$$ln\frac{C_t}{C_0} = -k \times t, \quad (3)$$

where C_t is the concentration under predetermined time.

The *CR-ZHP-1* sample, which was impregnated with a 0.1 M $ZrOCl_2$ solution before ZHP precipitation, is the most attractive from the point of view of sorption kinetics (in the case of chloride solutions). Regarding sorption of anions, the sample that have been saturated with more concentrated $ZrOCl_2$ solution for following ZHD deposition, is the most effective.

Composite ion-exchangers are regenerated easier and more complete than the pristine resins. The degree of uranium desorption from *CR* is 85 (using H_2SO_4 solution for regeneration) and 50% ($NaHCO_3$ solution). The S_{des} values are 90 (H_2SO_4) and 66% ($NaHCO_3$) for the *AR* sample. At the same time, the organic-inorganic ion-exchangers are regenerated more completely (S_{des}=90%) with the $NaHCO_3$ solution and the most completely (S_{des}=100%) with the H_2SO_4 solution. No change of sorption degree has been found for the composites after 5 cycles of sorption-regeneration.

Conclusions. Organic-inorganic ion-exchangers containing ZHP and HZD demonstrate more significant sorption ability towards soluble U(VI) compounds than the pristine resins. Depending on modification conditions, the composites show also higher sorption rate despite the inorganic constituents. This was shown particularly for the solutions, which model liquid wastes of uranium processing or mine waters. Other advantages of the organic-inorganic ion-exchangers are more facile regeneration and, as a result, a possibility of multiple application.

Acknowledgements. The work was supported by projects within the framework of programs supported by the National Academy of Science of Ukraine “Fundamental problems of development of new materials for chemical industry” (grant N 49/12).

References

1. *Gupta C., Singh H.* Uranium Resource Processing: Secondary Resources. Springer-Verlag, Berlin, Heidelberg, New York, 2003.
2. *Hodge H.C, Stannard J.N., Hursh J.B.* Uranium, Plutonium, Transplutonic Elements. Springer-Verlag, Berlin, Heidelberg, New York, 1973.
3. *Ostendorp D.* Uranium Concentration in Drinking Water from Small-scale Water Supplies in Schleswig-Holstein, Germany // Gesundheitswesen (Bundesverband der Arzte des Offentlichen Gesundheitsdienstes. 2015. V.77. P. 286-288.
4. *Yaroshenko N.A., Perlova O.V., Sazonova V.F., Perlova N. A.* Sorption of Uranium Compounds by Zirconium-Silica Nanosorbents // Russ. J. Appl. Chem. 2012. V. 85, N 6. P. 849−855.

5. *Perlova O.V., Sazonova V.F., Perlova N.A., Yaroshenko N.A.* Kinetics of Sorption of Uranium(VI) Compounds with Zirconium–Silica Nanosorbents // Russ. J. Phys. Chem. A. 2014. V.88, N 6. P.1012–1016.
6. *Perlova N.O., Sazonova V.F., Perlova O.V., DzyazkoYu.S., Polikarpov A.P.* New sorbents for removal of uranium(VI) compounds from diluted aqueous solutions // II Ukranian-Polish scientific conference "Membrane and Sorption processes and technologies" (Kyiv, December 2-4, 2015). Abstracts/ Eds.: Sobczuk H., Vakuliuk P. – Kyiv: NaUKMA, 2015. P. 165–166.
7. *Dzyazko Yu.S., Ponomaryova L.N., Volfkovich Yu.M., Trachevskii V.V., Palchik A.V.* Ion-exchange resin modified with aggregated nanoparticles of zirconium hydrophosphate. Morphology and functional properties // Micropor. Mesopor. Mater. 2014. V.198. P.55–62.
8. *Gapel G.* Speciation of actinides // Handbook of elemental speciation II. Species in the environment, food, medicine and occupational health / Eds. R. Cormelis, J.A. Caruso, H. Crews, K.G. Heumann. Chichester, UK: Wiley, 2005. P.509–563.
9. *Khan M.H., Warwick P., Evans N.* Spectrophotometric determination of uranium with arsenazo-III in perchloric acid // Chemosphere. 2006. V. 63. P. 1165.

УДК 544.726:546.791.6-381

СОРБЦІЙНЕ ВИЛУЧЕННЯ СПОЛУК УРАНУ (VI) ОРГАНО-НЕОРГАНІЧНИМИ ІОНІТАМИ

Н.О. Перлова[1], О.В. Перлова[1], І.Ю. Галуцька[1], Ю.С. Дзязько[2],
О.В. Пальчик[2], В.Ф. Сазонова[1]
[1]Одеський національний університет імені І.І. Мечникова, вул. Дворянська, 2, 65082, Одеса, Україна
e-mail: n.perlova@yandex.ua
[2]Інститут загальної та неорганічної хімії ім. В.І. Вернадського НАН України, Пр. Академіка Палладіна, 32/34, 03142, Київ, Україна
e-mail: dzyazko@gmail.com

Резюме. *Органо-неорганічні композити на основі йонообмінних смол, які містять гідрофосфат цирконію (катіоніт) та гідратований діоксид цирконію (аніоніт) застосовані для вилучення розчинних сполук U(VI) з модельних розчинів. Перевагами композитів у порівнянні з вихідними смолами є вища сорбційна ємність, більш висока швидкість сорбції, а також полегшена регенерація.*

Ключові слова: *органо-неорганічні іоніти, гідрофосфат цирконію, гідратований діоксид цирконію, йони уранілу, очистка стічних вод.*

UDC 544.6.018.22

THE NATURE OF INTERPHASE POTENTIAL UNDER FORCED MOVEMENT OF THE PROTON IN WATER/OXYGEN SYSTEM

K.D. Pershina
Joint Department of Electrochemical Energy Systems, Vernadsky av. 38a,
Kiev -142, 03680 Ukraine
e-mail: katherinepersh@gmail.com

Abstract. *The effect of oxygen bubbles on the formation of the membrane interfacial potential under microgravity in water media was considered. The braking of the proton motion and changes of pH under microgravity in water/oxygen systems depend on the O_2 gas bubble size distribution, that have a much larger variance in acid solutions than in basic solution.*

Keywords: *membrane, proton, oxygen, interphase potential*

Introduction. The main point that has to be considered in the water management is the behavior of the proton in presence of oxygen and porous membrane. This is ideal since the electrode needs to remain hydrated to promote high levels of proton transfer in presence of O_2 and is especially important for design of effective portable fuel cells [1]. In such case the water transfers protons through the membrane due own structure and exchanging of pressure in porous media [2, 3]. The presence of dodecahedral substitutional sites in the structure of liquid water promotes the hydration of individual water molecules, introduced into these cavities [4, 5]. The substitution of water molecules by oxygen molecules change the structure of existing hydrated complexes of water with change in degree of proton-donor activity and the transport of oxygen to the cathode. These effects increase in the presence of porous membrane.

The aim of this work is to study the effect of oxygen bubbles on the formation of the membrane interfacial potential under microgravity in water media.

Experimental. In the experiment distilled water, degassed for 1.5 - 2 hrs by refluxing was used. Water (80 - 85 ^{0} C) was placed in a sealed measuring cell, which was cooled to 20±2 ^{0}C then pH and redox - potential Eh were measured. Temperature settings were selected according to the oxygen solubility in water (at 80 ^{0}C virtually no dissolved oxygen) ($[O_2] \approx 10^{-7}$ M), whereas at 20 ^{0}C $[O_2] \approx 3\times10^{-4}$ M. The mechanical action exerted on the water by filtration through filters of different structure. The measurements were performed on ion-meter EV-74 with glass and platinum electrode and Ag/AgCl reference electrode with measurement error ± 5%. The standard and isolated from the air thin-layer cell with the water layer thickness of 0.5 mm were used for measurements. The experiment was conducted in two stages. First, the initial pH and Eh were measured in the degassed distilled water. In the second step into the cell with degassed water fed oxygen for one minute. Oxygen was bubbled through a saturated NaOH solution to remove CO_2. Then measurements of pH and Eh were repeated.

The microtexture of samples was studied using the SEM Mira 3 FESEM Tescan USA Inc. with high resolution on the cathode with field emission SEM HV - 10 KeV and automatic measurement in the image.

Magnetization of the water was performed with an inhomogeneous magnetic field intensity H = 0.074 Tl during 30 s.

Results and discussion. The shift of Eh potential values of degassed water in the cathode region after filtration through membranes with various nature and pore size was experimentally found (fig. 1). In the absence of concentration changes, it formally indicates the decrease in oxygen content [6]. And in this case, a change in the redox potential is possible due to the impact of double electric layer, DL, at the interphase of the water cluster/amorphous water/membrane surface, i. e interphase potential, caused by the forced movement of the proton across porous membrane. It's known that the electrical surface potential of pure water arise due to the net alignment of the dipole and quadrupole moments of water molecules at the interface and only changes in the surface potential can be measured experimentally, the small surface potential of pure water is not easily determined. The general sign convention for the surface potential is taken as measured from the air into the solution and the electrical surface potential is estimated to be between 0.1 and 0.2 V, corresponding to having the water hydrogens pointing slightly toward the bulk [7].

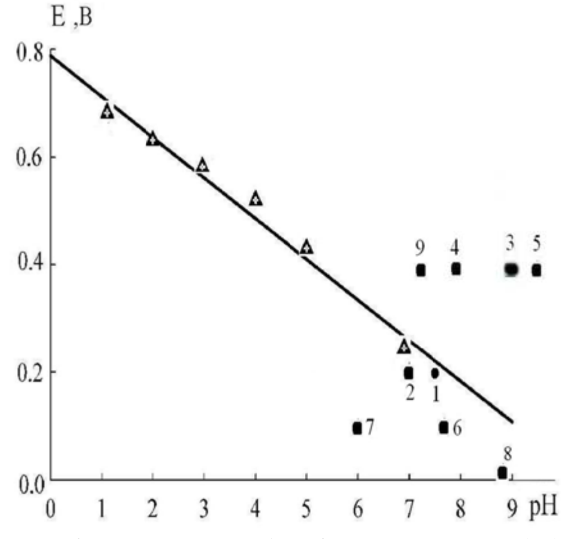

Fig. 1. *Isoelectric Point of Various Kinds of Water, Passed through Membranes of different Pore Size and Nature. Etalon - 0.01M Solution of NaCl with* O_2 *(▲).*
(1- Distilled Water; 2- Distilled Water without Oxygen; 3- Distilled Water without Oxygen, Passed through Polymer Membranes with pore size of 11-12nm ; 4- Distilled Water without Oxygen, Passed through Paper Membranes with Pore size of 200 nm; 5- Distilled Water Containing Oxygen, Passed through Polymer Membranes with Pore Size of 11-12 nm ; 6- Tap Water; 7 - Distilled Water Containing Carbon Dioxide ; 8 - Magnetized Distilled Water ; 9 - Distilled Water without Oxygen, Passed through Paper Membranes with Pore Size of 300nm).

In this case, the proton electrochemical potential can be expressed by the equation given by Nernst - Peters [7]:

$$\Delta\overline{\mu_{H^+}} = F\Delta\varphi - 2{,}3RT\Delta pH \qquad (1)$$

where ΔpH - interphase gradient of pH (or the concentration of protons) and Δφ - an electric potential difference at the phase interfaces (capacity of the DLs). The equation shows that the electrochemical potential difference of H^+ consists of two components - the concentration (pH gradient) and electrical (Δφ). The value of $\Delta\overline{\mu_{H^+}}$ can be regarded as the force acting on the protons, which determines the flow of H^+ across interphase border. If we taken the resulting potential to one coulomb of electricity, we get specific electromotive force (EMF) for the proton transfer:

$$\Delta E_{H^+} = \frac{\Delta\overline{\mu}}{F} = \Delta\varphi\frac{2{,}3RT}{F}\Delta pH \qquad (2)$$

Fixed experimental changes in pH and Eh potential values and the values of the isoelectric points removal corresponds to the mathematical regularity eq.2. If the pH removes in the basic site, the values of ΔE_H^+ increases with increasing of the ΔpH. It has created energy barriers for oxygen motion in this case. Thus, the membrane, under conditions of lack of dissolved oxygen, "encapsulates" it within a clusters, i.e. it translates into a molecular - dissolved state and eliminates the effect of proton EMF. In equilibrium state, the active (electrical) proton flux at the interphases is balanced by a passive flow of H^+ (concentration gradient). The stationary state is reached usually for 100 – 200 s.

The occurrence of the interphase potential explains the absence of differences in the values of the redox potential in the conditions of pH change by passing degassed water and water containing oxygen through the track (nano-scale) membrane (Fig. 2). The small pore sizes (11-12 nm) cause higher Laplace pressure values in this case.

$$P_L = \frac{2\sigma}{R} \qquad (3)$$

where σ - the surface tension, R - the pore radius of curvature.

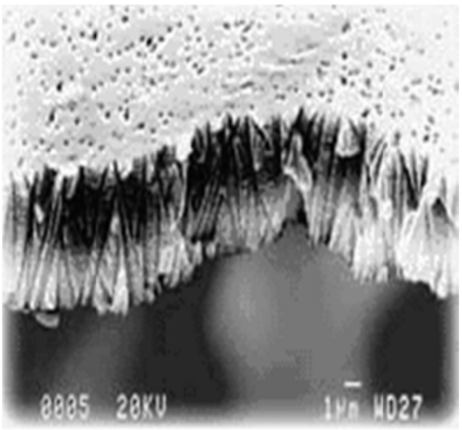

Fig. 2. *Electron Micrograph of the Track Membrane*

Taking into account that the bubble O_2 gas forms closed the membranes surface due to natural convection and that under microgravity environment the bubble curtain thickness increases with decreasing electrode potential, the O_2 gas bubble size distribution shows a much larger variance in acids solution than in basic solution under microgravity. The variance increases from ±0.05mm at −0.4V to ±0.2 mm at −0.8 V. [8]. And when the pore sizes are smaller than the size of the bubble the curvature radius increases exponentially, as result - the elimination of concentration component. Then according to the equation $2\ \Delta pH = 0$ and interfacial potential value becomes zero.

The presence of dissolved oxygen increase the concentration of protons at the interface of the oxygen / water, that causes the proton concentration gradient (fig 3). So to mitigate this effect the external pressure P_0 on the surface of the membrane should be increased or the pore size is to be increased, too.

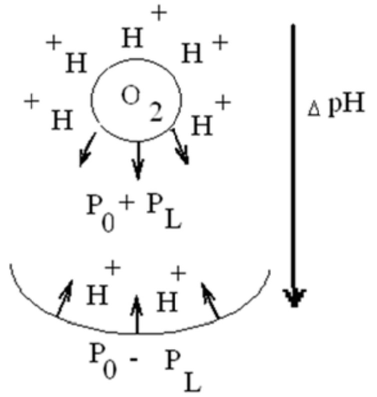

Fig. 3. *The Mechanism Scheme of the Proton Gradient Formation within the Nanoporous Membrane in the Presence of O_2 Bubble (External Pressure – P_0, Laplace Pressure- P_L).*

Conclusions. The membrane, under conditions of lack of dissolved oxygen, translates oxygen bubbles into a molecular - dissolved state and eliminates the effect of proton EMF. Changes of pH under microgravity in water/oxygen systems depend on the O_2 gas bubble size distribution, that have a much larger variance in acids solution than in basic solution. Modeling of cross-border potential have shown that when the pore sizes are smaller than the size of the bubble the curvature radius increases exponentially, as result - the elimination of concentration component and cross-border potential value becomes zero. This model is in agreement with experiment. If the porous size larger than size of oxygen bubbles –the cross-border potential is decreased. In case of the smaller porous (the smaller than bubble size) is observed an increase in concentration of the protons at the oxygen / water interphase. So to mitigate this effect should be increased external pressure P_0 on the surface of the membrane or increase the pore size.

References

1. *Paganelli G, Guezennec Y.G., Rizzoni G., Moran MJ.* Proton exchange membrane fuel cell system model for automotive vehicle simulation and control. // Journal of Energy Resources Technology-Transaction of the ASME. 2002. V. 124. P.20-27.
2. *Carrette U. S. L., Friedrich K. A.* Fuel cells: Principles, types, fuels, and applications.// Chem.Phys.Chem, 2002.V. 1:P.162-193.
3. *Pilatowsky I., Romero R.J., Isaza C.A., Gamboa S.A, Sebastian P.J., Rivera W.* Cogeneration Fuel Cell-Sorption Air Conditioning Systems. Springer. 2011. XIV 160 p..
4. *Kanno H. , Yokoyama. H., Yoshimura Y.* A new interpretation of anomalous properties of water based on Stillinger's postulate // J. Phys. Chem. 2001. V. 105, P. 2019- 2026.
5. *Chen B*. Hydrogen bonding in water. Phys. Rev. Lett. 2003. V. 91. P. 215503-215515.
6. *Kazdobin K.A., Pershina E.D., Kokhanenko E.V., Duma V.Yu.* Electrochemical Behavior of Diluted Aqueous Electrolytes Contaning Oxygen after Superimposition of Mechanical Effects // J.Water Chem.&Techn. 2009. V.31. P. 177-185.
7. *Petersen P. B., Saykally R. J.* On the nature of ions at the liquid water surface// Annu. Rev. Phys. Chem. 2006. V.57. P.:333–64.
8. *Matsushima H, Fukunaka Y., Kuribayash K.* Water electrolysis under microgravity Part II. Description of gas bubble evolution phenomena // Electrochimica Acta. 2006. V. 51. P. 4190–4198.

УДК 544.6.018.22

ПРИРОДА ТРАНСГРАНИЧНОГО ПОТЕНЦІАЛУ ПІД ЧАС ПРИМУСОВОГО РУХУ ПРОТОНУ В СИСТЕМІ ВОДА-КИСЕНЬ

К. Д. Першина
Міжвідомче відділення електрохімічної енергетики НАН України, проспект Вернадського 38 а, Київ -142,03680, Україна
e-mail: katherinepersh@gmail.com.

Резюме. *Розглянуто вплив бульбашок кисню на формування мембранного потенціалу на межі розділу фаз в умовах мікрогравітації у водних середовищах. Показано, що усунення руху протонів і зміни pH при мікрогравітації в системі вода / кисень залежить від розподілу розмірів бульбашок газу O_2, які мають набагато більшу дисперсію в розчині кислоти, ніж в лужному розчині.*

Ключові слова: *мембрана, протон, кисень, трансграничний потенціал.*

UDC 544.622+544.725.2

ELECTRODEIONIZATION REMOVAL OF $HCrO_4^-$ IONS FROM DILUTED SOLUTION. EFFECT OF MEMBRANE

Yu.S. Dzyazko[1], Ö. Arar[2], L.M. Rozhdestvenska[1], S.L. Vasilyuk[1]
[1]V.I. Vernadskii Institute of General and Inorganic Chemistry,
Palladin Ave. 32/34, 03680, Kyiv, Ukraine
e-mail: dzyazko@gmail.com
[2] Ege University, Faculty of Science, Department of Chemistry, Ege University,
Izmir 35100, Turkey
e-mail:ozgur.arar@ege.edu.tr

Abstract. *Transport of chromate ions in the systems involving granulated ion-exchangers and anion-exchange membranes of different origin was researched under various voltage. The role of the membranes as sorption barrier was considered. The method that allows one to estimate mobility of sorbed ions through ion-exchanger bed has been proposed. Electrodeionization of Cr(VI)-containing solution using inorganic ion exchange materials was studied.*

Keywords: *chromium, electrodialysis, electrodeionization, inorganic membrane, hydrated zirconium dioxide.*

Introduction. Electrodeionization (EDI) is a prospective technique for discontinuous desalination of diluted solutions [1, 2]. This method combines ion exchange and regeneration of the ion exchange resin due to ion transport through the packed bed and membrane. For instance, EDI can be applied to permeate [4], removal of toxic components (Ni^{2+} [5], Cu^{2+} [6], Cd^{2+} [7]) from water. The recovery of oxidizing ions ($HCrO_4^-$) is complicated by their interaction with ion exchange resins and polymer membranes [8-10], whereas ion transport through the inorganic membranes, which are stable against oxidation, is affected by concentration polarization [9]. The aim of the work was to establish regularities of $HCrO_4^-$ transport in the system of ion-exchanger and membrane in order to optimize the EDI process. This process has to involve ion exchange materials that are stable against oxidation.

Experimental. Such ion-exchange materials as *Dowex Marathon 11* anion exchange resin (*Dow Chemical*), granulated hydrated zirconium dioxide (synthesized similarly to [8]) in a form of hydrogel (*HZD*), *AMI-7001* polymer anion-exchange membrane (*Membrane International*), ceramic membrane modified with xerogel of hydrated zirconium dioxide were applied to investigations. The work involved electroregeneration of ion-exchangers, which were loaded preliminarily with chromate anions (no loading was provided for the membranes), and EDI using the inorganic ion-exchanger and membranes. The EDI stack is described in [8, 9], *Nafion-117* (*DuPont*) cation exchange membrane was used for separation of the cell compartment filled with ion-exchanger from the cathode chamber. The electrode compartments were filled with 0.1 M H_2SO_4 solutions.

Results and discussion. *Electroregeneration: polymer anion-exchange membrane and anion exchange resin.* The dependencies of $HCrO_4^-$ amount in the anolyte ($n_{Cr,a}$) on time (τ) show induction period, which corresponds to accumulation of ions in the anion-exchange membrane (Fig. 1). The initial flux of ions through the membrane ($N_{Cr,m}$) is not proportional to potential gradient though the resin bed ($grad\overline{E}$). It means, mobility of the species though the ion-exchanger ($\overline{u}_{Cr}$) cannot be determined from the $N_{Cr,m}-grad\overline{E}$ curve, as suggested in [11].

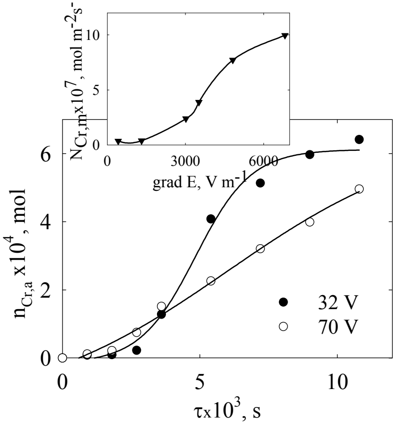

Fig. 1. *Dependence of $HCrO_4^-$ Amount in the Anolyte on Time. Insertion: Flux of These Species through the Polymer Membrane as a Function of Potential Gradient through the Bed of Anion-Exchange Resin. $\overline{C}_{Cr}$=41 mol m^{-3}.*

The flux through the membrane can be written as:

$$N_{Cr,m}=u_{Cr,m}C_{Cr,m}\frac{i}{\kappa_m}, \qquad (1)$$

were $u_{Cr,m}$ and $C_{Cr,m}$ are the mobility and concentration of species in membrane, $\kappa_{,m}$ is its electrical conductivity of the membrane, *i* is the current density. $C_{Cr,m}=\frac{n_{Cr,m}}{l_m S_m}$, where S_m is the membrane area, $n_{Cr,m}$ is the amount of Cr(VI) species in the membrane at *τ=0,* this value can be found via:

$$n_{Cr,m}=S_m\int_0^\tau \overline{u}_{Cr}\overline{C}_{Cr}\frac{i}{\overline{\kappa}}d\tau, \qquad (2)$$

where $\overline{\kappa}$ is the conductivity of the ion-exchanger bed. Thus:

$$N_{Cr,m}=u_{Cr,m}\overline{u}_{Cr}\frac{i^2}{l_m\kappa_{,m}}\int_0^\tau\frac{\overline{C}_{Cr}}{\overline{\kappa}}d\tau, \qquad (3)$$

where l_m is the membrane thickness, $\overline{C}_{Cr}$ is the concentration of Cr(VI) species in the ion-exchanger. It means:

$$\frac{dN_{Cr,m}}{d\tau}=\frac{u_{Cr,m}\overline{u}_{Cr}\overline{C}_{Cr}i^2}{\kappa_m\overline{\kappa}l_m}. \qquad (4)$$

The $u_{Cr,m}$, $\overline{\kappa}$ and the κ_m values are determined with independent methods. Indeed, the $dN_{Cr,m}/d\tau$ - i^2 curve is linear (Fig. 2). The diffusion coefficients through the resin ($\overline{D}_{Cr}$) for $HCrO_4^-$ (CrO_4^{2-}) species were estimated as:

$$\bar{u}_{Cr} = \frac{RT\bar{D}_{Cr}}{z_{Cr}F}, \qquad (5)$$

where R is the gas constant, T is the temperature, F is the Faraday constant, z_{Cr} is the charge number. These values are 1.2×10^{-12} ($HCrO_4^-$) and 5.1×10^{-13} (CrO_4^{2-}) $m^2\ s^{-1}$, they correspond to data for the similar ion-exchange resin [12]. Green colour of the resin (yellow after loading) was found after electroregeneration. This indicates Cr(VI)→Cr(III) transformation probably due to reduction by the ion exchange resin despite low initial Cr(VI) content ($\bar{c}_{Cr}$=41 mol m^{-3}).

Electroregeneration: polymer anion-exchange membrane and inorganic ion-exchanger. This system shows nonlinearity of the flux derivative *vs* square current density, moreover, $dN_{Cr,m}/d\tau \neq 0$ at i^2 and $dN_{Cr,m}/d\tau < 0$ reflecting a decrease of the flux over time. Nevertheless, calculations of linear region of the $dN_{Cr,m}/d\tau$ - i^2 curve give $\bar{D}_{Cr}$=4.5x10^{-12} m^2s^{-1} ($\bar{C}_{Cr}$ =165 mol m^{-3}), this value is in agreement with the magnitude obtained during investigation of sorption kinetics [8]. Cr(III) species in the inorganic ion-exchanger, which is stable against oxidation, were also found. Thus, the mechanism of ion transport through the ion-exchanger bed and polymer membrane involves following stages: (i) anion transport through the sorbent bed to the anode compartment; (ii) transport through the polymer membrane, which is accompanied by partial reduction of $HCrO_4^-$ ions; (iii) transport of Cr(III) cations from the anion-exchange membrane through the bed to cathode compartment. $HCrO_4^-$ ions destroy polymer materials, Cr(III) ions poison the amphoteric inorganic ion-exchanger since their mobility in the solid phase is extremely low.

Electroregeneration: inorganic materials. In this case, a change of the membrane conductivity under different voltage has to be taken into consideration. This is caused by concentration polarization that occurs also inside macropores of the inorganic membrane. The membrane resistance (R_m) increases gradually with voltage (the highest contributions of the potential gradient is due to the inorganic membrane and ion-exchanger) due to inhomogeneous membrane structure and decreases under high voltage due to overlimiting current conditions (Fig. 3).

Taking into consideration resistance of the inorganic membrane, resistance of the ion-exchanger ($\bar{R}$) and thickness of its bed ($\bar{l}$), equation (5) can be written:

$$\frac{dN_{Cr,m}}{d\tau} = \frac{u_{Cr,m}\bar{u}_{Cr}\bar{C}_{Cr}}{l_m^2\bar{l}} I^2 f(I^2). \qquad (6)$$

Here I is the current, f is the function of square current, $f(I^2) = \bar{R}R_м$. Derivation of eq. (6) gives $g(I^2)$ function:

$$g(I^2) = \frac{u_{Cr,m}\bar{u}_{Cr}C_{Cr}}{l_m^2\bar{l}} \left(\frac{d\left[f(I^2)\right]}{d(I)^2} I^2 + f(I^2) \right). \qquad (7)$$

In other words, the $g(I^2)$ function corresponds to a slope of the $dN_{Cr,m}/d\tau$ - I^2 curve to the abscissa axis. This function is approximated as $b_1 + b_2 I^2 (b_3 + I^2)^{-1}$, the term of eq. (7) in round brackets is expressed via $b_4 + b_5 I^2 + b_6 I^4$ (see Fig. 5, where b are the empirical coefficients).

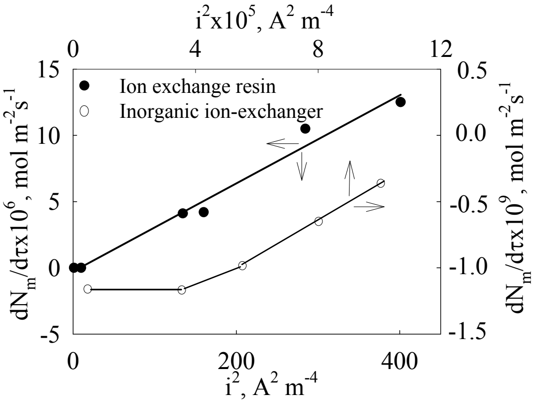

Fig. 2. *The Derivative of Initial Cr(VI) Flux with Respect to Time vs Square Current Density for the Systems Involving the Polymer Membrane.*

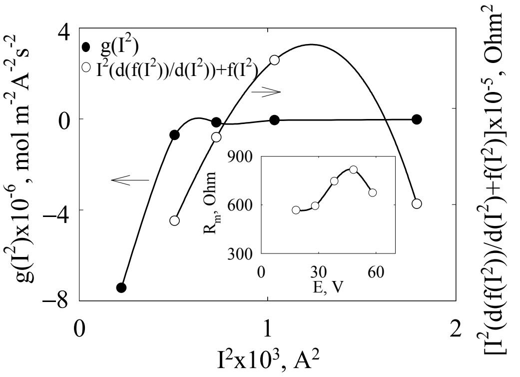

Fig. 3. *Functions of Square Current: g and Term in Round Brackets of eq. (7). Insertion: Membrane Resistance as a Function of Cell Voltage.*

When $I \to 0$, eq. (7) is simplified:

$$\bar{u}_{Cr} = \frac{b l_m^2 \bar{l}}{u_{Cr,m} \bar{C}_{Cr}}, \tag{8}$$

where $b = b_1/b_4$, this coefficient (mol $V^{-2}m^{-2}s^{-1}$) corresponds to rate of a change of ion flux through the membrane, if the potential drops through the membrane and ion-exchanger are 1 V Since $D_{Cr,m} = 1.80 \times 10^{-10}$ m^2s^{-1} [9[, $b_1 = -4.95 \times 10^{-5}$ mol m^{-2} A^{-2} s^{-2}, $b_4 = -7.49 \times 10^4$ Ohm^2, the diffusion coefficient of $HCrO_4^-$ has been estimated as 2.6×10^{-12} m^2 s^{-1}. The $\bar{D}_{Cr}$ values obtained for the systems involving polymer and inorganic anion exchange membranes are in a good agreement.

Electrodeionization: inorganic materials. Increasing in current reduces the flux of $HCrO_4^-$ species and degree of their removal from the mixed solution (Fig. 4). This is evidently due to concentration polarization of the membrane that increase its resistance and decrease the potential gradient through the bed of the inorganic ion-exchanger. When the current density is higher than the limiting value for $HCrO_4^-$ ions ($i_{lim,Cr}$) in 4 times, EDI is transformed into electrodialysis. The fluxes through the membrane are similar for the ion-exchanger and glass particles. In this case, the ion-exchanger behaves as inert components evidently due to higher rate of ion transport through the solution than through the ion-exchanger bed. The ion-exchanger particles only turbulizes the solution flow, no significant ion transport is realized through the bed.

Conclusions. In order to determine diffusion coefficient of sorbed ions through the ion-exchanger with electroregeneration method, the membrane has been taken into consideration as a sorption barrier. Using this approach, the $\bar{D}_{Cr}$ values have been found for ion-exchange materials of different origin. The order of diffusion coefficient for hydrogel of hydrated zirconium dioxide is 10^{-12} m^2 s^{-1}

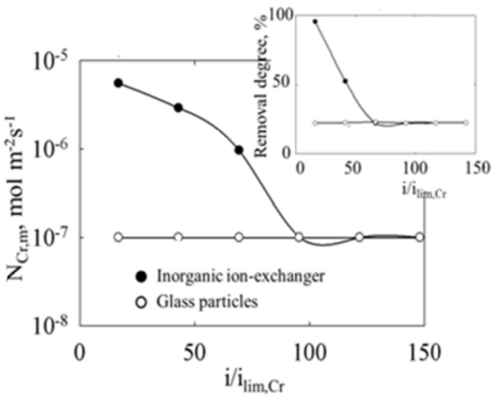

Fig. 4. *Flux of $HCrO_4^-$ Ions through the Inorganic Membrane as a Function of i/i_{lim}, Cr. It Is the Same for $HCrO_4^-$ Removal Degree (Insertion). The Solution Contained Initially (mol m^{-3}) Cr(VI) (0.1) and H_2SO_4 (0.5). Adapted from [9].*

similarly to that for the anion-exchange resin. Since $HCrO_4^-$ removal from diluted solution using polymer ion exchange materials is complicated by their oxidative destruction, inorganic membrane and highly hydrated inorganic ion-exchanger has to be applied to the EDI process. The removal conditions must exclude rapid increase of the membrane resistance due to concentration polarization. The system involving inorganic ion exchange materials can be recommended for recovery of other toxic components of solutions, which destroy polymer membranes and ion exchange resins. In the future, the task of optimization of composite membrane structure should be solved in order to eliminate negative effect of concentration polarization as much as possible.

References

1. *Alvarado L., Chen A.* Electrodeioniization: principle, strategies and applications // Electrochim. Acta. 2014. V. 132. P. 583-597.
2. *Arar Ö, Yüksel Ü, Kabay N., Yüksel M.*Various applications of electrodeionization (EDI) method for water treatment—A short review // Desalination. 2014. V. 342. P. 16-22.
3. *Turek M., Mitko K., Bandura-Zalska B., Ciecierska K., Dydo P.* Ultra-pure water production by integrated electrodialysis-ion exchange/electrodeionization // Membrane water treatment. 2013. V. 4. P. 237-249.
4. *Arar Ö, Yüksel Ü, Kabay N., Yüksel M.* Demineralization of geothermal water reverse osmosis (RO) permeate by electrodeionization (EDI) with mixed bed configuration // Desalination. 2014. V. 342. P. 23-28.
5. *Dzyazko Y.S., Ponomaryova L.N., Rozhdestvenskaya L.M., Vasilyuk S.L., Belyakov V.N.* Electrodeionization of low-concentrated multicomponent Ni^{2+}-containing solutions using organic-inorganic ion-exchangers // Desalination. 2014. V. 342. P. 52-60.
6. *Arar Ö., Yüksel Ü., Kabay N., Yüksel M.* Removal of Cu^{2+} ions by a micro-flow electrodeionization (EDI) system // Desalination. 2011. V. 277. P. 296-300.
7. *Dzyazko Yu. S., Volfkovich Y. M., Ponomaryova L. N., Sosenkin V. E., Trachevskii V. V., Belyakov V. N.* Composite ion-exchangers based on flexible resin containing zirconium hydrophosphate for electromembrane separation // J. Nanosci. Technol. 2016. V. 2. P. 43-49.
8. *Dzyazko Yu. S.; Rozhdestvenskaya L. M.; Vasilyuk S. L.; Belyakov V. N.; Kabay N.; Yuksel M., Arar Ö., Yuksel Ü.* Electrodeionization of Cr (VI)-containing solution. Part I: Chromium transport through granulated inorganic ion-exchanger // Chem.Eng.Commun. 2009. V. 196. P. 3-21.
9. *Dzyazko Yu. S., Vasilyuk S. L., Rozhdestvenskaya L. M., Belyakov V. N., Stefanyak N. V., Kabay N., Yulksel M., Arar Ö.. Yulksel Ü.* Electrodeionization of Cr(VI) containing solution. Part II. Chromium transport through inorganic ion-exchanger and composite ceramic membrane // Chem.Eng.Commun. 2009. V. 196. P. 22 - 38.

10. *Bryjak M., Kabay N., Rivas B.L., Bundschuh J.* Innovative Materials and Methods for Water Treatment: Solutions for Arsenic and Chromium Removal, CRC press, Boca Raton, London, New York, Leiden, 2016.
11. *Spoor P. B., ter Veen W. R., Janssen L. J. J.* Electrodeionization 1: The migration of nickel ions in a rigid, microporous cation-exchange resin / // J. Appl. Electrochem. 2001. V. 31, P. 523–530.
12. *Rivero M, J., Primo O., Ortiz M. I.* Modelling of Cr(VI) removal from polluted groundwaters by ion exchange // J. Chem. Technol. Biotechnol. 2004. V. 79. P. 822-829.

УДК 544.622+544.725.2

ЕЛЕКТРОДЕІОНІЗАЦІЙНЕ ВИДАЛЕННЯ ІОНІВ $HCrO_4^-$ З РОЗБАВЛЕНИХ РОЗЧИНІВ. ВПЛИВ МЕМБРАНИ

Ю.С. Дзязько[1], Ö. Arar[2], Л.М. Рождественська[1], С.Л. Василюк[1]

[1] Інститут загальної та неорганічної хімії ім. В.І. Вернадського НАН України.

пр. акад. Палладіна 32/34, 03680, Київ, Україна

e-mail: dzyazko@gmail.com

[2]Егейський університет, науковий факультет, кафедра хімії,
35100, Ізмір, Туреччина
e-mail:ozgur.arar@ege.edu.tr

Резюме. *При різних напругах вивчено перенос іонів у системах, які включають гранульовані іоніти та аніонообмінні мембрани різної природи. Розглянуто роль мембрани як сорбційного бар'єру. Запропоновано спосіб, що дозволяє визначати рухливість сорбованих іонів у шарі іоніту. Досліджено електродеіонізацію Cr(VI)-вмістного розчину із застосуванням неорганічних іонообмінних матеріалів.*

Ключові слова: *хром, електродіаліз, електродеіонізація, неорганічна мембрана, гідратований діоксид цирконію.*

UDC 66.081.6: 637.142.2

REVERSE OSMOSIS FOR CONCENTRATIION OF SUGAR BEET JUICE AFTER THE SECOND CARBONATION

Yu.G. Zmievskii, V.G. Myronchuk

National University of Food Technologies, Ministry of Education and Science of Ukraine, Vladimirskaya str. 68, 01601, Kiev, Ukraine,

e-mail:yrazm@meta.ua

Abstract.*Preliminary experiments of concentrationof sugar beet juice after the second carbonation were carried out.A dead-end cell with a reverse osmosis membrane was used.The dependence of the permeate flux vs pressure, which was varied from 0 to 6 MPa,has been obtained. Duringjuice concentration, a linear decrease of the flux was observed. It means no fouling of the membrane surface.Preliminary calculations show that the use of reverse osmosis provides at least 30% of energy consumption.*

Keywords: *reverse osmosis, sugar beet juice, concentration, membrane, dry matter.*

Introduction. Recently applicationfield of membrane processes expands intensively, especially in food industry. Membrane separation provides high quality of the products, they allows one to minimize energy consumption and, as a result, to save gas, coal and electricity.Traditionally vacuum evaporationis used for solution concentration in food technologies.The energy consumption of the evaporation systems for solvent removal is higher almost in 5 times than that for reverse osmosis (the comparison is for seawater desalination) [1].This limits prospects of evaporation techniques and expends opportunities of advanced technologies involving membrane separation.For example, nanofiltration or reverse osmosis are used for pre-concentration of dry matter of milky whey before evaporation [2].

Sugar industry is related to energy-intensive branches of food industry, thus, alternative technologies have to be developed. Previous analysis shows a possibility to provide 33% decrease of energy consumption for concentration of sugar beet juiceby means of application of reverse osmosis before evaporation [3].It is advisable to use this method due to following reasons.It is necessary to process large volume of theliquidduring short period, thus, bulky and expansive equipment is needed. Moreover, sugar plants work only 30-90 days a year.Membrane techniques would provide fast processing of large amount of perishable feedstock. The aim of the investigation was to evaluate a possibility to use reverse osmosis as a preliminary stage of sugar beet juice after second carbonization.

Experimental.ARM Nanotech membrane (RF) was used for the research, its effective area was $1.3 \cdot 10^{-3}$ m^2.A dead-end cell was applied tobaromembraneseparation. Pressure test of the membrane wasperformed by filtration of deionized water at ≈20°C to achieve a constant flux.

Sugar beet juice produced byUzynsky sugar plant (Ukraine) in September 2016 was processed.The liquid contained initially15.2 % of dry matters determined with a URL-1 refractometer (Analitpribor, Ukraine).

Results and discussion. After the second carbonization,sugar beet juicecontains no large colloidal particles and most of impurities. This provides good conditions for subsequent membrane separation.However, the temperature of the liquid after carbonization is 85-90° C, the working temperature of reverse osmosis membranes is up to 45°C. Thus, heat exchangers are required to provide necessaryconditions for the membrane.

Fig. 1 shows the experimental results.It can be seen that the flow of permeate is practically absent, when pressure is lower than 1 MPa. This is due to high osmotic pressure (π) of juice. According to [4], following equation has been obtained:

$$\pi = 0{,}0033 \cdot C^3 - 0{,}3124 \cdot C^2 + 11{,}333 \cdot C - 104{,}41 \qquad (1)$$

whereCis thecontent of dry matter, % (15 % □ C □ 75 %).It allows one to calculate the osmotic pressure (bar) of juice after the second carbonization at 80°C.

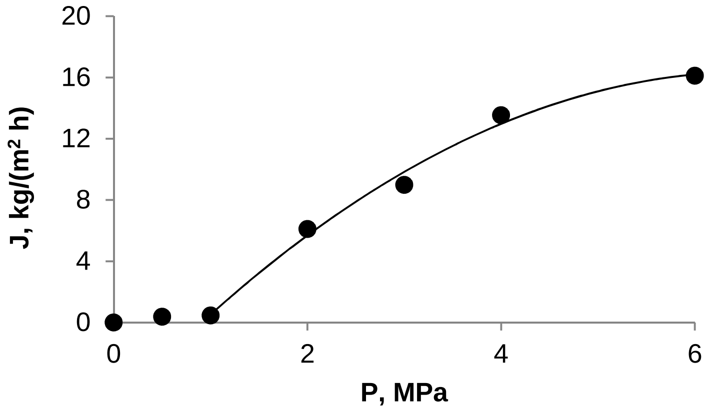

Fig. 1. *Permeate Flux as a Function of Pressure.*

This equation can be used to approximate the results, because the solution temperature was much lower than 80 °C.In addition, the values of osmotic pressure of juice, whichcontains similar amount of solids, but which wastreated by various methods, is also different within certain limits.Equation (1) and data [4] show that reducing of the temperature from 80 to 25 °C leads to a decrease of osmotic pressure π of 13%. In this case, the π value is about 0.56 MPa and conditionsof ΔP - π (where $\Delta P$is the working pressure) have to be the most suitable for reverse osmosis.

Fig. 1 shows that the permeate flux (*J*) increases linearly within 1-4 MPa, then no linearity is observed.In all cases, selectivity of the membrane agaisttowards dry matter exceeds 99%.Since the pressure test was performed preliminarily, the results cannot be caused by a change of the membrane structure affected by pressure. The reason of nonlinearity is assumed to be concentration polarization or membrane fouling. In order to confirm these assumptions, juice was concentrated at 6 MPa until to the minimal permeate flux (almost zero), as shown in Fig. 2.

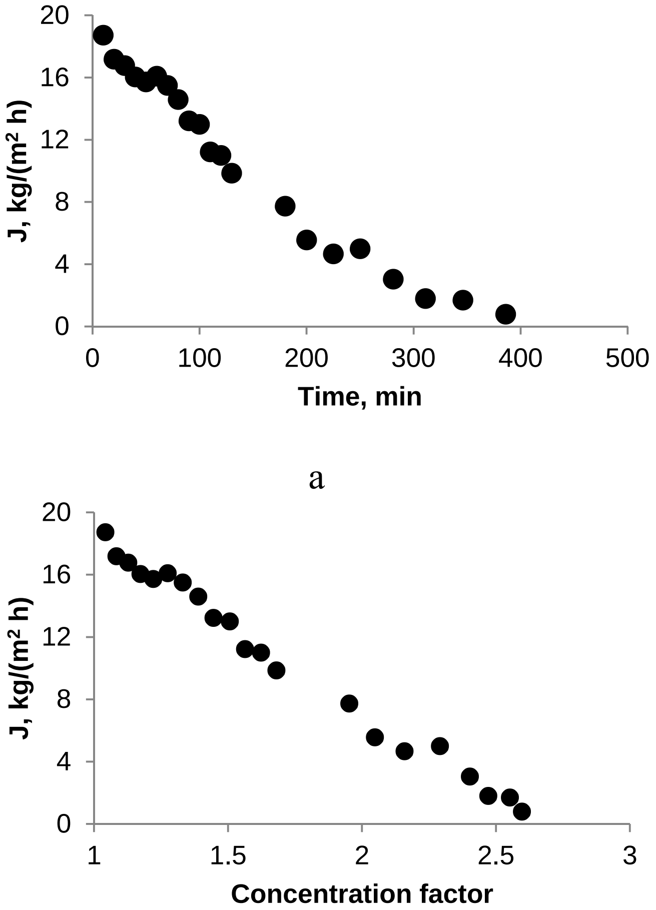

a

b

Fig. 2. *Permeate Flux as a Function of Time (a) and Concentration Factor(b).*

Fig. 2 shows uniform decrease of the permeate flux with increasing in time and grows of concentration factor, Thus, concentration polarization is a reason of nonlinearity of the curve of Fig. 1.It means, hydrodynamic conditions should be improved during the transition from laboratory research to industrial tests.

Based on our experience, we assume that the minimalpermeate flux should be at least 10 kg/(m^{2}h). Before concentrating in a vacuum evaporator,about 40 % of water can be released from juice. It is almost 55 % of solvent being removed.

Industrial plant consumes about 300-390 tons of fuel for processing of 6 000 tons of sugar beets (343-445 thousand m^3 of natural gas) for concentration of juice.The energy consumption of the device for reverse osmosis is less in 5 times than that for vacuum evaporator. Thus, the membrane method allows us 30% of reduce of energy consumption.

Conclusions. Reverse osmosis at 6 MPa removes 55 % of required amount of solvent from sugar beet juice after the second carbonization.Permeate flux is varied within the interval of 18.7 to 0.8 kg/(m^2 h), selectivity towards dry matter was 99%.Theoretically, sugar plant can reach more than 30 % of energy consumption,when reverse osmosis is used for pre-concentration.However, this process requires further study and new experimental data.Economic advantages of this technology should be estimated in details.

References

1. *Spiegler K.S., El-Sayed Y.M.* Theenergeticsofdesalinationprocesses // Desalination. 2001. V. 134. P. 109-128.
2. *Salehi F.*Current and future applications for nanofiltration technology in the food processing // Food and Bioproducts Processing. 2014. V. 91. P. 161-177.
3. *Madaeni S.S., Zereshki S.* Energy consumption for sugar manufacturing. Part I: Evaporation versus reverse osmosis // Energy Conversion and Management. 2010. V. 51. P. 1270–1276.
4. *Gul S., Harasek M.* Energy saving in sugar manufacturing through the integration of environmental friendly new membrane processes for thin juice pre-concentration // Applied Thermal Engineering. 2012. V. 43. P. 128-133.

УДК 66.081.6: 637.142.2

ЗВОРОТНИЙ ОСМОС ДЛЯ КОНЦЕНТРУВАННЯ СОКУ ЦУКРОВОГО БУРЯКА ПІСЛЯ ДРУГОЇ САТУРАЦІЇ

Ю.Г. Змієвський, В.Г. Мирончук

Національний університет харчових технологій,Володимирськавул.68, 01601, Київ, Україна,

e-mail:yrazm@meta.ua

Резюме.Проведено попередні дослідження процесу концентрування дифузійного соку після другої сатурації. Застосовували непроточну мембранну комірку іззворотноосмотичною мембраною, робоча температура становила 20±3 °С. Отримано залежність питомої продуктивності від тиску, який змінювали в діапазоні від 0 до 6 МПа. Під час концентрування дифузійного соку спостерігалось лінійне зниження продуктивності мембран, що вказує на відсутність забруднення поверхні розділення. Попередні розрахунки показують, що впровадження результатів досліджень у виробництво дозволить знизити споживання енергоносіїв мінімум на 30 %.*

Ключові слова: *зворотний осмос, дифузійний сік, концентрування, мембрана, суха речовина.*

UDC 544.723+544.726

REMOVAL OF Pb (II) IONS FROM WATER SOLUTIONS WITH ION EXCHANGE RESINS, OXIDES AND HYBRID SORBENTS

T.V. Maltseva, K. O. Kudelko, E.A. Kolomiets

V.I. Vernadsky Institute of General and Inorganic Chemistry NAS Ukraine,
Palladin Ave. 32/34, 03680, Kyiv, Ukraine
e-mail: maltseva@ionc.kiev.ua

Abstract. *The (hydr)oxides with chemical composition* $Mn_{0-1}M_{1-0}O_2{\cdot}nH_2O$ *(M = Zr (IV), Ti (IV), Sn (IV),) and predomination of negative surface charge were synthesized by sol-gel precipitation. The surface properties of (hydr)oxides were characterized by acid-base titration and adsorption/desorption of nitrogen. The organic-inorganic hybrid materials with sorption affinity for ions of Pb (II) have been obtained by introducing of hydroxides in organic matrix. The value of the distribution coefficient of Pb (II) ions on some materials reaches* 10^5 $cm^3{\cdot}g^{-1}$*.*

Keywords: *sorbents, organic-inorganic hybrid, lead ions, distribution coefficient.*

Introduction. Man-made sources of lead pollutions include: emissions of products formed during high-temperature processes, the exhaust gases of internal combustion engines, waste water, mining and processing of metals, transportation, abrasion resistance and its dispersion during the operation of machines and mechanisms. Only as a result of metallurgical plants the Earth's surface annually receives not less than 89 thousand tons, with the exhaust gases of about 260 thousand tons. [1]. Most perspective sorbents for heavy metal ions removal are inorganic nanoscale materials which can be obtained by sol-gel method.

This research devoted, at first, to a synthesis of individual and double inorganic and hybrid organic-inorganic compounds with predetermined surface properties and, at second, to their applications in environment, namely, for removal heavy metals from diluted water solutions. In literature, there are several researches about high selectivity of this group of individual hydroxides (Zr (IV), Ti (IV), Sn (IV)) towards toxic multivalent metal ions [2]. The addition of individual hydroxides to a proton-donor oxide matrix should obtain the materials with predomination of negative surface charge. The affinity of such materials to heavy metal ions is expected to be stronger in comparison to individual hydrated oxides. In addition, the introduction of “acid” (hydr)oxides in organic cation-exchange matrix should result in a high affinity of such hybrid materials to multicharged cations.

Experimental. *Synthesis.* The individual, double (hydr)oxides and hybrid organic-inorganic materials were synthesized by sol-gel precipitation with usage of salts and ammonia. The chemical composition of the (hydr)oxides was determined by analytical methods.

Surface area. The nitrogen adsorption/desorption isotherms were measured at 77.4 K using the "AUTOSORB-NOVA-6" instrument (by Quantachrome) after outgassing the samples at 463 K for 20 h. The surface area was calculated by the BET (Brunauer–Emmett–Teller) method. The pore volume and the pore size distribution were calculated by the BJH (Barrett-Joyner-Halenda) and DFT (density functional theory) methods.

Adsorption properties. For adsorption tests, 0.5 g of adsorbents were contacted with 50-200 mL of M (II) solutions having different concentrations in "Elpan type-375" shaker for 24 h. Adsorption from aqueous solution of $Pb(NO_3)_2$ was studied in the range of $1\cdot10^{-3}$-$5\cdot10^{-2}$ M. The samples were filtered prior to analysis to determine the concentration of the Pb (II) ions. The initial and equilibrium concentration of Pb (II) ions was determined by atomic adsorption spectroscopy. Final pH values of the solutions were measured using laboratory type pH-meter "I-160 M". Adsorption capacity (Q) and distribution coefficient (K_d) were calculated.

Results and discussion. The surface properties of inorganic individual and double (hydr)oxide adsorbents found to be as follow: PZC values in 0.12 M KNO_3 vary from 3.5 ($MnO_2\cdot H_2O$) to 6.3 ($TiO_2\cdot nH_2O$); value of the surface area is varied from 53 ($TiO_2\cdot nH_2O$) to 270 $m^2\cdot g^{-1}$ ($Mn_{0.4}Sn_{0.6}O_2\cdot H_2O$). The pore size is between 1.7-2.1 nm and micro pore percent is between 3-80. All inorganic adsorbents show predominant cation-adsorptive properties in I-I and II-I salts.

Figure 1 shows the results of investigation on adsorption of Pb (II) ions. It can be concluded from obtained data that several investigated adsorbents can remove Pb (II) ions from much diluted solutions.

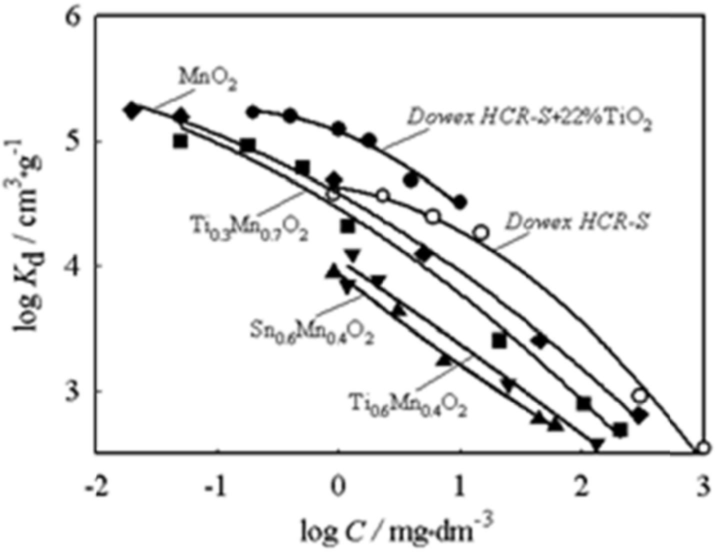

Fig. 1. *Removal of Pb (II) Ions from $Pb(NO_3)_2$ Solutions by Oorganic, Inorganic and Hybrid Adsorbents (in Logarithmic Coordinates).*

Table 1 presents distribution coefficient of Pb (II) ions in 0.1-1.0 mg·dm^{-3} equilibrium solution for all adsorbents which have been studied.

Table 1. Distribution Coefficient of Pb (II) Ions in 0.1-1.0 mg·dm^{-3} Solution

Adsorbent (·nH_2O)	**$K_d \cdot 10^{-4} \pm 0.5 \cdot 10^{-3}$, cm^3·g^{-1}**	**pH±0,3**
ZrO_2	0.5	3.4
SnO_2	0.2	2.2
TiO_2	2.0	4.2
MnO_2	10.0	1.9
$Mn_{0.4}Zn_{0.6}O_2$	0.9	3.8
$Mn_{0.4}Sn_{0.6}O_2$	0.8	2.5
$Mn_{0.4}Ti_{0.6}O_2$	1.0	4.5
$Mn_{0.7}Ti_{0.3}O_2$	10.0	4.0
Dowex HCR-S	7.0	4.8
Dowex HCR-S+12%SnO$_2$	10.0	3.6
Dowex HCR-S+44%SnO$_2$	14.0	3.0
Dowex HCR-S+22%TiO$_2$	12.0	4.3

The most promising adsorptive materials for the removal of Pb (II)ions are inorganic adsorbents which are hydrated MnO_2, $Mn_{0.7}$ Ti $_{0.3}O_2$; hybrid adsorbents which are *Dowex HCR-S*+12%SnO_2, *Dowex HCR-S*+44%SnO_2; *Dowex HCR-S*+22%TiO_2.

In the study of the absorption of Pb (II) ions from dilute solutions on the organic cation exchanger *Dowex HCR-S,* the local area of non-exchange electrolyte absorption was observed on adsorption isotherm. That is why in spite of high values of distribution coefficients which are closed to ones for inorganic adsorbents. So that it can be concluded that organic resins are not selective.

Conclusions. The (hydr)oxides with predomination of negative surface charge and chemical composition $Mn_{0-1}M_{1-0}O_2 \cdot nH_2O$, where M = Zr (IV), Ti (IV), Sn (IV) were synthesized by sol-gel precipitation. The surface properties of (hydr)oxides were characterized by acid-base titration [3] and adsorption/desorption of nitrogen. PZC values in 0.12 M KNO_3 vary from 3.5 to 6.3. The value of the surface area is varied from 53 to 260 m^2·g^{-1} . The pore size is between 1.7-2.1 nm and micro pore percent is between 3-80. By introducing of (hydr)oxides in organic matrix, organic-inorganic hybrid materials with a sorption affinity for ions of Pb (II) has been obtained. The distribution coefficients K_d of Pb (II) ions were calculated from adsorption isotherms. The application of such inorganic and organic-inorganic hybrid materials for the removal of Pb(II) ions from dilute solutions has showed promising results. The most promising adsorptive materials among the adsorbents tested are inorganic adsorbents such as hydrated MnO_2, $Mn_{0.7}$ Ti $_{0.3}O_2$; hybrid adsorbents such as *Dowex HCR-S*+12%SnO_2, *Dowex HCR-S*+44%SnO_2; *Dowex HCR-S*+22%TiO_2.

References

1. Lead Standard in Drinking Water // Scientific Committee on Health and Environmental Risks, P. 12, http://ec.europa.eu/health/scientific_committees/environmental_risks/docs/scher_o_128.pdf.
2. *Lefavre G., Kneppers J., Fedoroff M.* Sorption of uranyl ions on titanium oxide studied by ATR-IR spectroscopy // J. Coll. Int. Sci. 2008. V. 327. P. 15-20.
3. *Kosmulski M*. pH-dependent surface charging and points of zero charge II. Update // J. Coll. Int. Sci. 2004. V. 275. P. 214–224.

УДК 544.723+544.726

Видалення іонів свинцю з водних розчинів з використанням органічих, оксидів та гібридних сорбентів

Т.В.Мальцева, К.О. Куделко, Е.А. Коломієць
Інститут загальної та неорганічної хімії ім. В.І. Вернадського НАН України,
пр. акад. Палладіна, 03142 32/34 Київ, Україна
e-mail: maltseva@ionc.kiev.ua

Резюме. *(Гідр)оксиди з хімічним складом $Mn_{0-1}M_{1-0}O_2{\cdot}nH_2O$ (M = Zr (IV), Ti (IV), Sn (IV)) та переважно негативним поверхневим зарядом синтезовано золь-гель осадженням. За допомогою методів кислотно-основного титрування та адсорбції/десорбції азоту досліджено властивості поверхні (гідр)оксидів. Введення частинок (гідр)оксидів в органічну матрицю призвело до отримання органо-неорганічних гібридних матеріалів з адсорбційною спорідненістю до іонів Pb(II). Визначено значення коефіцієнту розподілу Pb(II) іонів на деяких матеріалах і досягає 10^5 см^3·г$^{-1}$.*

Ключові слова: *сорбенти, органо-неорганічні гібридні, іони свинцю, коефіцієнт розподілу.*

UDC 544.723+547.458

ADSORPTION OF DYES, HERBICIDES AND HEAVY METALS BY COMPOSITES OF SILICA WITH AMINO- AND SULFO CONTAINING POLYSACCHARIDES

T.M. Budnyak[1], V.A. Tertykh[1], M. Błachnio[2], A. Deryło-Marczewska[2],
A.W. Marczewski[2]
[1]Chuiko Institute of Surface Chemistry of NAS of Ukraine,
General Naumov Str. 17, 03164 Kyiv, Ukraine,
e-mail: tetyanabudnyak@yahoo.com
[2]Maria Curie-Sklodowska University,
Maria Curie Sklodowska Sq. 2, 20-031 Lublin, Poland
e-mail: mordenit@wp.pl

Abstract. *Adsorption on polysaccharide derivatives can be a low-cost procedure of choice in water decontamination for extraction and separation of compounds, and a useful tool for protecting the environment. In current study, polysaccharides-silica composites were synthesized by sol-gel method, physical and chemical adsorption of chitosan and carrageenan by silica surface. Obtained adsorbents were applied to adsorption of highly toxic compounds: cationic and anionic dyes, herbicides and heavy metals.*

Keywords: *chitosan, carrageenan, dyes, herbicides, silica*

Introduction. In recent years, the functional polymeric compounds are broadly used to modify the silica surface, which allows one to obtain the corresponding organo-mineral composites having sufficiently high capacity while maintaining good kinetic characteristics peculiar to inorganic adsorbents. In this respect, application for these purposes functional biopolymers, such as amino- and sulfo-containing polysaccharides chitosan and carrageenan, are of great interest [1,2]. Thus, abundant in nature polysaccharides as chitosan and carrageenan have good biocompatibility, a wide range of pH stability, expressed chelating properties. Furthermore, these biopolymers have opposite charge of functional groups what allows one to complement properties of polymers. From the other side, silica characterized by advanced surface stability in the acidic medium, acceptable kinetics, thermal stability, and resistance to microbial attack.

Experimental. Hybrid materials were prepared using various synthetic methods: adsorption and covalent binding of polymer on the silica, forming of inorganic matrix in polymer solution (sol gel method). The effect of route of polymer coating creation on thermal stability and ability to degradation, surface morphology, including pore size distribution and average surface area, as well as other physicochemical characteristics of such hybrid biocomposites have been described.

Results and discussion. It was found that physically adsorbed on the silica surface chitosan and carrageenan are effective as adsorbents with respect to highly toxic contaminants such as heavy metals, synthetic cationic and anionic dyes and herbicides from aqueous solutions, what is crucial in the development enterosorbents or adsorbents for water treatment. The hybrid biocomposite chitosan-silica gel was applied to study adsorption of sulfonated azo dyes. It was found that this composite is effective towards next dyes: Orange II and Acid Orange 8 (0.20 mmol/g), Orange G (0.12 mmol/g), Acid Red 88 (0.48 mmol/g) and Acid Red 1 (0.09 mmol/g).

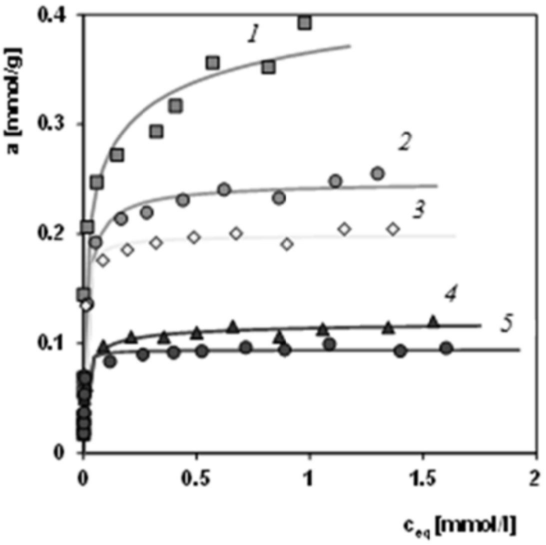

Fig. 1. *Comparison of Isotherms of the Dyes on the Chitosan-silica gel composite: Acid Red 88 (1), Orange II (2), Acid Orange 8 (3), Orange G (4), Acid Red 1(5).*

The influence of temperature to the ability of synthesized composites to adsorb Acid Orange 8 dye was studied (Fig. 2). The strong decrease of adsorption with temperature increase was observed. Maximum adsorption capacity at 5°C determined from the Langmuir-Freundlich eqluation is about one third higher than the value at 45°C obtained. The estimated thermodynamics parameters ΔG°, ΔH°, and ΔS° for the system Acid Orange 8 dye – chitosan-fumed silica adsorbent at 5 °C, 25 °C and 45 °C confirmed the exothermic and spontaneous character of the adsorption process. The kinetics study was shown that 10 minutes (at 45°C) and 20 minutes (at 25°C) is enough to achieve 50 % of dye removal, and 6 hours of the process is enough for achiving the adsorption equilibrium at those temperatures. Fast kinetic in the range of temperature 25°C □ 45°C favors to use adsorption on these type of composites as a preliminary technics in wastewater treatment plant. The applying obtained results to several kinetics models, such as first-order equation, pseudo-first order equation, second-order equation, pseudo-second order equation, mixed 1,2-order equation and multi-exponential equation, was shown very good correlation between experimental data and multi-exponential equation.

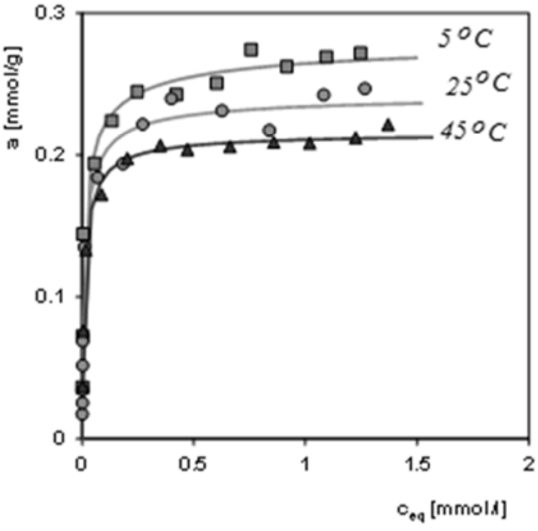

Fig. 2. *Temperature Effect on Adsorption of Acid Orange 8 from Aqueous Solutions on Composite Chitosan-Fumed Silica at Various Temperatures.*

Biohybride carrageenan-fumed silica has shown the highest adsorption capacity towards cationic synthetic dyes: Bismark Brown (0.54 mmol/g), Acridine Orange (0.88 mmol/g), Malachite Green (0.55 mmol/g), Methylene Blue (0.61 mmol/g), Crystal Violet (0.52 mmol/g). The study of adsorption of herbicides has shown that composite chitosan-fumed silica could adsorb up to 0.31 and 0.35 mmol/g of 4-chlorophenoxyacetic and 2,4-dichlorophenoxyacetic acid, respectively.

The composite synthesized by covalent binding of chitosan on the silica surface was found to show high adsorption activity with respect to milligram amounts of toxic metal oxoanions and moderately adsorbed cations. Thus, the composite extracted metal ions Zn(II), Cu(II), Cd(II), Pb(II) and Fe(III) with adsorption capacity range from 0.03 mmol/g for Fe(III) to 0.17 mmol/g for Zn(II) in the neutral medium, and adsorbed oxoanions V(V) and Mo(VI) from the acidic medium with adsorption capacity 1.6 and 1.5 mmol/g, respectively, and 0.5 mmol/g for Cr(VI) at neutral pH. Moreover, it was found that after functionalization of the surface of organomineral composite with iodoacetic acid, adsorption capacity are highly increased with respect to studied cations of heavy metals up to the range from 0.14 mmol/g for Pb(II) to 0.60 mmol/g for Zn(II) in the neutral medium.

Conclusions. It was found that the biocomposites based on polysaccharides, such as chitosan, carrageenan and silica are effective as adsorbents with respect to highly toxic contaminants such as synthetic cationic and anionic dyes, herbicides, and heavy metals from aqueous solutions, what is crucial in the development enterosorbents or adsorbents for water treatment.

Acknowledgements. The research leading to these results was financed from the People Programme (Marie Curie Actions) of the European Union's Seventh Framework Programme FP7/2007-2013/ under REA grant agreement No° PIRSES-GA-2013-612484.

References

1. *Grini G.* Recent development in polysaccharide-based materials used as adsorbents in wastewater treatment // Prog. Polym. Sci. 2005. V. 30. P. 38–70.
2. *Yagub M.T., Sen T.K., Afroze S., Ang H.M.* Dye and its removal from aqueous solution by adsorption: a review // Adv. Colloid Interface Sci. 2014. V. 209. P. 172–184.

УДК 544.723+547.458

АДСОРБЦІЯ БАРВНИКІВ, ГЕРБІЦИДІВ ТА ВАЖКИХ МЕТАЛІВ КОМПОЗИТАМИ КРЕМНЕЗЕМУ З АМІНОВМІСНИМИ ТА СУЛЬФАТНИМИ ПОЛІСАХАРИДАМИ

Т.М. Будняк[1], В.А. Тьортих[1], М. Блахньо[2], А. Дерило-Марчевська[2], А.В. Марчевський[2]

[1]Інститут хімії поверхні ім. О.О. Чуйка НАН України, вул. Генерала Наумова 17, 03164 Київ,Україна
e-mail: tetyanabudnyak@yahoo.com
[2]Університет Марії Кюрі Склодовської, пл. М. Кюрі Склодовської 2, 20-031 Люблін, Польща
e-mail: mordenit@wp.pl

Резюме. *Адсорбція похідними полісахаридів може застосовуватися як дешевий метод очистки води та як корисний інструмент для захисту навколишнього середовища. У цьому дослідженні композити полісахарид-кремнезем були синтезовані шляхом застосування золь-гель методу, фізичної і хімічної адсорбції хітозану і каррагинану поверхнею кремнезему. Екстракція високотоксичних сполук: катіонних і аніонних барвників, гербіцидів і важких металів синтезованими адсорбентами була досліджена.*

Ключові слова: *хітозан, каррагинан, барвники, гербіциди, кремнезем.*

UDC 539.211 : 544.723+54.31

BORONIC-ACID FUNCTIONALIZED MAGNETITE NANOCOMPOSITES FOR FRUCTOSE SENSING

Ye.V. Pylypchuk[1*], Yu.O. Zubchuk[1], P.P. Gorbyk[1]
K.O. Doroshenko[2*], N.G. Antoniuk[2]
[1] O.O. Chuiko Institute of Surface Chemistry, 17, General Naumov Street, Kyiv, 03164, Ukraine
**e-mail: ievgenpylypchuk@gmail.com*
[2] National University of Kyiv-Mohyla Academy, 2, Skovorody Street, 04655, Kyiv, Ukraine
**e-mail: ekaterinka.doroshenko@mail.com*

Abstract.*Method for boronic acid immobilization on the magnetite surface reported.Immobilization of boronic acid on the nanocomposite surface was confirmed using Fourier-Transform infrared spectroscopy. Proof of principle experiments using obtained nanocomposites showed possibility of their potential application for fructose sensing.*

Keywords: *multifunctional nanocomposites, absorption of fructose,magnetite, Alizarin Red S, boronic acid.*

Introduction. Recognition of different simple sugars in human blood is an important taskforcurrent medicine. The most promising way to construct fructose-sensitive materials is to use the ability of boronic acid to form reversible covalent complexes with 1,2- and 1,3-diols [1-2]. Boronic acids has relatively small toxicity and can be considered as "green" compounds [3].

Magnetite, Fe_3O_4 is natural mineral with high biocompatibitily [4]. Sensor applications in combination with magnetic properties of boronic acid-containing Fe_3O_4 nanocomposites allow us to create highly biocompatible multifunctional "green" materials for fructose detection.

Experimental. Magnetite was modified by 3-APTES using standart method [5]. 5-Formil-2-furyl boronic acid (furyl borate) was immobizlied on the surface of Magnetite/3-APTES composite in ethanolic solution. Immobilization of Alizarine Red S was performed in phosphate buffer (pH=7.4).

Results and discussion. The general scheme of Fe_3O_4/3-APTES/boronic acidnanocomposite synthesis is shown in Fig. 1. In the IR spectra of the obtained composite and initial furyl borate (Fig. 2) characteristic absorption bands are observed. They can be attributed to formilgroupinfuryl borate (1735 and 1803 cm^{-1}, probably splitting is due to intramolecular interactions of formil residuewith hydroxyl groups of boronic acid).After interaction withaminomagnetite, absorption bands of formil disappear, what may indicate the formation of Fe_3O_4/3-APTES/boronic acidcomposite. Absorption bandsof –B–C bondare is observed at 900 cm^{-1}, absorption bandsof –B– O bond is observed at 1350 cm^{-1}.

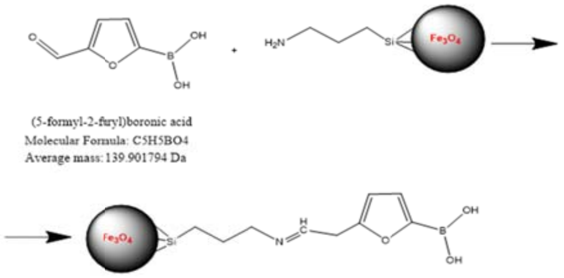

Fig. 1. *Scheme of synthesis of Fe_3O_4/3-APTES/Boronic Acid Nanocomposite*

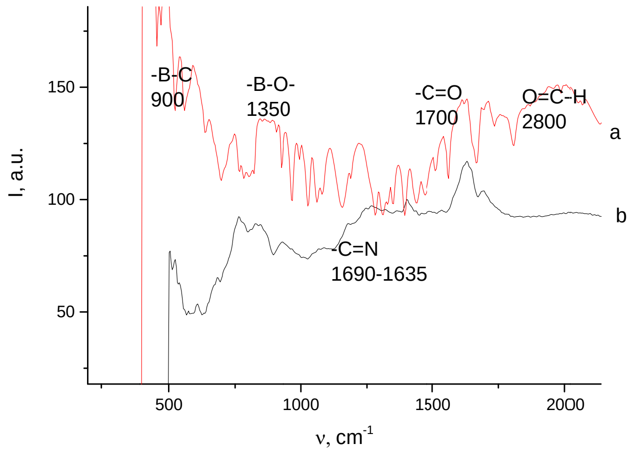

Fig. 2*. IR spectra of furfurylborate (a) and nanocomposite Fe_3O_4/3-APTES/boronic acid (b).*

Based on the data obtained by IR spectroscopy furylborate was successfully immobilized on the surface of magnetite.

*The study of competitive interaction and nanocompositeFe_3O_4 / 3-ARS / furfurylborate with Alizaryn Red S and Fructose***.** The method is based on the ability of immobilized boronic acid to bind cis-diol form of hydrocarbons specificly(Fig. 3) [6].

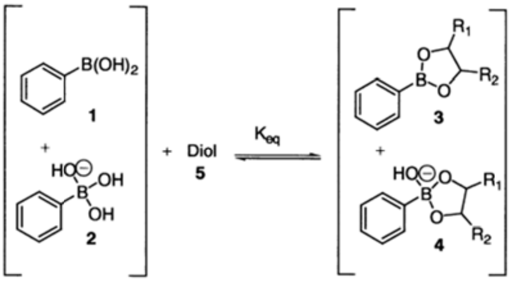

Fig. 3. *The binding of cis-diol with boronic acid [7].*

AlizarinRed S (ARS) in phosphate buffer (pH = 7.4) is used as an indicator in these types of reactions, λ_{max} = 423 nm.

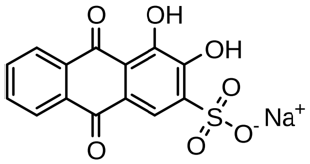

Molecular Weight 342.26

According to the literature, a competitive reaction between sugar and ARSh occurs in the processof absorption of sugars on the surface of the material which contain acidic surface groups with Boron (Fig. 4):

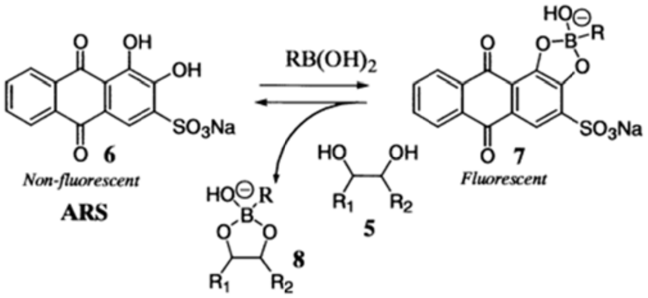

Fig. 4. *The competitive reaction between sugars and ARS.*

Thus, there is a "switch" of ARS molecules from non-fluorescence condition to fluorescence one. Thus, the content of cis-diols in solution can be quantitatively evaluated with the fluorescence of obtained conjugate. In addition, there is a shift of the maximum of absorption band of cis-diol derivate in the visible range. In our work itis demonstrated with the formyl-furylboric acid and ARS in phosphate buffer (Fig. 5).

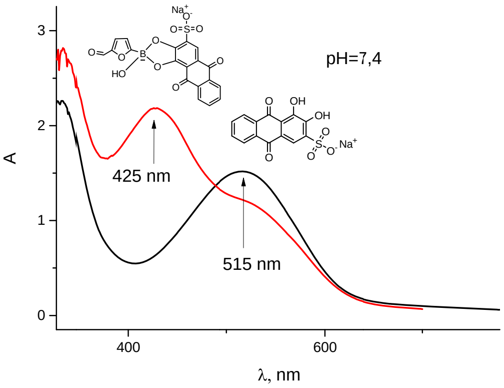

Fig. 5. *The absorption spectrum of ARS in phosphate buffer (1) and its conjugate acid with formyl-furfurylboric acid.*

Scheme of ARS binding with the surface of Fe_3O_4/3-APTES/boronic acid nanocomposite is showen in Fig. 6.

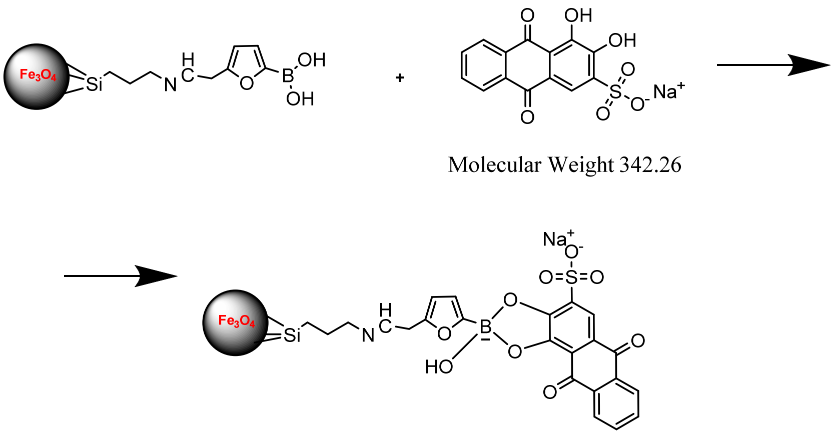

Fig. 6. *Scheme of ARS binding with the surface of Fe_3O_4/3-APTES/boronic acid nanocomposite*

Based on literature data, in case of the addition of carbohydrate in the form of cis-diol form the competitive replacement ARS on the surface of the composite to sugar molecules should occur.

Release of ARS when fructose is added was confirmed by photocolorimetric method. A model experiment was being conducted that based on competitive sorption phenomena between ARS at the surface of nanocomposites and fructose. It passes according to this scheme (Fig. 7).

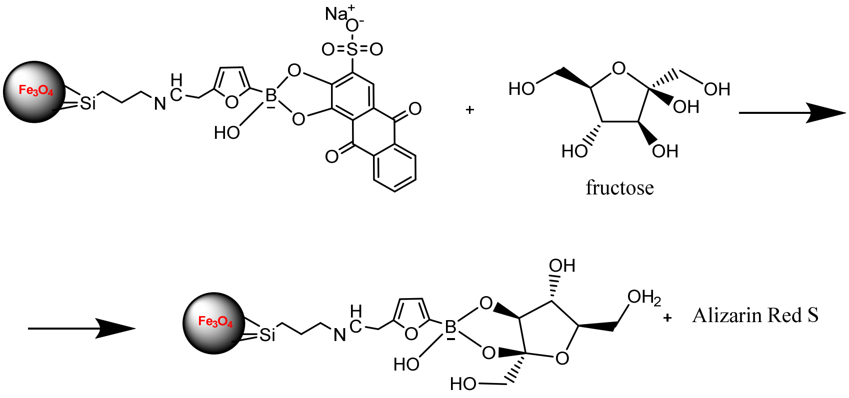

Fig. 7. *Competition between ARS and fructose.*

Conclusions. Modification of Fe_3O_4 by boronic acid could be realized throughout imine bond formation using formil-furyl boronic acid and NH_2-containing magnetite. Obtained Fe_3O_4/3-APTES/boronic acidcomposite show characteric adsorption band in FTIR spectra and able to interact with 1,2-diols (e.g. ARS). Preliminary experiments confirmed possibility to detect glucose using Fe_3O_4/3-APTES/boronic acid/Alizarin Red S nanocomposites according to competitive interaction in phosphfte buffer.

Acknowledgements. This research was supported by project N 38-16 *"Synthesis and properties of novel supramolecular nanostructures and* *composites, absorbing microwave electromagnetic and neutron radiation"* in framework of NAS of Ukraine comprehensive program of basic research "Fundamental problems of new nanomaterials and nanotechnologies".

References

1. *Cambre J. N., Sumerlin B. S.* Biomedical applications of boronic acid polymers // Polymer. 2011. V. 52. P. 4631-4643.
2. *Salazar-Mendoza D., Cruz-Huerta J., Ho□pfl H., Hernández-Ahuactzi I. F., Sanchez M.* Macrocycles and Coordination Polymers Derived from Self-Complementary Tectons Based on N-Containing Boronic Acids // Crystal Growth and Design. 2013. V. 13. P. 2441-2454.
3. *Savsunenko O., Matondo H., Frencechi-Messant S., Perez E., Popov A., Rico-Lattes I., Lattes A., Kaprichev Ye.* Functionalized vesicles based on amphiphilic boronic acids: a system for recognizing biologically important polyols // Langmuir. 2013.V. 29. P. 3207-3213.
4. *Kołodyńska D., Gęca M., Hubicki Z.* Development of New Effective Sorbents Based on Nanomagnetite // Nano Res. lett. 2016. V. 11.1. P. 1-10.
5. *Pylypchuk Ye., Zubchuk Yu., Petranovska A., Turanska S., Gorbyk P.* Syntesis and properties of Fe_3O_4/hydroxyapatite/pamidrinic acid/DTPA/Gd^{3+} // Him. Fiz. Techn. Pov. 2015. V. 3. P. 326-335.
6. *Emanuel V., Karyagin Y., Emanuel U.* Comparison of methods for determining of glycolysised hemoglobin // Lab. Medicine. 2002. V. 5. P. 98-104.
7. *Springsteen G., Wang B.* A detailed examination of boronic acid–diol complexation // Tetrahedron. 2002. V. 58. P. 5291–5300.

УДК 539.211 : 544.723+54.31

НАНОКОМПОЗИТИ НА ОСНОВІ МАГНЕТИТУ ФУНКЦІОНАЛІЗОВАНОГО БОРНОЮ КИСЛОТОЮ ДЛЯ ВИЗНАЧЕННЯ ФРУКТОЗИ.

Є. В. Пилипчук[1*], Ю. О. Зубчук[1], П. П. Горбик[1]
К. О. Дорошенко[2*], Н. Г. Антонюк[2]
[1]Інститут хімії поверхні ім. О.О. Чуйка, вул. Генерала Наумова17, 03164,Київ, Україна,
**e-mail: ievgenpylypchuk@gmail.com*
[2]Національний університет «Києво-Могилянська академія», вул.Г. Сковороди 2, 04655, Київ, Україна.
**e-mail: ekaternka.doroshenko@gmail.com*

***Резюме.** Висвітлено метод іммобілізації фурфурилборної кислоти на поверхню магнетиту. Іммобілізацію на поверхні нанокомпозиту підтверджено за допомогою ІЧ спектроскопії з Фур'є-перетворенням. Контрольно-перевірочний експеримент отриманого нанокомпозиту показав потенційну можливість застосування його для визначення фруктози.*

***Ключові слова:** поліфункціональні нанокомпозити, абсорбція фруктози, магнетит, алізарин червоний S, борна килота.*

Колективна монографія «Environmental Protection: from Sorbents to Membranes» - під ред. проф. Н. Кабай, докт. хім. наук Ю. С. Дзязько, проф. М. Арда, докт. хім. наук К. О. Каздобіна - 108 с.

Рецензенти: Проф. Утлеш С., докт. техн. наук, проф. Мирончук В. Г., докт. Іпек І., докт. хім. наук, проф. Сазонова В. Ф.

Рекомендовано до **друку** Вченою радою ІЗНХ ім. В. І. Вернадського НАН України (протокол № 15 від 19 жовтня 2016 р.).

Видавництво «АРТ ОК»
СВІДОЦТВО про внесення до державного реєстру видавців ДК № 4842 від 31.01.2015
03150, м. Київ, вул. Велика Васильківська, 143/2, 5 поверх, 7 офіс тел.: +38 044 222 63 42,
e-mail: info@art-ok.com.ua, www.art-ok.com.ua

Піписано до друку 19.10.2016 р. Формат 60х84/16. Наклад 300 примірників.
Замовлення № 01/11